

AD-778 167

BEACH MOBILITY TESTS AND ANALYSIS OF
LARGE, CARGO-HANDLING VEHICLES

J. G. Hicks, et al

Army Mobility Equipment Research and
Development Center
Fort Belvoir, Virginia

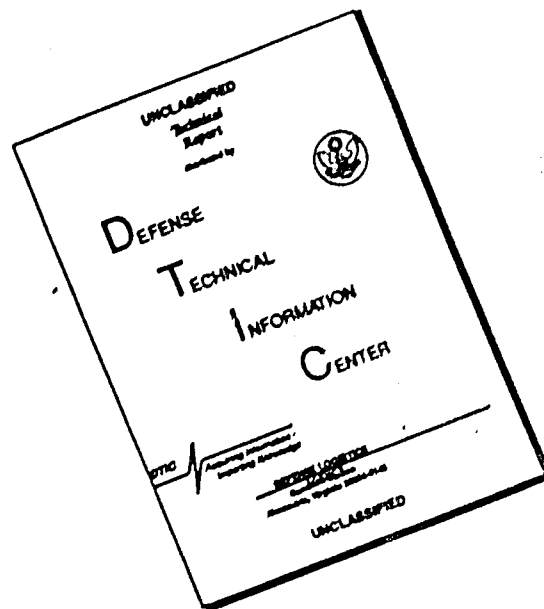
April 1974

DISTRIBUTED BY:

NTIS

National Technical Information Service
U. S. DEPARTMENT OF COMMERCE
5285 Port Royal Road, Springfield Va. 22151

DISCLAIMER NOTICE



THIS DOCUMENT IS BEST QUALITY AVAILABLE. THE COPY FURNISHED TO DTIC CONTAINED A SIGNIFICANT NUMBER OF PAGES WHICH DO NOT REPRODUCE LEGIBLY.

ACCESSION for	
NTIS	WFO 2 1971
DGC	100 1 1971
UNANNOUNCED	
JUSTIFICATION	
BY	
DISTRIBUTION AVAILABLE TO ALL S	
Class	
A	

Destroy this report when no longer needed.
Do not return it to the originator.

The citation in this report of trade names of commercially available products
does not constitute official endorsement or approval of the use of such products.

UNCLASSIFIED

SECURITY CLASSIFICATION OF THIS PAGE (When Data Entered)

AD 778 167

REPORT DOCUMENTATION PAGE		READ INSTRUCTIONS BEFORE COMPLETING FORM
1. REPORT NUMBER 2096	2. GOVT ACCESSION NO.	3. RECIPIENT'S CATALOG NUMBER
4. TITLE (and Subtitle) BEACH MOBILITY TESTS AND ANALYSIS OF LARGE, CARGO-HANDLING VEHICLES		5. TYPE OF REPORT & PERIOD COVERED Final Report
7. AUTHOR(s) J. G. Hicks A. Thomas W. F. Clark C. Orth C. Tacey		6. PERFORMING ORG. REPORT NUMBER
9. PERFORMING ORGANIZATION NAME AND ADDRESS U. S. Army Mobility Equipment Research and Development Center, Mechanical Technology Department, STSFB-HMM, Fort Belvoir, Virginia 22060		8. CONTRACT OR GRANT NUMBER(s)
11. CONTROLLING OFFICE NAME AND ADDRESS U. S. Army Mobility Equipment Research and Development Center, Fort Belvoir, Virginia 22060		10. PROGRAM ELEMENT, PROJECT, TASK AREA & WORK UNIT NUMBERS IG763702DG1407
14. MONITORING AGENCY NAME & ADDRESS (if different from Controlling Office)		12. REPORT DATE April 1974
		13. NUMBER OF PAGES 219
		15. SECURITY CLASS. (of this report) UNCLASSIFIED
		15a. DECLASSIFICATION/DOWNGRADING SCHEDULE
16. DISTRIBUTION STATEMENT (of this Report) Approved for public release; distribution unlimited.		
17. DISTRIBUTION STATEMENT (of the abstract entered in Block 20, if different from Report)		
18. SUPPLEMENTARY NOTES		
19. KEY WORDS (Continue on reverse side if necessary and identify by block number) Sand Mobility Beach Mobility Vehicle Performance Cone Index Mobility Models Reproduced by NATIONAL TECHNICAL INFORMATION SERVICE U. S. Department of Commerce Springfield VA 22151		
20. ABSTRACT (Continue on reverse side if necessary and identify by block number) Beach mobility tests were performed on 6000-, 10,000-, and 50,000-pound-capacity rough terrain forklift trucks and a 20-ton-capacity rough terrain crane. Data included drawbar pull, maximum negotiable slope, and soil characteristics. An extension of the Cone Index Mobility Model is proposed to account for the additional effects of differences in front/rear tire inflations and axle loadings, and radial tires. Test observations and data analysis suggest that new approaches in developing sand mobility prediction techniques may be fruitful.		

DD FORM 1473

JAN 73

EDITION OF 1 NOV 65 IS OBSOLETE

UNCLASSIFIED

SECURITY CLASSIFICATION OF THIS PAGE (When Data Entered)

SUMMARY

This report describes beach mobility tests that were conducted by the U. S. Army at the Naval Amphibious Base, Little Creek, Virginia, during September and October 1973. Analysis of the data has resulted in a suggested modification to the Cone Index Mobility Model to be used when predicting performance of large material handling vehicles on sandy beaches or in desert areas.

Drawbar pull (DBP) and maximum negotiable slope (S_{\max}) tests were performed on the military designed, 20-ton-capacity, rough terrain crane, and the 6000-pound-capacity (6K) and 10,000-pound-capacity (10K) rough terrain forklift trucks. A commercial, 50,000-pound-capacity (50K) rough terrain forklift/container handler was also tested. Extensive testing with the 10K and the 50K vehicles provided sufficient data for the extension of the mobility model.

A FORTRAN computer program was developed for the proposed prediction technique which calculates performance parameters from vehicle description and soil strength data.

PREFACE

The testing at Little Creek, Virginia, from 7 September through 19 October 1973 was done under Project 1G763702DG1407. The testing was performed to obtain data needed for in-house technical decisions. Supervision and consultation were rendered by J. R. Blanchfield, Principal Engineer.

The authors are grateful for the support and cooperation of Ed Rush and his colleagues of Waterways Experiment Station. Their aid in gathering and interpreting data was most helpful.

Particular thanks is given to Percy Davidson for managing the test equipment and gathering the tire data. The valuable aid rendered by Mr. Davidson, equipment operators Arthur Limerick and Robert Combs, and photographer Harold Mohaupt is greatly appreciated.

CONTENTS

Section	Title	Page
	SUMMARY	i
	PREFACE	ii
	ILLUSTRATIONS	v
	TABLES	vi
	GRAPHS	vii
I	INTRODUCTION	
	1. Background	1
II	INVESTIGATION	
	2. Test Procedures and Data Handling	
	a. Soils Measurements	3
	b. Drawbar Pull Tests	5
	c. Dune Slope Tests	8
	3. Data Analysis	
	a. Performance/Soil Strength Relationship	13
	b. Tire Inflation Effects	17
	c. Axle Loading Effects	20
	d. Radial Tire Effects	22
	e. Mobility Model Modification	22
III	DISCUSSION	
	4. Presentation of Results	
	a. Computer Program Calculations	24
	b. Soil Mechanics	25
IV	CONCLUSIONS AND SUBSEQUENT AREAS FOR INVESTIGATION	
	5. Conclusions	26
	6. Subsequent Areas for Investigation	27
	APPENDICES	
	A. Test Data	31
	B. Drawbar Pull -- Maximum Slope Equivalency	127

CONTENTS (cont'd)

Section	Title	Page
	APPENDICES (cont'd)	
C.	Computer Program Description	129
D.	Graphical Representation of Computer	134
	ABBREVIATIONS, ACRONYMS, AND SYMBOLS	201

ILLUSTRATIONS

Figure	Title	Page
1	Test Site at the Naval Amphibious Base, Little Creek, Virginia	2
2	Prepared Slope Area	3
3	Dune Under Construction	9
4	10K RTFLT Ascending a Dune	10
5	Vehicle Stalled on a Slope	12
6	Drawbar Pull – Maximum Slope Correlation for 50K RTFLT	15
7	Drawbar Pull – Maximum Slope Correlation for 10K RTFLT	16
8	Performance Variation with Average Tire Inflation for 50K RTFLT	18
9	Three Methods for Data Point Adjustment to Reach a Curve	28
10	Cone Index Profile	28
A3-1	Sample DBP – Slip Curve (10K RTFLT)	46
A3-2	Sample DBP – Slip Curve (50K RTFLT)	47
A-6	Drawbar Pull Test Lane Cone Index Profile	110
B-1	DPB – GVW Equivalentcy – Level Surface	128
B-2	DPB – GVW Equivalentcy – Inclined Surface	128

TABLES

Table	Title	Page
1	10K RTFLT, Standard Tire, Equal Axle Load	19
2	50K RTFLT, Standard Tire, Equal Axle Load	20
A-1	Master Analysis Sheets	33-36
A-2	Prepared Slope Data	38-44
A-3	Drawbar Pull Data	48-92
A-4	Motion Resistance Tests	94-104
A-5	Vehicle Contact Pressures	106-108
A-6	Drawbar Test Lane Cone Index Profile	111-114
A-7	Soil Moisture and Density Data	115
A-8	Grain Size Distribution	116
A-9	Drawbar Test Lane Evaluation Profile	118
A-10	Prepared Slope Evaluation Profile	120-124
A-11	Vehicle and Tire Parameters	125-126

GRAPHS IN APPENDIX D

No.	Equipment	Size	Page
1	Standard Tires, Equal axle load	50K RTFLT	134
2	Standard Tires, Equal axle load	50K RTFLT	135
3	Standard Tires, Equal axle load	50K RTFLT	136
4	Standard Tires, Equal axle load	50K RTFLT	137
5	Standard Tires, Equal axle load	50K RTFLT	138
6	Standard Tires, Equal axle load	50K RTFLT	139
7	Standard Tires, Unequal axle load	50K RTFLT	140
8	Standard Tires, Unequal axle load	50K RTFLT	141
9	Standard Tires, Unequal axle load	50K RTFLT	142
10	Standard Tires, Unequal axle load	50K RTFLT	143
11	Standard Tires, Unequal axle load	50K RTFLT	144
12	Standard Tires, No axle load	50K RTFLT	145
13	Standard Tires, No axle load	50K RTFLT	146
14	Standard Tires, No axle load	50K RTFLT	147
15	Standard Tires, No axle load	50K RTFLT	148
16	Standard Tires, No axle load	50K RTFLT	149
17	Radial Tires, Equal axle load	50K RTFLT	150
18	Radial Tires, Equal axle load	50K RTFLT	151
19	Radial Tires, Equal axle load	50K RTFLT	152
20	Radial Tires, Equal axle load	50K RTFLT	153
21	Radial Tires, Equal axle load	50K RTFLT	154
22	Radial Tires, Equal axle load	50K RTFLT	155
23	Radial Tires, Unequal axle load	50K RTFLT	156
24	Radial Tires, Unequal axle load	50K RTFLT	157
25	Radial Tires, Unequal axle load	50K RTFLT	158
26	Radial Tires, Unequal axle load	50K RTFLT	159
27	Radial Tires, Unequal axle load	50K RTFLT	160
28	Radial Tires, Unequal axle load	50K RTFLT	161
29	Radial Tires, No axle load	50K RTFLT	162
30	Radial Tires, No axle load	50K RTFLT	163
31	Radial Tires, No axle load	50K RTFLT	164
32	Radial Tires, No axle load	50K RTFLT	165
33	Radial Tires, No axle load	50K RTFLT	166
34	Radial Tires, No axle load	50K RTFLT	167
35	Standard Tires, Equal axle load	10K RTFLT	168
36	Standard Tires, Equal axle load	10K RTFLT	169
37	Standard Tires, Equal axle load	10K RTFLT	170
38	Standard Tires, Equal axle load	10K RTFLT	171

GRAPHS IN APPENDIX D (cont'd)

No.	Equipment	Size	Page
39	Standard Tires, Equal axle load	10K RTFLT	172
40	Standard Tires, Unequal axle load	10K RTFLT	173
41	Standard Tires, Unequal axle load	10K RTFLT	174
42	Standard Tires, Unequal axle load	10K RTFLT	175
43	Standard Tires, Unequal axle load	10K RTFLT	176
44	Standard Tires, Unequal axle load	10K RTFLT	177
45	Standard Tires, No axle load	10K RTFLT	178
46	Standard Tires, No axle load	10K RTFLT	179
47	Standard Tires, No axle load	10K RTFLT	180
48	Standard Tires, No axle load	10K RTFLT	181
49	Standard Tires, No axle load	10K RTFLT	182
50	Radial Tires, Equal axle load	10K RTFLT	183
51	Radial Tires, Equal axle load	10K RTFLT	184
52	Radial Tires, Equal axle load	10K RTFLT	185
53	Radial Tires, Equal axle load	10K RTFLT	186
54	Radial Tires, Equal axle load	10K RTFLT	187
55	Radial Tires, Unequal axle load	10K RTFLT	188
56	Radial Tires, Unequal axle load	10K RTFLT	189
57	Radial Tires, Unequal axle load	10K RTFLT	190
58	Radial Tires, Unequal axle load	10K RTFLT	191
59	Radial Tires, Unequal axle load	10K RTFLT	192
60	Radial Tires, No axle load	10K RTFLT	193
61	Radial Tires, No axle load	10K RTFLT	194
62	Radial Tires, No axle load	10K RTFLT	195
63	Radial Tires, No axle load	10K RTFLT	196
64	Radial Tires, No axle load	10K RTFLT	197
65		20-ton RTC	198
66		6K RTFLT	199
67		6K RTFLT	200

BEACH MOBILITY TESTS AND ANALYSIS OF LARGE, CARGO-HANDLING VEHICLES

I. INTRODUCTION

1. **Background.** A number of mobility models have been created for the purpose of predicting the performance of military vehicles in off-road environments. In this report, the primary concern is the specific case of the mobility of large materials-handling equipment (MHE) items on sand. The cone index model, conceived and developed at the U. S. Army Corps of Engineers Waterways Experiment Station (WES), Vicksburg, Mississippi, demonstrates how well empirical mathematical relations can be used to predict wheeled-vehicle mobility on weak soils.¹ This model distinguishes itself from other mobility models by its dependence on a single soil strength quantity—the Cone Index (CI). The tacit assumption is made that all factors which affect soil strength, such as moisture content, vegetation, and grain size, need not be determined if the CI is known. Mathematically, this means that the mobility-dependent variable—usually draw-bar pull (DBP) or maximum negotiable slope (S_{max})—is a function of only one soil parameter. One asset of the Cone Index Mobility Model (CIMM) is its simplicity and the ease with which CI data can be obtained and then used in the formula. The excellent correlation that exists between mobility variables and soil strengths, through the CI quantity, is indeed fortunate; and the purpose of the present work is to further exploit this correlation. Statistical analyses performed during the original model derivation indicate that the basic equation is highly significant at the .01 probability level.

There are some anomalies associated with the CIMM which are not yet fully understood. One is the difference between the observed mobilities of a vehicle in natural and in prepared (harrowed) terrains of the same soil strength (CI). The formulas which embody the CIMM were derived from field test data; and the inability of the model to compute results which compare accurately with laboratory tests or prepared terrain data is not considered a serious deficiency.

However, there are effects which are not included in the equations that quite readily lend themselves to quantification. These are differences in front-rear tire inflation pressures and front-rear axle loadings. The present investigation sheds some light on both of these effects.

¹U. S. Army Engineer Waterways Experiment Station, "Trafficability of Soils," Tech. Memo. No. 3-240, 17th Supplement, May 1973.

TEST SITE **NAVAL AMPHIBIOUS BASE** **LITTLE CREEK, VIRGINIA** (MAP NOT TO SCALE)

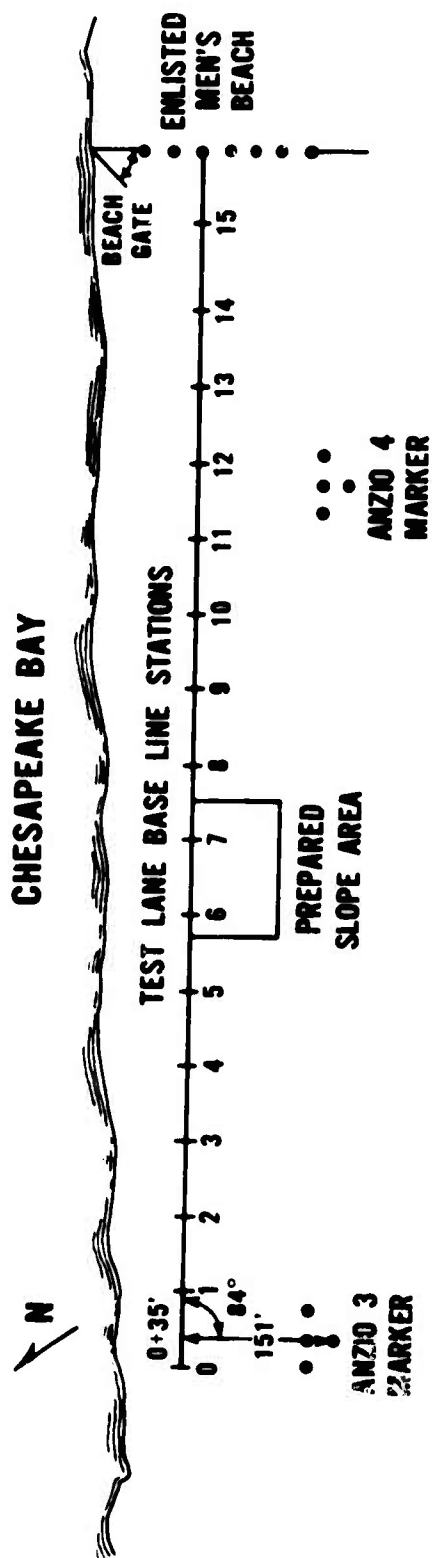


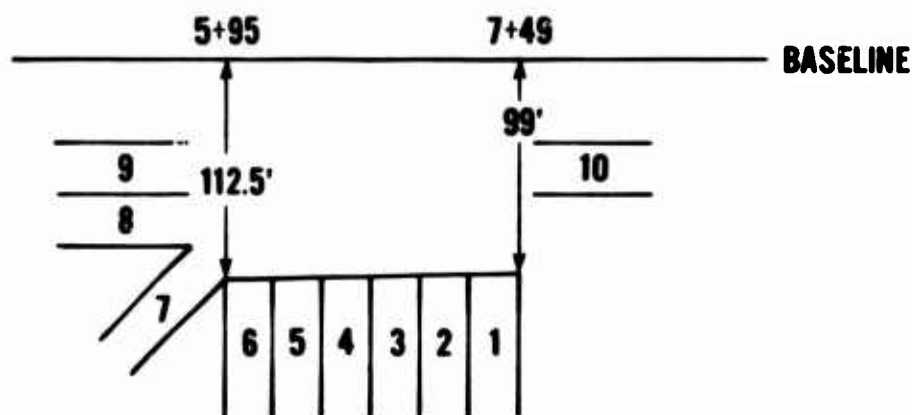
Fig. 1. Test site at the Naval Amphibious Base, Little Creek, Virginia.

II. INVESTIGATION

2. Test Procedures and Data Handling.

a. **Soils Measurements.** The specific details of the techniques used to gather the required data are outlined in the *Preliminary Plan of Test-Beach Mobility Tests of Off-Road MHE Items*. The plan and all collected data are contained in Office Report T9M 74.² Therefore, the procedures presented and the data used herein have been summarized for brevity.

The test area was a natural, all-sand beach typical of most beaches on the eastern seaboard. A drawbar pull lane was established parallel to the tide line but approximately 100 feet inland. Existing dunes provided the foundation for the slope test area where sand from the surrounding area was piled up and graded to form the desired slopes. Diagrams of the test area are shown in Figs. 1 and 2. Abbreviated tabulations of the natural characteristics of the test area are shown in Appendix A.



PREPARED SLOPES

1 - 11%	6 - 4%
2 - 10%	7 - 6%
3 - 8%	8 - 13%
4 - 9%	9 - 12%
5 - 5%	10 - 15%

NOTE: ALL SLOPES ARE 75'
LONG AND 30' WIDE

Fig. 2. Prepared slope area.

²USAMERDC Office Report T9M-74.

(1) **Test Course Preparation.** Since any sustained operation on a beach causes surface disturbance, the courses were processed and maintained by back-dragging with a dozer blade or a bundle of timber to remove ruts and other surface irregularities. The operation was performed before each test operation on both the drawbar lane and the prepared slopes.

(2) **Grade and Alignment.** The centerline of the courses was established and maintained with off-set stakes. Longitudinal and transverse grades were measured with an Engineer's Level and a Philadelphia Leveling Rod.

(3) **Sand Data.** The several tests and items of test apparatus are described in the following sub-paragraphs.

(a) **Cone Index.** An index of shearing resistance of soil was measured with the cone penetrometer. The value represents the resistance of the soil to penetration of a 30-degree cone of 0.5-in.² base, or projected area. The number, although considered dimensionless, actually denotes pounds of force on the handle divided by the area of the cone base in square inches. The standard cone penetrometer permits CI readings to be taken up to 300. However, to obtain measurements in firm sand exceeding a 300 CI, a 30-degree cone with a 0.2-in.² base area and a 3/8-in. diameter shaft was used. The 0.2-in.² cone permitted taking CI readings up to 750 (dial readings are multiplied by a factor of 2.5). CI measurements were made at intervals along the test course starting at the surface and continuing to a depth of 18 inches (at 3-inch depth intervals) or until the cone reading exceeded 300. The penetrations were spaced across the test course at each sample station. Three to ten readings were made to establish an arithmetic mean value at each location. Testing was repeated at time intervals considered appropriate to detect any change that might occur in the shearing resistance and friction capacity of the various layers.

(b) **Moisture.** Moisture is defined as the water content of a soil mass and is the ratio of the weight of water to the weight of dry soil (usually expressed as percentage). A testing pattern was established to provide the moisture content of the surface and at depths of 1 to 3 inches and 6 to 9 inches. Samples were taken at appropriate time intervals to detect major changes in the moisture condition. Frequent sampling for moisture content was not required since the tests were performed during the dry season, and there was no radical change in moisture except during a short period of inclement weather which affected the surface for only a short time.

Sand condition nomenclature as established by WES was used to classify the material as follows:

Dry Sand: Light-colored, loose, and free flowing when poured from the hand. Dry sand usually occurred on the surface of all areas of the beach except on the wetted foreshore, but it never extended deeper than about 5 inches before becoming moist. Sand classed as dry on the basis of observation usually contained less than 1.5% moisture by weight.

Moist Sand: Usually lies directly beneath the dry-sand layer. It was usually darker in color, showed slight cohesion, and was cool to the touch. In general, moist, coarse sand was found to contain about 1.5 to 5.0% moisture, and moist fine sand, about 10 to 12% moisture. The conditions shown were used to classify the test courses.

(c) **Density.** The dry density is defined as the weight of soil per unit volume normally expressed in pounds per cubic foot. A 2.9-in.-diameter, thin-walled steel cylinder was used to obtain all density samples. Since there is no reliable correlation between density and CI, the sampling was limited. Samples were taken at 6 to 9 inches below the surface.

(d) **Grain Size Analysis.** Grain size distribution tests were conducted on samples obtained along the centerline of the drawbar test lane at 50-ft intervals and at depths of 1 to 3 inches and 6 to 9 inches below the surface. The tests were conducted by shaking the sample through a stack of wire screens with openings of known size. The definition of particle diameter is, therefore, the side dimension of a square hole. The National Bureau of Standards screen sizes used to classify sand are No. 4 with 0.187 in. openings; No. 10 with 0.0787 in. openings; No. 40 with 0.0165 in. openings, and No. 200 with 0.0029 in. openings.

b. Drawbar Pull Tests.

(1) **Purpose.** The comprehensive plan followed during the Beach Mobility Test of Off-Road MHE Items is shown in Office Report T9M-74. Analytical evaluation of the test results will provide the following:

(a) Quantitative evaluation of the mobility characteristics of the current military off-road materials handling equipment which will then serve as the performance criteria and minimum design objective for future equipment items.

(b) Validation and/or revision of the current mobility prediction formula to cover the larger and heavier MHE items required by the U. S. Army.

(c) Establishment of specific design relationships which will be used in future development of MHE. The establishment of specific performance design relationships will assure the attainment of the required mobility while avoiding the penalties intrinsic in overdesign.

(2) **Objective.** This report is primarily concerned with the objective described in paragraph (b), above. The test procedures are summarized and the test results are arranged in accordance with the Data Analysis (Section II-3).

The following operating procedures, techniques, and instrumentation were employed during the tests at Little Creek, Virginia.

(a) **Procedures and Techniques.** The drawbar pull ability was based on the pull exerted at the drawbar with the vehicle in the lowest forward gear and the all-wheel-drive mode, while traveling over the test course under full throttle. The load-measuring instrument (load Cell SR-4) was connected in series with a cable attached to the drawbar of the test unit and a retarding vehicle. The cable was as near parallel to the test course surface as vehicular configuration would allow. The test vehicle was allowed to obtain maximum ground speed at maximum engine speed prior to the application of various retarding forces. Once a stabilized ground speed was reached, various incremental retarding forces were applied to the drawbar of the test vehicle for short durations throughout the test course. The instrumentation used was capable of simultaneously recording the ground speed, drawbar force, engine speed, pulling wheel speed, and duration of test. Data obtained was used to plot curves of drawbar force versus test vehicle wheel slip in percent.

This drawbar pull procedure was used throughout the evaluation of the 20-ton rough terrain crane (RTC) and the 10K rough terrain forklift truck (RTFLT) during the standard tire phase of the test. Difficulty was encountered in maintaining a travel efficiency of 90% or greater when the test vehicles were operating at full throttle with no retarding force applied to the drawbar. Excessive wheel slip resulted primarily from excessive power being delivered to the drive wheels, and test course soil conditions were considered marginal in terms of go -- no go.

As a result of discussions between Mr. Ed Rush, WES representative, and MERDC test personnel, the drawbar technique as previously

described was modified. Modification to the drawbar technique was done primarily to satisfy the needs of the drawbar pull versus vehicle wheel slip curves.

The change in drawbar pull technique was initiated on 1 October 1973 at the outset of the radial ply tire phase of the 10K RTFLT test and continued for the duration of the tests.

The major change in drawbar technique consisted in allowing the test vehicle and the retarding vehicle to obtain a stabilized speed of 1 to 2 mph corresponding to approximately half maximum engine speed. Incremental drawbar loading was applied by the retarding vehicle, and each load increment was held until the combined speed of both units reached a stabilized ground speed at which time the desired phenomena were recorded. To obtain higher slip points, the test vehicle operator attempted to maintain a constant ground speed regardless of the drawbar load. The test vehicle throttle position was varied from half throttle initially to full throttle at the conclusion of the test run. There were no significant changes in the instrumentation.

(b) Instrumentation and Measurements. The instrumentation consisted of a Honeywell Model 1858-T79 graphic recorder with compatible signal conditioning units to handle strain gage and pulse-type signals and with the ability to handle 18 separate pieces of data. The test data were recorded simultaneously on 8-inch-wide, photo-sensitive direct printpaper. The following phenomena were measured and recorded during the test using the aforementioned instrumentation:

1 **Travel Distance:** The test unit was equipped with a fifth wheel of known circumference (6.98 ft) and divided into fourths with each fourth being represented by an event mark on the data record.

2 **Engine Speed (rpm):** A 10:1 reduction coupling was installed at the tachometer output of the test vehicle engine with each event mark on the data record representing one-tenth of the engine speed occurring during the test interval.

3 **Vehicle Wheel Revolutions:** During the first phase of testing, lugs were welded to a wheel on the test vehicle. A switch was mounted on the test vehicle in such a manner that rotation of the vehicle wheel tripped the switch and the event was recorded on the data record. During the later phases, a lug was placed on the drive shaft of the test vehicle and calibrated in vehicle distance traveled per shaft

revolution. As in the previous method, the lug tripped a switch and the event was recorded on the data record. The advantage of placing the lug on the vehicle drive shaft was an improved accuracy resulting from the higher number of event marks recorded per distance of test vehicle travel.

4 Drawbar Force: The applied drawbar retarding forces were measured using an SR-4 Strain Gage Load Cell and were recorded simultaneously with other events.

5 Resistance to Towing: The force required to tow the various test vehicles and the speed of towing were recorded using the aforementioned fifth wheel and load cell.

6 Duration of Test: Recorded simultaneously with occurring phenomena is a 1-second time line with every tenth line accentuated. From the aforementioned recorded data, the information required for the development of a Drawbar Pull Versus Percent Wheel Slip Curve can be developed. The calculations are shown in Appendix A-3.

c. **Dune Slope Tests.** Ten dunes, each with a different slope, were constructed to accommodate the maximum negotiable slope tests. The dunes were built with a D-7 bulldozer and were allowed to settle for 2 weeks before tests were begun. Slope values ranged from 4 to 22%. Figures 3 and 4 illustrate the layout of the dunes and Figs. 1 and 2 show plan views of the test site. The soil strength of the dunes was generally less than the DBP test lane when tests were begun, but near the end of testing the dunes had become somewhat stronger than the test lane.

The test procedure generally was to run the vehicle on progressively steeper slopes until it became immobilized. Stalls which occurred on the curved portion near the top or bottom of the slope were not considered as valid runs. The length of the dunes was approximately 90 feet, and valid stall positions were those which occurred between 20 and 70 feet from the bottom.

Before slope tests began, it was realized that a vehicle could negotiate the lower portion of a dune yet would stall on the same slope at a higher position. This would occur because the dunes invariably had a positive strength gradient from bottom to top. This gradient existed mainly because the base of the dune was below the level of the original beach surface and consequently had a higher moisture content than the top. Also, there was more bulldozer traffic on the lower portion of the dune which aided settlement with its vibrations. In one respect, this gradient was a blessing in disguise since multiple data points could be obtained for the same test case. Frequently, stall points were acquired on two adjacent dunes with the vehicle climbing higher on the



W6496

Fig. 3. Dune under construction.



W6527

Fig. 4. A 10K RTFLT ascending a dune.

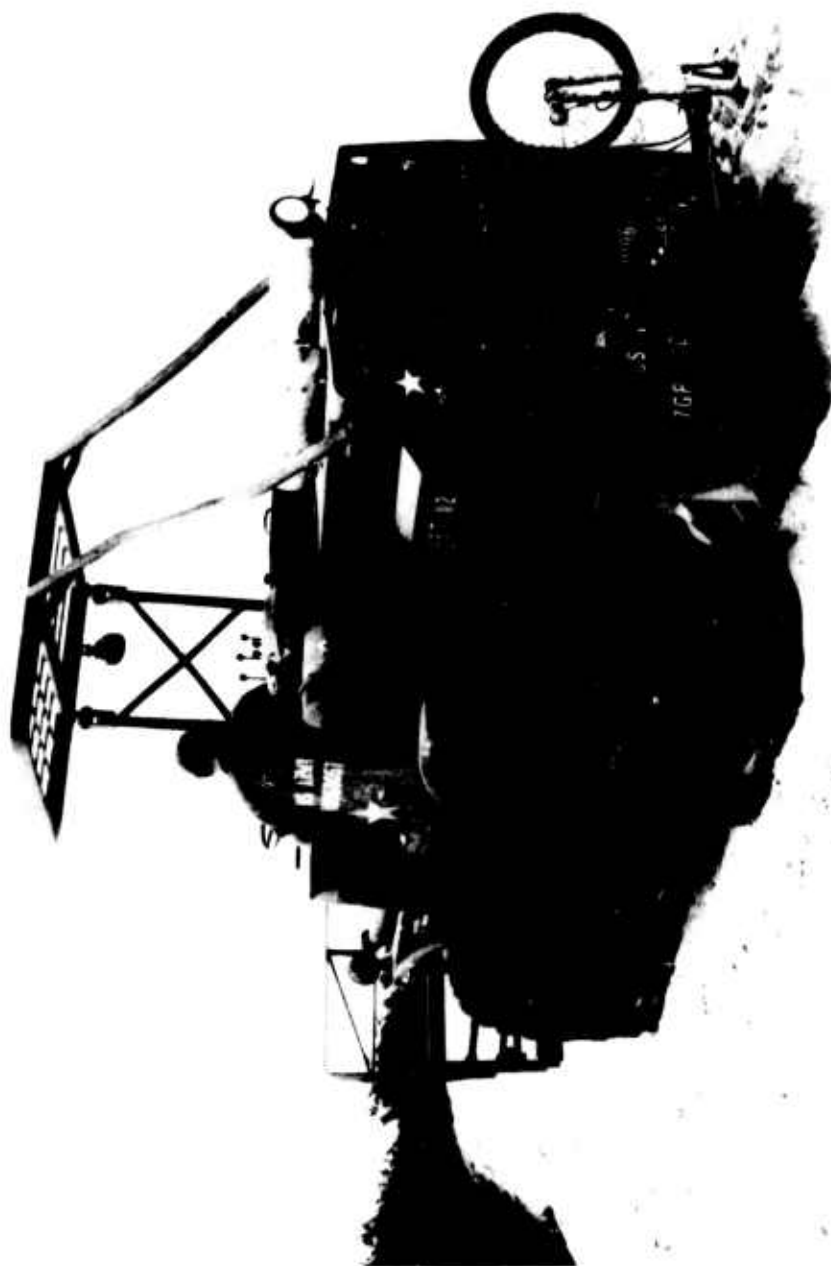
incline with the smallest slope. In a few cases, it was possible to obtain three data points since adjacent dunes varied only about 2% in slope.

Initially, the vehicle was stopped on level at the base of the incline. Ascent was made at full throttle with all four wheels driving when possible. Power was reduced soon after slip was observed to prevent further disturbance of the sand. Complete immobility did occur immediately after the top layer of sand was sheared by the tire. There was never any gradual approach to stall – the vehicles literally “fell into” the dune with a catastrophic onset of immobility. In some cases, the vehicle was backed down the slope after stall and then started again to verify the “go” area. This maneuver would also indicate if the vehicle inertia actually carried it beyond its true stall position. Another method employed to determine inertia effects was to make a low-speed run very close to the tracks of the full-throttle run and compare the stall positions. In no case did the vehicle fail to start when stopped in a “go” area. However, the low-speed runs invariably stalled from 5 to 10 feet down slope of the corresponding full-throttle run. It is estimated that the change in the 0- to 9-inch average of the CI would vary only about 5 points (PSI) over a 10-foot span. Consequently, these differences were not accounted for in the data analysis.

Figure 5 is a typical picture of a vehicle at its stall position on an incline. To facilitate the gathering of data, the truck was backed away in its ascent tracks. Cone penetrometer readings were made to the left and right of the tracks as well as in the center of the stall area. Five strength profiles were taken in each of these three regions and the arithmetic mean was used as the strength parameter in the analysis. In the 50K RTFLT analysis 0- to 9-inch and 0- to 12-inch averages were used, while 0- to 6-inch and 0- to 9-inch values were considered in the 10 K RTFLT tests. A suggested alternate approach to specifying strength values is developed in Section IV-6 but is not used in the present analysis.

The other important variables that were measured after each test run were the longitudinal and side slopes of the dune. Five to ten readings were taken with a hand inclinometer. The mean of these values was averaged with the slope which was computed from elevation profile data obtained with the Engineer's Level. Axle position elevations were computed by linearly interpolating between the two adjacent elevation readings. The largest observed discrepancy between slopes determined from inclinometer and elevation measurements was only 0.4% slope. A slight error was introduced when distance measurements along the dune surface were tacitly assumed to be equal to the horizontal values. This results in only a 0.5% difference in slope on the steepest dune.

At the conclusion of a test run, the dune was repaired with the bulldozer. After the dunes were smoothed, the bulldozer was run back and forth in an attempt to settle the soil in the ruts.



W6509

Fig. 5. Vehicle stalled on a slope.

3. Data Analysis.

a. **Performance/Soil Strength Relationship.** Sufficient data was taken on the 50K and 10K RTFLT to provide a basis for the analytical development of a recommended mobility model. The Master Data sheets in Appendix A show all the test cases. However, the analyses presented herein concern only a modification to the well established CIMM. Care was taken to retain the basic character of the CIMM formulas. It should be understood that these modifications are suggestive in nature and should not be interpreted as the ultimate. The empirical equations of the original CIMM were derived from literally thousands of data points whereas the present analysis is based on approximately 100 data points. Consequently, the proposed extension of the CIMM to large material handling vehicles should be refined or revamped as additional data becomes available. Greater quantities of data, even with the same scatter range, would increase the confidence level as calculated by statistical methods. All the analyses contained in this report are empirical in nature and have no theoretical basis.

The original CIMM prediction equation is as follows:

$$\text{DBP or } S_{\max} = 28.87 \log_{10} \text{ CI} + 10.1 \text{ CAF} - 1.52 \text{ NPW} - 0.61 \text{ TP} - 43.82 \text{ or } 45.82 \quad (1)$$

The modified CIMM (of Section II-3e), including terms which compensate for the effects of unequal axle loads, differences in front and rear tire inflation pressures, and the type of tire construction being used, is as follows:

$$\begin{aligned} \text{DBP or } S_{\max} = & 28.87 \log_{10} \text{ CI} + 10.1 \text{ CAF} - 1.52 \text{ NPW} - 0.205 \text{ TP} \\ & + \frac{2.17 (\text{TP}_F - \text{TP}_R)}{\text{TP}} + \frac{1.16 (\text{AL}_F - \text{AL}_R)}{\text{GVW}} - K_{\text{FL}} \end{aligned} \quad (2)$$

The modifications to the CIMM directly reflect the performance measured during the testing at Little Creek, Virginia, under conditions with the closest possible similarity to the natural environment. Certain indices of performance have historically been used to describe the off-road capabilities of vehicles. The most accepted indices are drawbar pull and maximum slope which are related. However, before DBP and S_{\max} can be correlated, compared, and used to establish trends, they must first be adjusted to a common soil strength condition. It would not be meaningful to compare the DBP and slope performance of a vehicle at different soil strengths. Since the desired relationship should preserve the logarithmic character of the CIMM formula, we assume that

$$S_{\max} = K \log_{10} \text{ CI} + C \quad (3)$$

where C represents the remaining terms of the CIMM formula, all of which are being

held constant for the present. Equation (3) may be used as an adjustment formula by casting it as a difference relationship:

$$\Delta S_{\max} = K \log_{10} \frac{CI_1}{CI_2} \quad (4)$$

Here, ΔS_{\max} represents the correction to be applied to performance data (drawbar pull or slope) at soil strength condition CI_2 so that it may be compared directly with data at condition CI_1 . There only remains to calculate the value of K . This was accomplished by solving Equation (4) for K while using the test data for values of CI and ΔS_{\max} . The average value of K obtained from the 50K and 10K RTFLT was 8.04. It should be noted that this constant corresponds to the 28.87 coefficient in the original CIMM. Also, the greater the range in CI , the more accurate will be the calculation of K . The 0- to 9-inch average of CI ranged from 110 to 180 over which the foregoing analysis was performed.

It should be pointed out that the calculated K of 8.04 was used only in the adjustment formula equation (4) and not in the modified prediction equation (15). The CIMM coefficient when used in the adjustment formula gave unrealistically high adjustments. However the CIMM value which affects the curvature of the S_{\max} versus CI curve gives better accuracy in the *prediction formula* — particularly, at low soil strengths. Consequently, the modified prediction formula developed in this report preserves completely the effect of soil strength on performance.

Equation (4) was utilized to adjust the slope data to the soil strength condition of the DBP test lane. However, before a comparison could be made, it was also necessary to correct the DBP values for side-slope effects. This was accomplished by using the WES formula:

$$DBP = \frac{\sqrt{DBP'^2 + \sin^2 \theta}}{\cos \theta} \quad (5)$$

where the prime represents values measured on the side slope. The DBP values may now be correlated directly with the maximum negotiable slope data. Theoretically, DBP as a percentage of the gross vehicle weight should be equal to the maximum negotiable slope. Appendix B treats this in some detail.

Figures 6 and 7 are graphs of the two performance variables shown plotted against each other for the 50K and 10K RTFLT tests. Perfect agreement of the data is represented by a line passing through the origin and having a slope of unity. Better correlation can be seen to exist for the 50K RTFLT than for the 10K RTFLT.

- No Adjustment for CI Variations
- × Adjustment made for CI Variations

NOTE: 0-9' CI for DBP assumed to be 114
 No 2% difference in DBP & S max was assumed

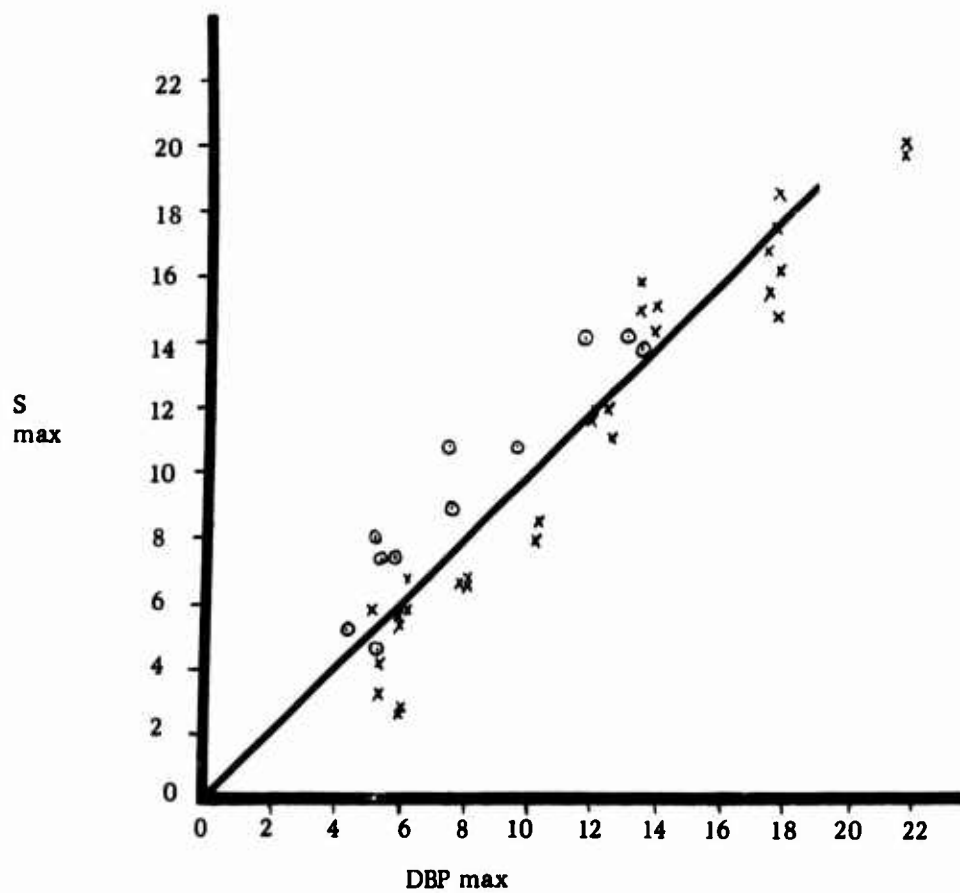


Fig. 6. Drawbar pull-maximum slope correlation for the 50K RTFLT.

- No Adjustment for CI Variations
- × Adjustment made for CI Variations

NOTE: 0-9" CI for DBP assumed to be 114
 No 2% difference in DBP & S_{max} was assumed

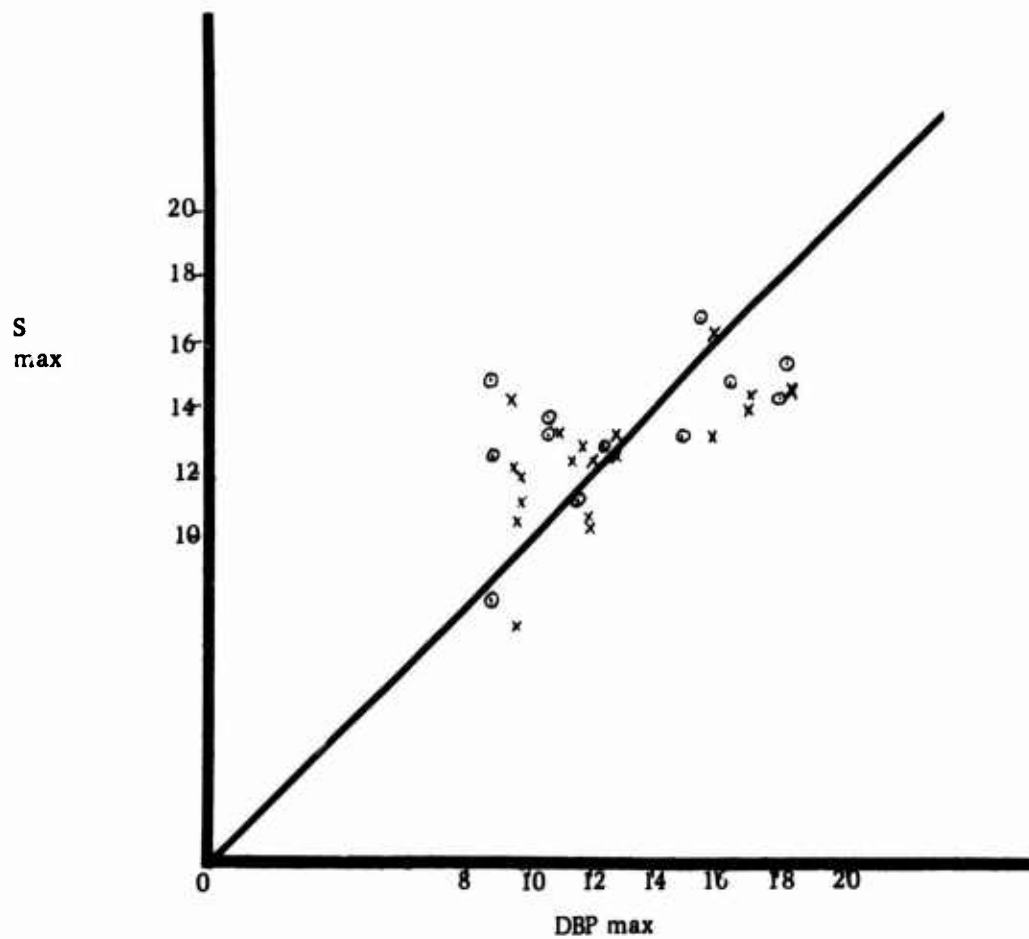


Fig. 7. Drawbar pull-maximum slope correlation for the 10K RTFLT.

This can be attributed, at least in part, to the sequence of testing. The 10K RTFLT was tested first, and it is felt that test procedures, particularly drawbar pulls, were more refined during the 50K RTFLT tests.

Statistical calculations were performed to indicate quantitative confidence levels of the data. The correlation coefficient for the 50K RTFLT was computed to be 0.92 for CI values averaged over the 0- to 9-inch depth range. The 0- to 12-inch range coefficient was 0.85 which suggests that soil strengths below the 9-inch level need not be considered. Correlation coefficients for the 10K RTFLT were determined to be 0.60 and 0.62 for the 0- to 6-inch and 0- to 9-inch ranges respectively. This scatter is due in part to the lack of homogeneity of the beach strength which is discussed further in Section IV.

b. **Tire Inflation Effects.** The next relationship of interest is the variation of performance with changes in average tire pressure. Figure 8 is a plot of an average performance quantity versus average tire inflation. This performance parameter is a weighted average of maximum negotiable slope and drawbar pull. Slope performance was weighted twice that of the DBP for three basic reasons. First, the soil strengths on the dune slopes were monitored much more closely than in the test lane. It was not possible to locate the position of maximum DBP on the test lane as accurately as the stall position on the slope. Consequently, the CI data on the slope should be more representative of operating conditions than the test lane soil strength data. Second, the dune slope data may be more reliable than DBP measurements because dune performance could be reproduced with a greater degree of accuracy. Third, a slope test is simpler in nature and does not require sophisticated support equipment nor instrumentation devices which can introduce additional errors.

A linear relationship was assumed to exist between performance and average tire inflation as in the CIMM. The slope of this relation was obtained by a least squares analysis and a group averaging technique. Results were nearly identical. However, there was a difference in the slopes of the curves for the 10K and 50K RTFLT. The values for the 10K and 50K RTFLT are minus 0.17 and minus 0.23 respectively as compared to minus 0.6 in the CIMM.

A series of tests was performed for the purpose of investigating the effects of differences in front and rear tire inflation pressures. A set of data was gathered for both the 10K and 50K RTFLT. Front and rear inflations were varied through a range with each axle taking on three discreet values. For these tests, a payload was selected for each truck such that both front and rear axles were carrying the same load.

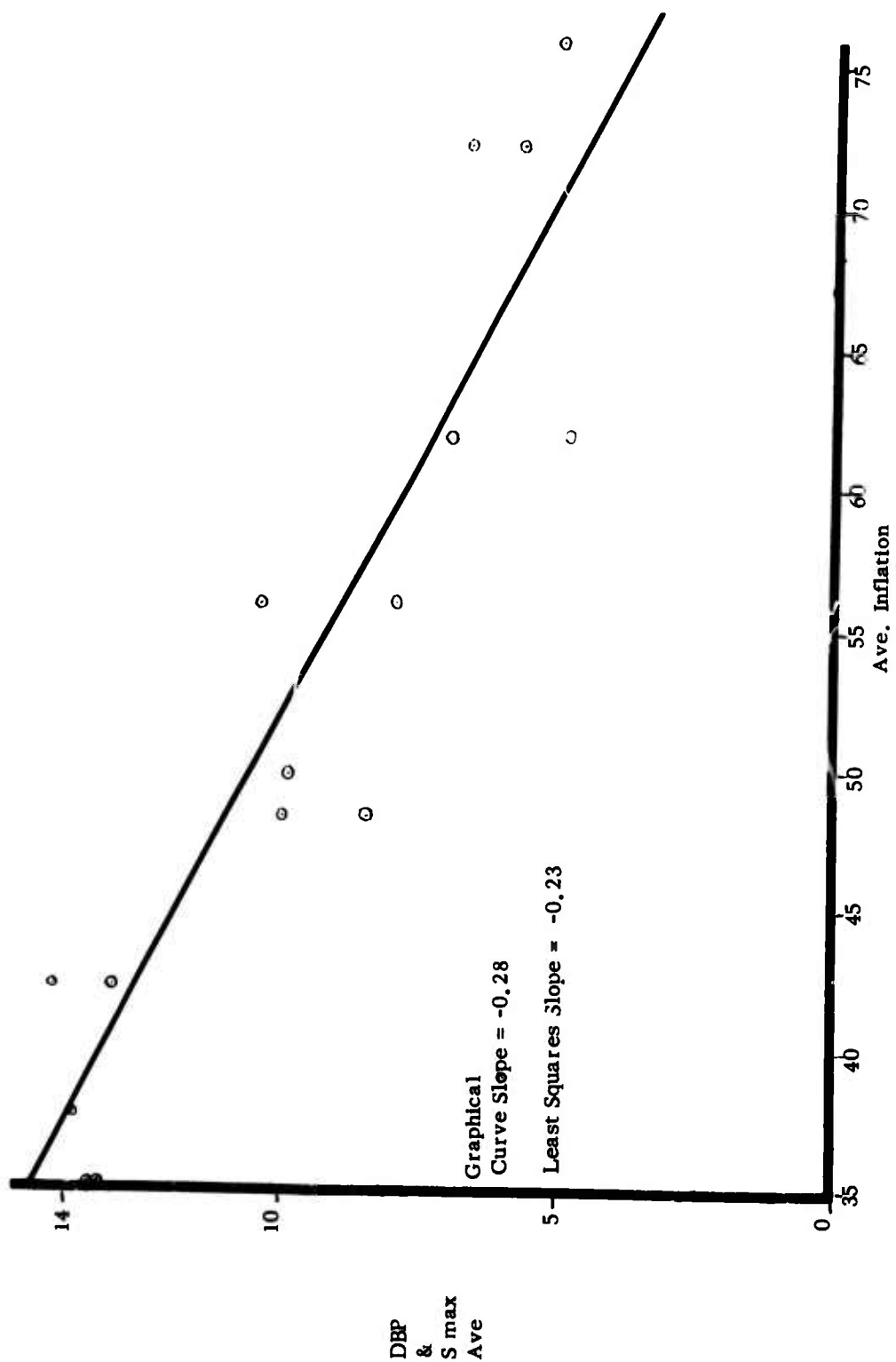


Fig. 8. Performance variation with average tire inflation for the 50K RTFLT.

It was necessary to make a basic mathematical assumption regarding the relationship between performance and inflation difference in order to arrive at an appropriate adjustment term for inflation difference effects. The simplest imaginable relation would be that the change in performance is proportional to the inflation difference:

$$\Delta \text{DBP} \propto \Delta \text{TP},$$

$$\text{or} \quad \Delta \text{DBP} = K_{\text{ID}} \Delta \text{TP}. \quad (6)$$

Since the drawbar pull is nondimensional, it is convenient to normalize inflation pressure with the average inflation which gives

$$\Delta \text{DBP} = K_{\text{ID}} \frac{\Delta \text{TP}}{\text{TP}_{\text{ave}}} \quad (7)$$

Solving equation (7) for K_{ID} results in

$$K_{\text{ID}} = \frac{\Delta \text{DBP} \times \text{TP}_{\text{ave}}}{\Delta \text{TP}} \quad (8)$$

where K_{ID} is nondimensional, and all the quantities on the right-hand side are obtained from test results. For the 10K RTFLT, the inflation test cases used in calculating K_{ID} were 30F - 40R, 40F - 30R, 30F - 50R, 50F - 30R, 40F - 50R, and 50F - 40R. Each axle carried the same load. A trend was easily established and better performance was always noted when the low-inflation tire followed the high-inflation tire. This is not surprising since the first tire through the sand "encounters" a higher strength than does the following tire (soil measurements taken immediately after passage of a test truck were significantly lower than those taken before its traversal of the lane). For cases where the soft tire led, there was little tractive effort produced by the rear tires. When the soft tire followed, it was better able to negotiate the softer sand and, therefore, contributed to the machine's mobility. CI measurements were also taken in the tire ruts on the dune slopes. The strength was considerably less there than between the ruts. In some cases, readings were only about half those in the undisturbed region.

Table 1 shows a tabulation of K_{ID} values computed for the 10K RTFLT.

Table 1. 10K RTFLT, Standard Tire, Equal Axle Load

Case	K_{ID}
30F - 40R, 40F - 30R	2.8
30F - 50R, 50F - 30R	2.7
40F - 50R, 50F - 40R	2.0

Much to the puzzlement of the authors, this trend could not be seen as clearly for the 50K RTFLT. Values for K_{ID} were erratic as seen in Table 2:

Table 2. 50K RTFLT, Standard Tire, Equal Axle Load

Case	K_{ID}
50F - 62R, 62F - 50R	4.3
35F - 50R, 50F - 35R	0.3
35F - 62R, 62F - 35R	- 0.4

So, two of the three 50K RTFLT test cases indicate that front-rear inflation differences have an insignificant effect on mobility. It was felt that the trend established by the 10K RTFLT data and supported by one of the 50K RTFLT cases should not be discarded. The effect was taken into consideration in the proposed modifications discussed in Section II-3e.

c. **Axle Loading Effects.** There were two cases in the 10K RTFLT tests and one case in the 50K RTFLT tests which shed light on the effects of unequal axle loading on performance. For each of the inflation cases, runs were made with equal-axle loading, with no-load, and with full-rated load. The CIMM equation predicts a slight improvement in performance with increasing gross weight. Discussions with WES personnel have revealed that some doubt exists as to the validity of this predicted effect. This doubt was used as partial justification for an assumption necessary to permit an analysis of the effects of unequal-axle loading. No determination of unequal-axle loading effects could be made without making some assumption about the effects of gross loading. It was assumed that the observed performance variation with loading was due to unequal-axle loading and not to changes in gross weight. Also, no determination of the effects of changes in gross weight can be made without knowledge of the effects of unequal-axle loading. No tests were performed where gross vehicle weight was varied while the distribution was held constant. Consequently, the CIMM-predicted gross load effect could not be verified or refuted, and it was assumed to be inconsequential for purposes of deriving a relation for unequal-axle loading effects.

Also, no tests were performed where GVW was held constant while the distribution was varied. Measured performance variations may have been due to changes in both variables, but for lack of a creditable relation for GVW effects, it was assumed that unequal-axle loading was the predominant loading parameter. It should be understood that the term in the original CIMM equation which contains gross vehicle weight, specifically the contact area factor, was not modified. So GVW effects are still in the modified mobility prediction equation presented in Section II-3e, but were neglected in the derivation of the unequal-axle loading relation (Equation (9)).

A second assumption was made to facilitate development of an analytical expression to describe quantitatively the effects of unequal-axle loading. It was assumed that the change in performance varied directly as the difference in axle loads. Algebraically,

$$\Delta \text{DBP} \propto (\text{AL}_F - \text{AL}_R),$$

$$\text{or} \quad \Delta \text{DBP} = K_{\text{AL}} (\text{AL}_F - \text{AL}_R). \quad (9)$$

To insure nondimensionality throughout the equation, the axle loading difference is divided by the gross vehicle weight. Solving for K_{AL} results in

$$K_{\text{AL}} = \frac{\Delta \text{DBP} (\text{AL}_F - \text{AL}_R)}{\text{GVW}} \quad (10)$$

This constant was computed using the 50F - 45R and 35F - 30R cases for the 10K RTFLT and the 35F - 35R case for the 50K RTFLT. The average value for K_{AL} for these cases is 1.16.

The last proposed adjustment to the CIMM involves the constant term on the right-hand side which serves to shift the S_{max} versus CI curve in the Y-direction. Terms of this type can be viewed as "floating" constants in the sense that they raise or lower the entire curve a predetermined amount. However, in the present analysis, it was convenient to allow this quantity to vary with vehicle size so a good curve fit would exist for all of the vehicles.

This floating term was derived after all other adjustments were completed. The procedure used was to first perform calculations corresponding to the present data cases utilizing the new adjustments while keeping the CIMM floating constant intact. Then, the differences between calculated predictions and data values were averaged for the 10K RTFLT and 50K RTFLT separately. Since values for these two different size vehicles were different, a quantity was derived which varied linearly with vehicle weight between the adjustment values for the 10K RTFLT and 50K RTFLT. The algebraic relation is

$$K_{\text{FL}} = 15.5 + 0.08 \frac{\text{GVW}}{1000} \quad (11)$$

This quantity is used to replace the 43.82 or 45.82 constant in the CIMM equation (Eq (13)).

d. **Radial Tire Effects.** Radial tires improved the mobility for both the 10K and 50K RTFLT. Only a slight increase in performance was observed for the 10K RTFLT, whereas the 50K RTFLT showed substantial improvement. However, there were only two test cases for each truck where standard and radial tire performances could be compared.

For the 10K RTFLT, the usable data cases were 50F - 45R empty and with rated load. Before the 50K RTFLT analysis could be performed, it was necessary to make some adjustments for differences in axle loading since standard and radial cases did not correspond exactly in this respect. From the 62F - 35R (empty and loaded) radial cases, the performance value for 62F - 35R equal-axle loading was estimated and compared with the corresponding standard tire case. Also, from the 50F - 50R loaded radial data, the 50F - 50R equal-axle radial case was approximated and compared with standard tire results.

The average performance improvement for the 10K RTFLT was 1.2% of slope while the 50K RTFLT value was a highly significant 10.9%. A correction factor, based on gross vehicle weight, was derived for radial tire effects and introduced into the computer program, but it is not shown in the prediction formula. A linear variation between the two gross weights was again assumed and resulted in the following:

$$\begin{array}{lcl} \text{Radial Tire} \\ \text{Correction Factor} \end{array} = 0.0001072\text{GVW} - 2.017. \quad (12)$$

The correction factor is added to the results of the performance prediction formula. Equation (12) should be employed only when the standard tire ply rating is used rather than the radial tire ply rating.

e. **Mobility Model Modification.** The CIMM formula for calculation of the maximum drawbar pull or negotiable slope is:

$$\text{DBP or } S_{\max} = 28.87 \log_{10} \text{CI} + 10.1 \text{CAF} - 1.52 \text{NPW} - 0.61 \text{TP} - (43.82 \text{ or } 45.82). \quad (13)$$

If this equation is solved for CI and the slope is redefined as that on which the vehicle is operating rather than the maximum negotiable value, Equation (13) then becomes a means for calculating the vehicle cone index (VCI). Performing these algebraic manipulations on the above formula results in

$$\text{VCI} = \text{Antilog}_{10} (0.0346S - 0.35 \text{CAF} + 0.0526 \text{NPW} + 0.0211 \text{TP} + 1.587). \quad (14)$$

The VCI is now interpreted as the minimum soil strength required to ensure mobility on an incline of slope S. The conventional definition of VCI dictates that the vehicle

be on level in which case S would be identically zero in Equation (14). Equation (13) is frequently plotted as S_{\max} versus CI. The value of CI when this curve crosses the CI axis is by conventional definition the VCI. Consequently, the VCI (on level) may be obtained graphically, and solving Equation (14) may be superfluous.

Data gathered in the Little Creek tests has made possible the investigation of three of the constants in Equation (13). Earlier portions of this report were devoted to the calculation of these quantities plus two terms that were added to the CIMM formula.

In summary, the modifications consist of: (1) re-calculated coefficients for the CI and inflation pressure terms, (2) replacement of the "floating" constant with a quantity that varies with vehicle weight, (3) addition of terms which accounts for the effects of differences in front and rear tire inflations and axle loadings, and (4) a correction term to be applied when radial tires are used.

Applying these changes to Equation (13) gives:

$$\begin{aligned} \text{DBP or } S_{\max} = & 28.87 \log_{10} \text{ CI} + 10.1 \text{ CAF} - 1.52 \text{ NPW} - 0.205 \text{ TP} \\ & + \frac{2.17 (\text{TP}_F - \text{TP}_R)}{\text{TP}} + \frac{1.16 (\text{AL}_F - \text{AL}_R)}{\text{GVW}} - K_{\text{FL}} , \end{aligned} \quad (15)$$

which is the equation that is recommended for use in predicting beach mobility characteristics of large MHE vehicles. The corresponding relation for VCI is:

$$\begin{aligned} \text{VCI} = & \text{Antilog} \left(\left[-10.1 \text{ CAF} + 1.25 \text{ NPW} + 2.05 \text{ TP} - \frac{2.17 (\text{TP}_F - \text{TP}_R)}{\text{TP}} \right. \right. \\ & \left. \left. + \frac{1.16 (\text{AL}_F - \text{AL}_R)}{\text{GVW}} - K_{\text{FL}} \right] / 28.87 \right) \end{aligned} \quad (16)$$

Equation (15) does not take into account the 2% difference in DBP and S_{\max} that occurs in the CIMM formula (Equation (13)). Analysis of Figs. 6 and 7 does not suggest that any adjustment could improve DBP- S_{\max} correlation since the data points are quite evenly distributed about the perfect-agreement line.

Some mention should be made of the dimensions for Equations (13) through (16). The original CIMM relationships were derived without regard to correct dimensionality. Consequently, there occurs such mathematical anomalies as the logarithm of PSI. This shortcoming does not detract from the ability of the model to accurately predict vehicle mobility, but it does restrict the allowable units for each

term in the formulas. The required units are: DBP as percentage of GVW, S as percent, CI in PSI, areas in square inches, inflations in PSI, and loadings and weights in pounds.

The present work makes no attempt to derive a set of dimensionally homogeneous formulas but serves to refine and extend the CIMM relationships. Usually, empirical expressions which are derived by regression techniques (such as the CIMM) contain terms which are nondimensional groupings of the independent variables. This permits exponents and coefficients to be adjusted rather arbitrarily without loss of dimensional homogeneity.

Appendix C defines the computer program of the proposed mobility prediction technique.

III. DISCUSSION

4. Presentation of Results.

a. **Computer Program Calculations.** The graphs in Appendix D are the tabulated results from the computer program using the CIMM formulas. S_{\max} (maximum negotiable slope) was calculated in the computer program and these values were plotted versus the corresponding values of the CI. Values of S_{\max} can range from -30 to +50, and values of CI can range from 0 to 500. The tire pressures are given as (front)/(rear). The graphs for the 10K RTFLT radial tire pressures are given as (front)/(rear)/(average).

For the cases using standard tires, two formulas were graphed. One is the CIMM formula which does not account for different front and rear tire inflation pressures: i.e., the average tire pressure is used in the calculation of S_{\max} . These results are indicated by "OLD" after the tire pressures. The second formula plotted is the modified CIMM formula which takes into account the front tire inflation pressure and the rear tire inflation pressure. For example, if the tire pressures are 50 front and 40 rear (50/40), the plot is slightly higher than the converse case (40/50). Most graphs show plots for each case. The results from the second formula are indicated by "NEW" after the tire pressures.

Radial tires were tested on both the 10K and 50K RTFLT's. Results from the modified CIMM formula are presented for the radial tire case only.

Computer runs were made for all tire pressure combinations tested at Little Creek. The actual test data results are plotted on the corresponding graphs resulting from the computer output. Additional tire pressure combinations were run, and the results were graphed for inclusion in this report.

b. **Soil Mechanics.** Soil measurements are presented in detail or summary form as required to illustrate values used in Section II-3, Data Analysis. The information and tabulated values are outlined as follows:

(1) **Test Course Maintenance.** The repetitive processing of the test lane and slope surface resulted in conditions considered uniform within the parameters used in the data analysis.

(2) **Grade and Alignment.** Uniformity of the longitudinal and transverse grades remained good throughout the test. On the drawbar lane, as on the prepared slopes, frequent reshaping was required to eliminate the ruts caused by the action of pulling wheels. Since this operation was performed many times, some change in the slope grades occurred. As a result, it was necessary to measure the slope each time vehicle stall occurred.

(3) **Sand Data.** Abbreviated results of the tests are shown in Appendix A and are as follows:

(a) **Cone Index (Tables A1a through A1d in Appendix A-1).** The values shown were used to compare Profiles of Depth vs Cone Index for consistent trends. General classification of the beach for sustained operation would be "NO GO" for both test and support equipment vehicles.

(b) **Moisture Test (Table A7 in Appendix A-7).** The tabulations show the moisture range encountered during the test; and, except for very short periods of inclement weather, the drawbar test lane was classified as dry to a depth of 3 inches. The prepared slopes were dry on the surface and slightly moist at increased depths.

(c) **Density (Table A7 in Appendix A-7).** The data shown was used to identify the beach and to afford comparison of the beach with the prepared slopes. Based on density, the degree of consolidation is similar. However, a comparison of CI will afford a better comparison of shearing resistance.

(d) **Grain Size Analysis (Table A8 in Appendix A-8).** The grain size data provides another means of determining the uniformity of the test areas and also serves to identify the beach sand.

V. CONCLUSIONS AND SUBSEQUENT AREAS FOR INVESTIGATION

5. **Conclusions.** Experimental data was utilized to numerically refine the CIMM to secure an analytical method capable of predicting the performance of large MHE vehicles in sand. This was accomplished by adjusting three of the constants in the original CIMM formula and adding two additional terms. These changes stem from data analyses of the present tests and have no theoretical basis. Consequently, the coefficients and terms developed here are intermediary and should be adjusted as further tests are performed.

A rather large data scatter was observed early in the drawbar pull tests. This situation improved quickly and decisively as procedures were modified. One might expect the data scatter to increase with vehicle size because the generated drawbar pull as a percentage of its gross weight usually decreases with size. Smaller vehicles generally have lower tire inflations and pull much more relative to their weight.

Another observation should be mentioned regarding an item which was beyond the control of the experimenters. This was the nature and size of the beach. The sand strength was not completely homogeneous along the test lane and there was insufficient space to make each drawbar pull run on a virgin part of the beach. Also, some general deterioration of sections of the test lane was observed near the end of the experiments. A 500-ft extension of the lane helped remedy this situation.

Close visual observation of the tire-sand interactions on the dune slopes suggests that mobility exists only when the tire is displacing the loose surface layer and has not exceeded the surcharge. (The term "surcharge" refers to the natural phenomenon of a crust effect involving the upper few inches of sand. After a period of time, undisturbed sand develops a significant self attraction, or cohesive force.) Whether the sand failed in shear when the tire first slipped or failed in bearing due to contact pressure is not clear. It is suspected that immobility was due primarily to bearing failure since slip probably would not occur on such small slopes. Theoretically, slip occurs only when the percent slope exceeds the coefficient of friction between the tire and sand or the tangent of the angle of repose whichever is smaller. (For example, a parked vehicle would not start to slide down any of the slopes used for the tests nor would there be any sand sliding due to gravitational effects alone.) Since these values were larger than the steepest dune, bearing failure most likely preceded tire slippage (shearing failure) in all of the present tests. The cone penetrometer does not measure either pure bearing or pure shear resistance, so the foregoing conclusions cannot be supported with the soil strength data.

In Figs. 6 and 7 the data points are quite evenly distributed about the perfect-agreement line. Consequently, there seems little justification in using different equations

when predicting maximum slope and drawbar pull. If the tire-sand interaction mechanism is the same on level as on an incline, theory indicates that DBP and S_{\max} should be numerically equal. Since the data and theory agree on this point, it can be concluded that the traction mechanism giving rise to DBP and slope negotiating ability is, in fact, the same. Appendix B shows analytical details of the DBP-Maximum Slope equivalency.

6. Subsequent Areas For Investigation. Future analyses of the type performed in Section II-3 should investigate the possible dependence between so-called independent variables such as CI, inflation pressure, unequal-axle loads, and gross weight. In the original derivation of the CIMM formula, as well as in the present work, the above quantities were assumed to be completely independent of each other. In reality, this may very well not be the case. Substantial additional data would be required to gain insight into this possibility. Each independent variable would have to be held constant while varying the others through a range. If each of N variables is to have M discrete values, then M^N number of tests would have to be performed.

Two of the greatest assets of the CIMM is its mathematical simplicity and the ease with which the soil strength is described via the CI value. The CI then is one of the most, if not the most, important independent variables in the equations for maximum negotiable slope and drawbar pull. When the mobility prediction equations are used, the immediate question which comes to mind is which CI value to use. Previously, for smaller vehicles, the average of CI values at the surface, at the 3-inch depth, and at the 6-inch depth has been used. This constitutes what is referred to as the 0- to 6-inch critical layer.

Results of the present analysis suggest that a 0- to 9-inch or a 0- to 12-inch layer is more appropriate for the larger vehicles with higher inflation pressures. An alternate procedure will now be presented which, when used with the CIMM formulas, will eliminate the problem of assuming a proper critical layer.

In general, the procedure consists of adjusting the data points until they fit the prediction curve and observing the resulting CI. The depth corresponding to this CI is taken as the critical depth.

It is apparent that there are an infinite number of paths along which a data point could be adjusted to reach the curve. In Fig. 9 three linear paths present themselves as logical and they are easily defined mathematically. These paths are defined as: (1) minimum distance between data point and calculated curve, (2) vertical path (CI remaining constant), and (3) horizontal path (DBP remaining constant). Paths (1) and (2) are judged to be not acceptable since motions in these directions incur changes in DBP. Since DBP is not the variable in question, it should remain unchanged. Consequently,

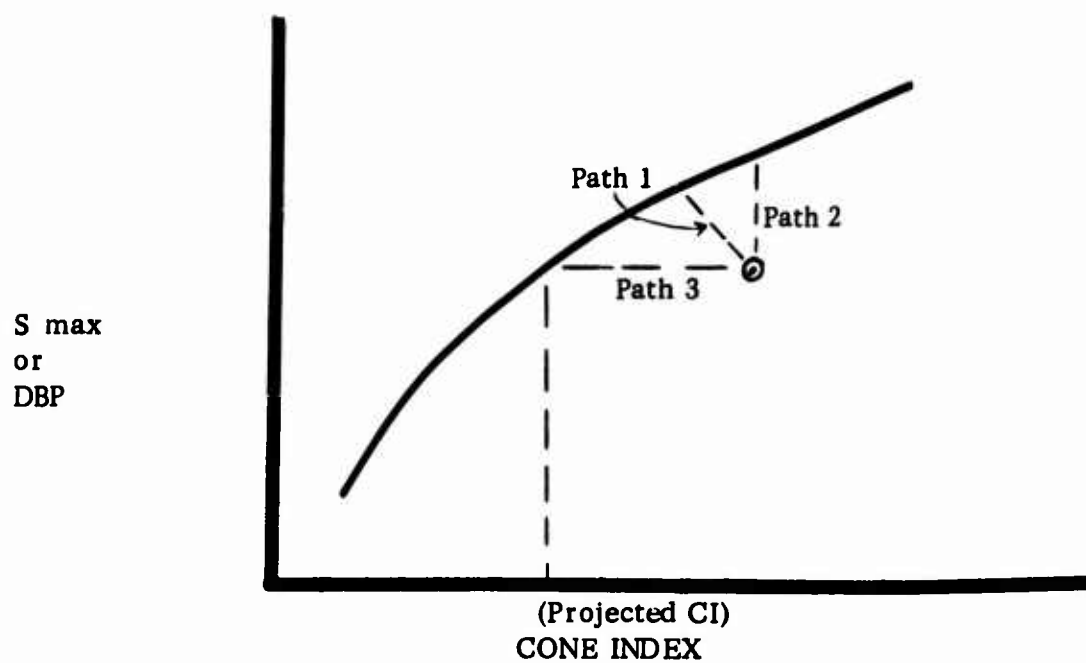


Fig. 9. Three methods for data point adjustment to reach a curve.

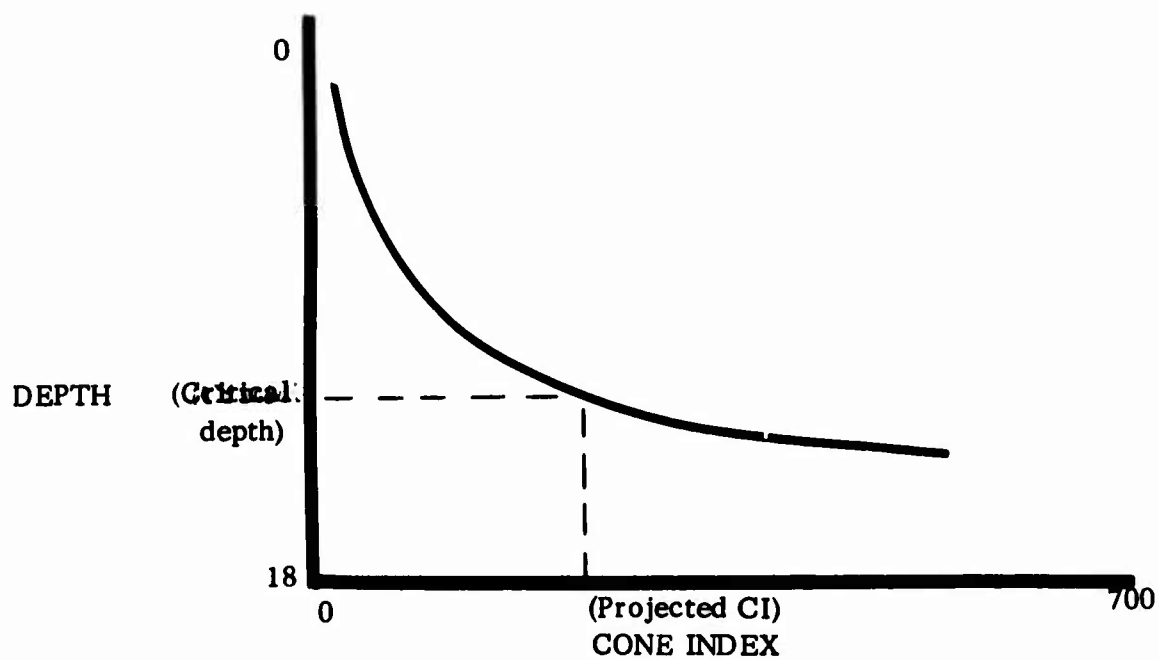


Fig. 10. Cone index profile.

Path (3) is selected which results in a change only in the cone index reading—which is the variable in question.

The cone index value of the intersection of the Path 3 projection and the computed curve is obtained for use in Fig. 10. This graph represents the cone index profile corresponding to the performance curve in Fig. 9. The depth at which the projected CI value from Fig. 9 occurs as determined in Fig. 10 is defined as the critical depth.

It should be understood that the foregoing discussion simply presents an alternate procedure to acquire a CI value for the mobility prediction equation. It is equivalent to fitting the data to the curve rather than the conventional procedure of fitting the curve to the data. Schemes like this, which might appear unorthodox, can be resorted to only because of the wide latitude one has in selecting a value for CI. Apparently, there is no convincing argument for using the critical layer average other than the fact that performance data for certain sized vehicles can be correlated well using that quantity. However, as vehicle size and tire inflation change, so does the optimum critical layer definition. The above proposed technique would eliminate the trial and error search for an optimum critical layer and would provide an explicit scheme for determining a CI value.

Observation of the present tests and analysis of the data seem to suggest that a fresh and more simplified approach to beach mobility prediction may be plausible. Future investigations should include the consideration of tire contact area as a parameter. Conceivably, a performance prediction technique could be developed in which the only independent variables would be contact pressure and soil strength. This suggestion is based on the conviction that immobility is a direct consequence of catastrophic sand bearing failure. Contact pressure (i.e. contact area and wheel loading) would reflect entirely the necessary vehicle characteristics to be considered.

The following is a proposed method for approximating vehicle motion resistance when the rut depth can be estimated. The CI reading at a particular depth is numerically equal to the force in pounds applied to the penetrometer shaft divided by the area in square inches of the cone base. Since work is defined as force times distance, then the product of average CI and rut depth should give some indication of the work done on the sand by the tire. It would be a better indication if CI values were a direct indication of the sand bearing resistance. The work performed by the towed vehicle tire on the sand is the mechanism by which motion resistance is generated. The algebraic relationship would be $\text{Work per rut area} = \text{CI}_{\text{ave}} \left(\frac{\text{lb}}{\text{in}^2} \right) \times D \text{ (in)}$. Multiplication by rut width results in $\text{Work per unit length} = \text{CI}_{\text{ave}} \times D \times \text{Wd}$. Work per length has the same dimensions as force and in this case is interpreted as the drawbar pull

motion resistance force. The equation for estimating motion resistance would then be $MR = CI_{ave} \times D \times Wd$.

In statistics, the coefficient of correlation is a calculated quantity which indicates the goodness-of-fit of a curve to data points. The square of this value is the percent of variation in the dependent variable that can be attributed to differences in the independent variables. The correlation coefficient for the mobility prediction equation in the present work (0.92 for 50K RTFLT and 0.62 for 10K RTFLT data) is less than that for the corresponding CIMM equation (0.96). This is not to say that the original CIMM is the most accurate in predicting mobility of large vehicles with high tire inflations. Quite the contrary, the CIMM has been tailored to fit the data gathered in large vehicle tests. The lower correlation coefficient resulted mainly from the relatively small number of data points under consideration and also from their scatter. As greater quantities of large-vehicle data become available, the correlation coefficient should improve and the resulting formulas may be used with a higher degree of confidence. In summary, the formulas derived in the present work are more pertinent to large-vehicle mobility predictions but are not data-correlated as well as the CIMM because of large scatter and fewer data points.

APPENDIX A

TEST DATA

- A-1. Master Analysis Sheets**
- A-2. Prepared Slope Data**
- A-3. Drawbar Pull Data**
- A-4. Motion Resistance Tests**
- A-5. Vehicle Contact Pressures**
- A-6. Drawbar Test Lane Cone Index Profile**
- A-7. Soil Moisture and Density Data**
- A-8. Grain Size Distribution**
- A-9. Drawbar Pull Test Lane Elevation Profile**
- A-10. Prepared Slope Elevation Profile**
- A-11. Vehicle and Tire Parameters**

A-1. MASTER ANALYSIS SHEETS

The master analysis sheets (Tables A1a through A1d) are a compilation of the data obtained and were used in the calculations to modify the Conc Index Mobility Model.

Shown are slope CI averages, % slope (S_{\max}) where stall occurred, drawbar pull (DBP), and drawbar lane CI values. The weighted average is an average of S_{\max} adj and DBP giving twice the weight of DBP: $\left(\frac{2 \times (S_{\max}) + \text{DBP}}{3} \right)$. DBP is adjusted for side slope, and S_{\max} and the weighted average are adjusted to a common CI. The purpose of the weighting is discussed in the body of this report.

Table A-1a. 10 K RTFLIT Standard Tires

Inflation F - R	Date	Load Cond	Stone 0-6"	CI 0-9"	S max ave	S max Adj 0-6 0-9	DBP (%GVW)	DBP Adj	wt ave 0-6"	wt ave 0-9"	Lane 0-6"	CI 0-9"	Adj wt d ave 0-6"	Adj wt d ave 0-9"
30-30	24 Sept	Eq Ax	86.5	125	13.8	13.8	16.5	16.9	14.7	14.8	83.8	135.5	14.6	14.6
30-30	24 Sept		118.75	180.6	14.3	13.9	16.5	17.1	14.8	14.8	83.8	135.5	14.8	14.6
50-45	25 Sept		74.3	122.1	12.4	12.5	11.5	12.0	12.1	12.3	78.9	152	12.05	11.9
50-45	25 Sept		79.6	119.5	10.3	10.3	11.5	12.0	10.7	10.9			10.7	10.5
50-45	25 Sept	✓	112.1	172.8	12.8	12.3	11.5	12.4	12.0	12.2			12.0	11.8
50-45	27 Sept	No Load	72.1	109.8	10.6	10.7	11.5	11.9	11.0	11.2			11.0	10.8
50-45	27 Sept		112.1	172.8	12.8	12.3	11.5	12.4	12.0	12.2			12.0	11.8
50-45	27 Sept	✓	58.9	97.1	12.7	13	11.5	11.7	12.5	12.6			12.5	12.2
50-50	25 Sept	Eq Ax	95.2	146.5	7.3	7.1	8.8	9.6	7.6	7.7			7.6	7.3
50-50	25 Sept		100	147.2	10.5	10.5	8.8	9.6	9.7	9.9			9.7	9.5
50-50	25 Sept	✓	104.3	157.8	11.8	11.4	8.8	9.7	10.5	10.8			10.5	10.4
50-45	27 Sept	10 K	79.6	134.5	13.1	13.1	7.0	7.6	11.1	11.2			11.1	10.8
50-40	26 Sept	Eq Ax	101.2	153.0	12.3	12	10.6	11.4	11.5	11.7			11.5	11.3
40-40	26 Sept		135.8	196.9	13.3	12.3	14.9	15.9	13.2	13.5			13.2	13.1
40-30	26 Sept	✓	82.5	123.8	12.4	12.3	12.3	12.7	12.3	12.6			12.3	12.2
35-30	27 Sept	No Load					21.0	21.2						
25-30	26 Sept	Eq Ax	85	127.5	16.2	16.1	15.6	16.0	15.9	16.2			15.9	15.8
35-30	27 Sept	10 K	52.75	74.8	15.7	16.2	18.3	18.5	16.9	17.1			16.9	16.7
30-40	27 Sept	Eq Ax	66.27	123.7	14.3	14.3	5.5	9.4	12.6	12.6			12.6	12.2
30-40	27 Sept		100.8	156.3	11.2	11	8.8	9.7	10.3	10.3			10.3	9.9
30-50	27 Sept		69.1	118.4	13.3	13.4	10.6	11	12.5	12.6			12.5	12.2
40-50	27 Sept		77.9	130.3	12.1	12.1	8.7	9.5	10.9	11.1			10.9	10.7
40-50	27 Sept		55	81.5	13	13.5	8.8	9.3	11.9	12.1			11.9	11.7
50-30	28 Sept	✓	73.6	104.7	14.5	14.6	18.2	18.3	15.8	16.1	✓	✓	15.8	15.7

Table A-1b. 10 K RTFLT Radial Tires

[illegible]

Table A-1c. 50 K RTFLT Standard Tires

35

A-2. PREPARED SLOPE DATA

All vehicles were operated on prepared slopes during the tests. Each vehicle ascended progressively steeper slopes until stall occurred. At the point of vehicle stall, CI readings were taken and the percent slope was measured (Tables A2a through A2g). Though not shown, some 12-inch and all 15- and 18-inch depth penetrometer readings were taken. These were omitted because these values were not used in the analysis. Representative value ranges are shown below:

15-inch depth - 275 - 625

18-inch depth - 625 - 750

Some measurements exceeded these ranges and some overlapping occurred; however, in every case the average CI increased significantly with depth.

Table A-2a. 10 K RTFLT Standard Tires .2 Conc

Date - 1973	Press. F - R	Load Cond	SFC	Average Cone Index Readings			O-6" ave	O-9" ave	No. of Profiles	Slope No.	Slope %
28 Sept	50-30	Eq-Ax	12.5	76	132.3	198	73.6	104.7	12	1	15.3
27 Sept	35-30	10K	12.5	50.8	95	140.8	52.8	74.8	15	8	17
27 Sept	50-45	10K	27.5	67.3	144.3	299	79.7	134.5	14	1	13.7
27 Sept	50-45	No Load	17.3	62.5	143.3	265.5	74.3	122.1	15	1	13.1
27 Sept	50-45	Eq-Ax	17.3	62.5	143.3	265.5	74.3	122.1	13	1	13.6
27 Sept	30-40	Eq-Ax	27.5	91.5	168.8	305	95.4	147.8	10	9	14.8
27 Sept	30-40	Eq-Ax	23.8	77.5	201.3	322.5	100.8	156.3	10	1	11.8
27 Sept	30-50	Eq-Ax	12.5	56.3	138.8	266.3	69.1	118.4	10	1	14
27 Sept	50-45	No Load	13.8	67.5	135	222.5	72.1	43.9	10	2	11.4
25 Sept	46-46	Eq-Ax	25	94.8	194.8	310.5	104.8	156.3	12	2	10.4
25 Sept	46-46	Eq-Ax	25	105.5	222	320.3	117.5	176.5	16	1	13.2
27 Sept	40-50	Eq-Ax	16.3	62.5	155	287.5	77.9	130.3	10	1	13.2
27 Sept	50-45	No Load	11	55.1	110.8	211.8	58.9	97.1	15	1	13
26 Sept	35-30	Eq-Ax	25	68.8	161.3	255	85.1	127.5	10	8	17.3
26 Sept	40-30	Eq-Ax	25	77.5	145	247.5	82.5	123.8	10	1	12.6
26 Sept	40-40	Eq-Ax	25	128.8	253.8	380	135.8	196.9	10	1	13.9
26 Sept	50-40	Eq-Ax	25	96.3	182.5	310	101.2	153	11	1	13.1
24 Sept	30-30	Eq-Ax	30	110	216.3	366.3	118.8	180.6	10	9	14.7
24 Sept	30-30	Eq-Ax	25	86.5	148	200	86.5	125	12	8	
25 Sept	50-45	Eq-Ax	13.8	95	227.5	355	112.1	172.8	10	1	13.6
25 Sept	50-45	No Load	12.5	71.3	163.8	285	82.5	133	10	2	13.6
25 Sept	50-45	Eq-Ax	15	68.8	155	238.8	79.6	119.5	10	2	11.1
25 Sept	50-50	Eq-Ax	25	76.5	137.5	225	79.7	116	10	1	12.7
25 Sept	50-50	Eq-Ax	25	97.5	160	265	94.2	137	10	2	11.3
25 Sept	50-50	Eq-Ax	25	80	213.8	350	106.3	167.3	10	3	7.9

CMR Form 93

2. Cone

33 MAY 1963

Table A-2f. 6K RTFLT Sand Tires .2 Cone

[illegible]

36 443 82273

A-3. DRAWBAR PULL DATA

Drawbar pull (DBP) tests were performed on each vehicle (Tables A3a through A3ss). A fifth wheel was attached to the test vehicle and "pips" were recorded from this fifth wheel and also from either the right rear wheel or the drive shaft of the test vehicle. A load cell was used to measure the force generated by a holdback vehicle (see test procedure). These values were recorded on a paper recording tape.

From the tape, the number of pips over a certain time period was noted. From these values, the ground speed and the travel efficiency were calculated. The "Factor" noted on each sheet was obtained to find the rates of the fifth wheel and vehicle pips in a "no slip" condition by running the test vehicle with the fifth wheel attached on a hard, dry surface. The following equations were used:

$$\frac{(\text{\#5th wheel counts}) \times (\text{5th wheel Rolling Circumference*})}{\frac{\text{Time in seconds}}{1.467}} = \text{Ground Speed (mph)}$$

$$\frac{(\text{Factor}) \times (\text{5th wheel Count}) \times 100}{\text{Test Vehicle Count}} = \text{Travel efficiency (\%)}$$

$$100 - \text{Travel efficiency} = \text{Slip (\%)}$$

For the tests on the 20-Ton Rough Terrain Crane, the factor equation was not used to calculate travel efficiency. The equation used was:

Travel Efficiency (%) =

$$\frac{\left(\frac{\text{5th Wheel Rolling Circumference*}}{\text{Test Vehicle Wheel Rolling Circumference}} \right) \times (\text{5th Wheel Count}) \times 100}{\text{Vehicle Wheel Count}}$$

*5th Wheel Rolling Circumference used was 6.98 feet.

Drawbar pull was also shown as a percent of gross vehicle weight. This value was plotted against slip and representative graphs are shown in Figs. A3-1 and A3-2. From these graphs, the maximum DBP was obtained from the 10 to 60 percent slip range. These values were tabulated on the Master Analysis Sheets under the column heading DBP.

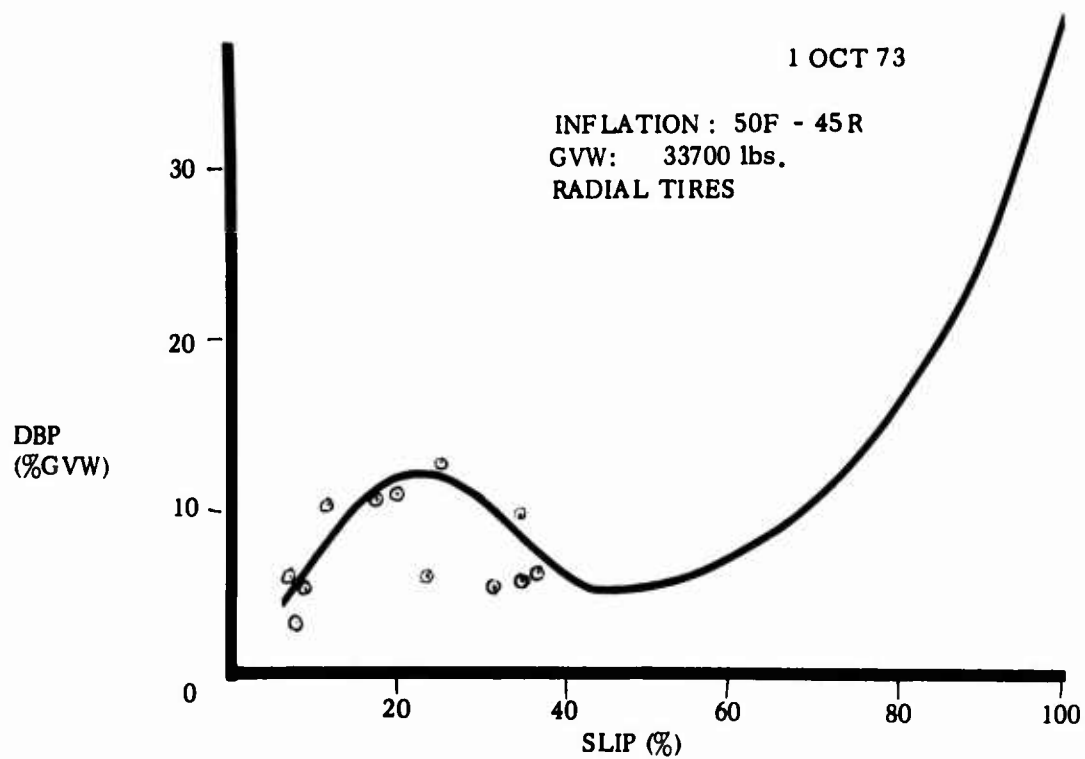
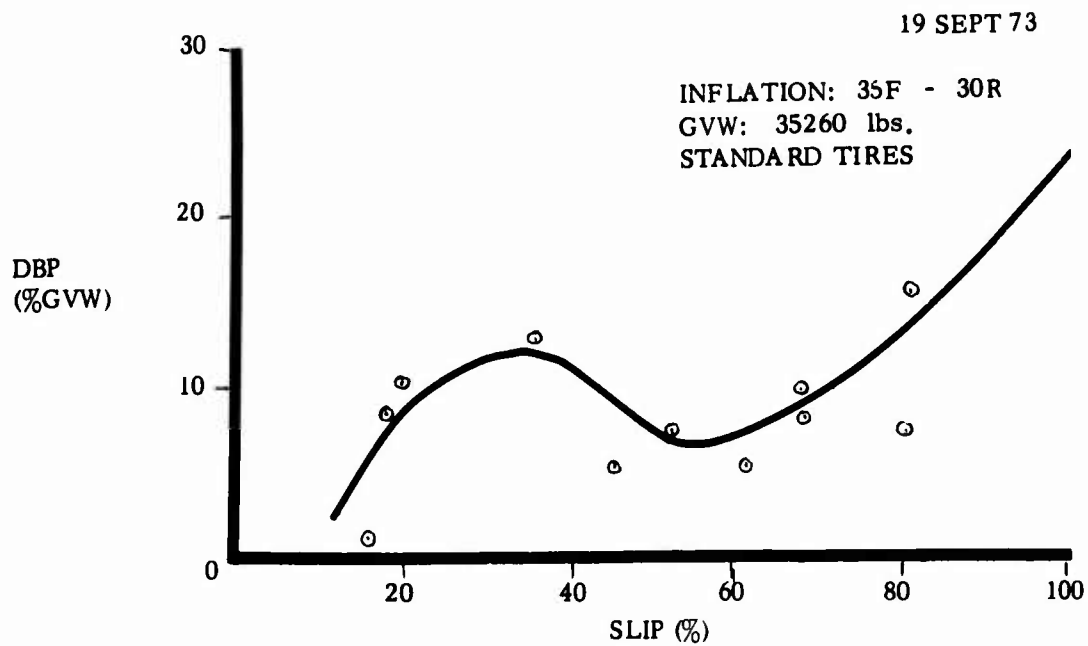


Fig. A3-1. Sample DBP - slip curve (10K RTFLT).

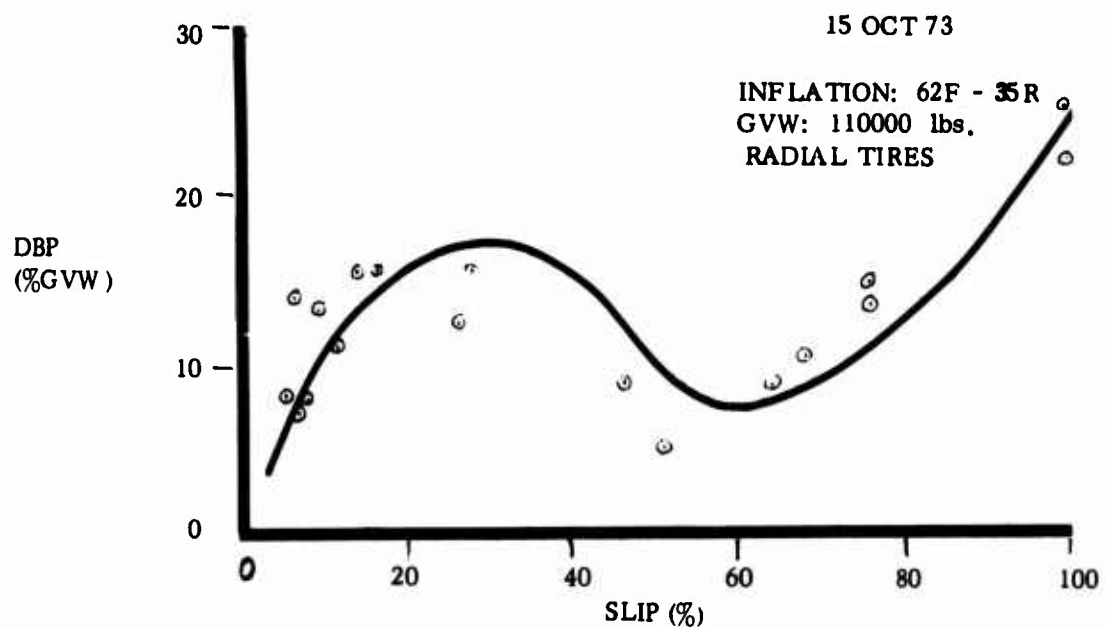
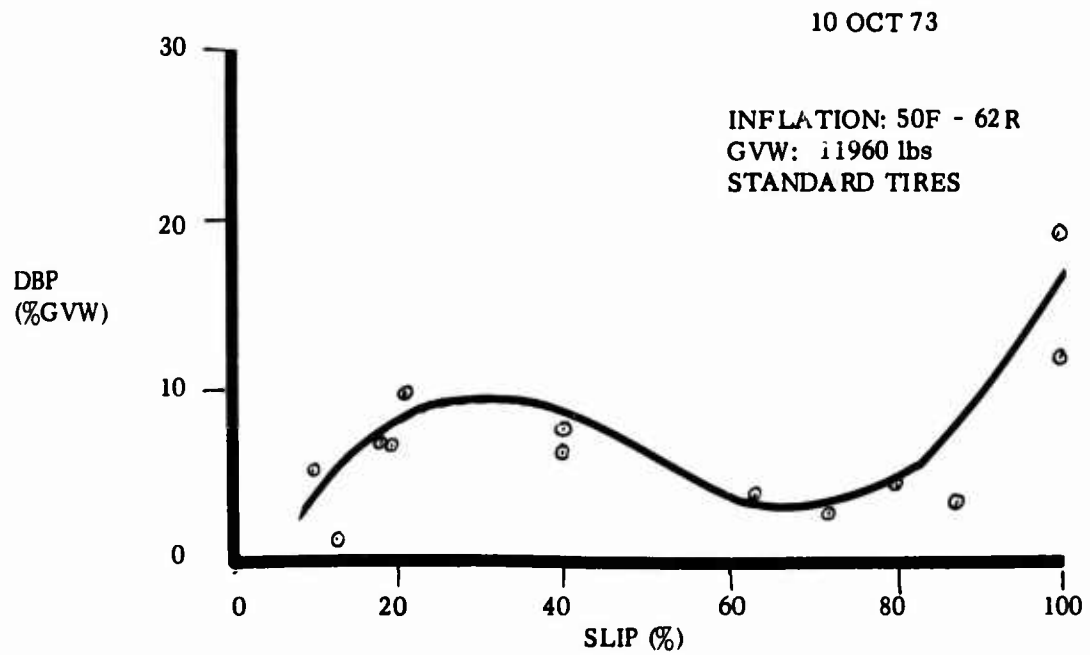


Fig. A3-2. Sample DBP - slip curve (50K RTFLT).

Date 19 Sept 1973

10K RTFLT

Table A-3a. Standard Tires

Inflation: F-20 R-15

GVW 33700

FACTOR .48

[illegible]

Date 19 Sept 1973

10K RTFLT

Table A-3b. Standard Tires

Inflation: F-20 R-15

GVW 44100

FACTOR .48

[illegible]

Sept 1973

Table A-3c. Standard Tires

Inflation: F- 30 R- 30

FACTOR .48

SMEFB Form 92

GVW 35260

FACTOR .48

[illegible]

Date 18 Sept 1973

10K RTFLT

Table A-3c. Standard Tires

Inflation: F- 30 R- 50

[illegible]

Date 18 Sept 1973

10K RTFLT

Table A-3f. Standard Tires

Inflation: F-35 R-30

GVW 33700

FACTOR .48

[illegible]

Date 19 Sept 1973

10K RTFLT

Table A-3g. Standard Tires

Inflation: F-35 R-30

GVW 35260

FACTOR .48

[illegible]

Date 18 Sept 1973

10K RTFLT

Table A-3h. Standard Tires

Inflation: F-35 R-30

GVW 44100

FACTOR .48

[illegible]

Date 20 Sept 1973

10K RTFLT

Table A-3i. Standard Tires

Inflation: F-40 R-30

GVW 35260

FACTOR .48

[illegible]

Date 20 Sept 1973

10K RTFLT

Table A-3j. Standard Tires

Inflation: F-40 R-40

GVW 35260

FACTOR .48

[illegible]

Date 14 Sept 1973

Table A-3k. Standard Tires

Inflation: F-40 R-50

10K RTFLI

GVW 35260

FACTOR .48

[illegible]

Date 18 Sept 1973

10K RTFLT

Table A-31. Standard Tires

Inflation: F-50 R-30

GVW 35260

FACTOR .48

[illegible]

Date 20 Sept 1973

10K RTFLT

Table A-3m. Standard Tires

Inflation: F-50 R-40

GVW 35260

FACTOR .48

[illegible]

Date 13 Sept 1973

10K RTFLT

Table A-3n. Standard Tires

Inflation: F-50 R-45

GVW 33700

FACTOR .48

[illegible]

Date 17 Sept 1973

10K RTFLT

Table A-3o. Standard Tires

Inflation: F-50 R-45

GVW 35260

FACTOR .48

[illegible]

Inflation: F-50 R-45

FACTOR .48

[illegible]

10K RTFLT

Inflation: F-50 R-50

GVW 35260

FACTOR .48

[illegible]

20-L

Inflation: F-45 R-25-R

GVW 33700

FACTOR 2.65

SMEFB Form 92

20-1

Inflation: F-45 R-25-R

GVW 44100

FACTOR 2.65

SMEFB Form 92

Date 1 Oct 1973

Table A-3t. Radial Tires

10K RTFLT

Inflation: F- 50 R-45

GVW 33700

FACTOR 2.65

[illegible]

Date 1 Oct 1973

10K RTFLT

Table A-3u. Radial Tires

Inflation: F-50 R-45

GVW 44100

FACTOR 2.65

[illegible]

Date 5 Oct 1973

50 K RTFLT

Table A-3w. Standard Tires

Inflation: F- 35 R- 35

[illegible]

Date 10 Oct 1973

50 K RTFLT

Table A-3x. Standard Tires

Inflation: F- 35 R- 35

[illegible]

Date 5 Oct 1973

50 K RTFLT

Table A-3y. Standard Tires

Inflation: F- 50 R- 35

GVW 119600

FACTOR 1.7

[illegible]

Inflation: F- 50 R- 62

[illegible]

50 K RTFLT

Inflation: F-62 R-35

SMEFB Form 92

Inflation: F-62 R-50

GVW 119600

FACTOR 1.7

[illegible]

Date 9 Oct 1973

50 K RTFLT

Table A-3dd. Standard Tires

Inflation: F- 62 R- 62

[illegible]

[illegible]

Date 3 Oct 1973

Table A-3ff. Standard Tires

50 K RTFLT

Inflation: F- 90 R- 55

[illegible]

Date 4 Oct 1973

50 K RTFLT

Table A-3gg. Standard Tires

Inflation: F- 90 R- 62

[illegible]

Date 17 Oct 1973

50 K RTFLT

Table A-3hh. Radial Tires

Inflation: F- 40 R- 25

[illegible]

Date 17 Oct 1973

50 K RTFLT

Table A-3ii. Radial Tires

Inflation: F- 50 R- 35

[illegible]

Date 17 Oct 1973

50 K RTFLT

Table A-3jj. Radial Tires

Inflation: F- 50 R- 50

[illegible]

Date 15 Oct 1973

50 K RTFLT

Table A-3kk. Radial Tires

Inflation: F- 62 R-35

GVW 110000

FACTOR 1.7

[illegible]

50 K RT:LT

Inflation: F- 62 R- 35

SMEFR Form 92

Date 15 Oct 1973

50 K RTFLT

Table A-3mm. Radial Tires

Inflation: F- 80 R- 35

[illegible]

Date 15 Oct 1973

50 K RTFLT

Table A-3nn. Radial Tires

Inflation: F-80 R-35

GVW 160,000

FACTOR 1.7

[illegible]

Date 11 Oct 1973

6K RTFLT

Table A-300. Standard Tires.

Inflation: F-35 R-25

GVW 29280

FACTOR 2.42

[illegible]

Date 11 Oct 1973

6K RTFLT

Table A-3pp. Standard Tires.

Inflation: F-48 R-35

GVW 29280

FACTOR 2.42

[illegible]

Date 12 Oct 1973

Table A-3qq. Sand Tires

6K RTFLT

Inflation: F-40 R-25

GVW 29280

ACTOR 2.14

[illegible]

Date 11 Sept 1973

20 Ton RT Crane

Table A-3rr. Standard Tires.

Inflation: F- 35 R- 35

[illegible]



Table A-3ss. Standard Tires

Inflation: F-55 R-55

[illegible]

A-4. MOTION RESISTANCE TESTS

For these tests, the test vehicle was towed in a pure rolling state (no power applied to driving wheels). Ground speed and resistance force were noted. The vehicles were towed back through their old tracks (OT) and also on a back-dragged (BD) or smooth beach surface (Tables A4a through A4g).

The speed check count was taken from the pips of either the 5th wheel or the test vehicle. The equation used is as follows:

$$\text{Ground Speed (mph)} = \frac{(\text{Speed Check Count}) \times K}{\frac{\text{Time in seconds}}{1.467}}$$

- K = 6.98 – 10K RTFLT (Radial Tires)
 20 Ton RT Crane
 (5th Wheel Rolling Circumference)
- 14.62 – 10K RTFLT (Standard Tires)
 (Vehicle Rolling Circumference)
- 1.035 – 50K RTFLT (Standard Tires)
- 1.04 – 50K RTFLT (Radial Tires)
 (From Vehicle "no slip" Rolling Factor (Appendix A-3))
- .712 – 6K RTFLT (Standard Tires)
- .82 – 6K RTFLT (Sand Tires)
 (From Vehicle "no slip" Rolling Factor (Appendix A-3))

Table A-4a. 10 K Rough Terrain Forklift Truck

Date	Type tire	Inflation F - R	Time (secs)	Speed Check Count	Ground Speed (mph)	Force (lbs)	GVW	Force (%) (GVW)	Remarks
13 Sept	STD	50-45	10	2	2	8750	33760	25.9	
			10	4	4	5750		17	
			10	3	2.99	9562.5		28.3	
			10	3	2.99	5000		14.8	
			10	3	2.99	7937.5		23.4	
17 Sept	STD	50-45	10	3	2.99	6875	44100	15.5	OT
			5	2	4	6000		13.6	
			5	2	4	9500		21.5	
			10	2	2	9437.5		21.3	BD
			10	2.2	2.2	9562.5		21.6	
			10	3	2.98	10250		23.1	
17 Sept	STD	50-45	10	1.9	1.89	6250	35260	17.7	BD
			10	2.46	2.45	5125		14.5	
			5	1.53	1.52	9750		27.6	
			5	.55	.55	9125		25.8	
			10	1.84	1.83	7063		20	
			10	2.89	2.88	6750		19.1	
			10	3.92	3.9	4938		14	
18 Sept	STD	50/50	10	1.39	1.38	4125	35260	11.7	OT
			10	2	1.99	5187.5		14.7	
			10	3.99	3.97	4500		12.7	
			10	3.99	3.97	4375		12.4	
			10	2.46	2.4	5000		14.2	BD
			10	3.65	3.6	6062.5		17.2	
			10	3.09	3.1	9500		26.9	
18 Sept	STD	50/50	10	8	8	4875	35260	13.8	OT
			10	8.3	8.3	3937.5		11.1	
			10	8	8	4250		12.0	
			10	8	8	4375		12.4	
			10	8	8	5000		14.1	
			10	10	10	4750		13.4	BD
			10	10	10	6625		18.7	
			10	11	11	8625		24.4	
			10	10.3	10.3	6000		17	

Table A-4a. 10 K Rough Terrain Forklift Truck (cont'd)

Date	Type tire	Inflation F - R	Time (secs)	Speed Check Coun	Ground Speed (mph)	Force (lbs)	GVW	Force (%) (GVW)	Remarks
18 Sept	STD	50-50	10	2.39	2.3	7000	35260	19.8	BD
			10	3.23	3.2	6875		19.5	
			10	3.2	3.2	9188		26	↓
			10	3.24	3.2	8125		23	OT
	↓	↓	10	3.23	3.2	7875	↓	22.3	↓
18 Sept	STD	35-30	10	1	1	7250	44100	16.4	OT
			10	1	1	5188		11.7	
			10	4	4	5750		13	
			10	2	2	5313		12	↓
			10	1	1	5125		11.6	BD
			10	1	1	5375		12.1	
			10	3	3	5625		12.7	
			10	4	4	4938		11.2	
	↓	↓	10	4	4	4500	↓	10.2	↓
18 Sept	STD	35-30	10	2	2	5375	33700	15.9	OT
			10	3	3	6250		18.5	
			10	4	4	6875		20.4	↓
			10	1	1	3625		10.7	BD
			10	3	3	3938		11.7	
			10	4	4	4688		13.9	
	↓	↓	10	4	4	5125	↓	15.2	↓
19 Sept	STD	35-30	10	4	4	4063	35260	11.5	OT
			10	4	4	3625		10.3	
			10	4	4	3250		9.2	↓
			10	1	1	3438		9.7	BD
			10	3	3	4125		11.7	
			10	7	7	3750		10.6	
	↓	↓	8	5	5	6125	↓	17.3	↓
19 Sept	STD	30-30	10	1	1	4875	35260	13.8	OT
			10	2	2	4500		12.7	
			10	3	3	4563		12.9	
			10	4	4	3625		10.3	↓
			10	2	2	5188		14.7	BD
			10	2	2	4563		12.9	
			10	3	3	4063		11.5	
	↓	↓	10	4	4	3938	↓	11.1	↓

Table 4-a. 10 K Rough Terrain Forklift Truck (cont'd)

Date	Type tire	Inflation F - P	Time (secs)	Speed Check Count	Ground Speed (mph)	Force (lbs)	GVW	Force (%) (GVW)	Remarks
19 Sept	STD	20-15	10	1	1	3125	33700	9.3	OT
			10	2	2	3250		9.6	
			10	4	4	3438		10.2	
			10	4	4	3500		10.4	↓
			10	2	2	3500		10.4	BD
			10	4	4	3500		10.4	
			10	4	4	3750		11.1	
			10	4	4	3125	↓	9.3	↓
19 Sept	STD	20-15	10	4	4	3438	44100	7.8	OT
			10	4	4	4875		11	
			10	4	4	4375		10	↓
			10	3	3	4688		10.6	BD
			10	3	3	5000		11.3	
			10	4	4	4563		10.3	
			10	5	5	4688	↓	10.6	↓
20 Sept	STD	50-40	10	2	2	6063	35260	17.2	OT
			10	4	4	6750		19.1	
			10	4	4	4938		14	
			10	3	3	6000		17	↓
			10	1	1	4688		13.3	BD
			10	1	1	5313		15	
			10	3.8	3.8	5000		14.2	
			10	7	7	5313	↓	15	↓
20 Sept	STD	40-40	10	2	2	8500	35260	24.1	BD
			10	4	4	7188		20.3	
			10	3	3	6250		17.7	↓
			10	2	2	8438		23.9	OT
			10	4	4	6250		17.7	
			10	4	4	5625	↓	15.9	↓
20 Sept	STD	40-30	10	2	2	5000	35260	14.2	OT
			10	4	4	5000		14.2	
			10	4	4	4688		13.3	↓
			10	3	3	4688		13.3	BD
			10	3	3	7063		20	
			10	4	4	5313		15	
			10	4	4	4375	↓	12.4	↓

[illegible]

Table 4-b. 10 K Rough Terrain Forklift Truck

Date	Type tire	Inflation F - R	Time (secs)	Speed Check Count	Ground Speed (mph)	Force (lbs)	GVW	Force (%) (GVW)	Remarks
1 Oct	Radial	50-45	2	2	4.75	8125	33700	24.1	OT
			5	2.8	2.66	7063		20.9	
			4	3.6	4.3	5625		16.7	
			4	3.1	3.68	9250		27.4	↓
			6	5	3.96	6563		19.4	BD
			6	5	3.96	6563		19.4	↓
	↓	↓	4	3.2	3.8	5688	↓	16.8	↓
1 Oct	Radial	50-45	6	5	3.96	6063	44100	13.7	OT
			5	4	3.8	6563		14.8	↓
			4	3	3.56	5000		11.3	↓
			5	4	3.8	5438		12.3	BD
			6	5	3.96	5813		13.1	↓
	↓	↓	5	4	3.8	5875	↓	13.3	↓
1 Oct	Radial	45-25 ^{20L} _R	5	4	3.8	8563	44100	19.6	OT
			5	4	3.8	5813		13.1	↓
			7	6	4.1	5313		12	↓
			5	4	3.8	4813		10.9	BD
			6	5	3.96	4813		10.9	↓
	↓	↓	6	5	3.96	4250	↓	9.6	↓
2 Oct	Radial	45-25 ^{20L} _R	5	4.2	3.99	4250	33700	12.6	OT
			5	4	3.8	4313		12.8	↓
			5	4	3.8	3750		11.1	BD
			6	5	3.96	4063		12	↓
	↓	↓	6	5	3.96	3438	↓	10.2	↓

Table 4-c. 50 K Rough Terrain Forklift Truck

Date	Type tire	Inflation F - R	Time (secs)	Speed Check Count	Ground Speed (mph)	Force (lbs)	GVW	Force (%) (GVW)	Remarks
3 Oct	STD	90-55	10	14.5	1.02	18500	110000	16.7	OT
			10	24.6	1.74	15700		14.1	
			7	17.3	1.74	16400		14.8	
			10	19	1.34	21000		18.9	BD
			10	24.2	1.71	16700		15	
			10	24.5	1.73	16400		14.8	
3 Oct	STD	90-55	4	2.04	.36	29000	160000	18	OT
			2	4	1.41	20500		12.7	
			3	7.15	1.68	18700		11.6	
			4	4.58	.81	22200		13.8	BD
			6	12	1.44	23200		14.4	
4 Oct	STD	96-62	10	9.1	.64	19600	119600	16.3	OT
			10	16.5	1.16	23800		19.8	
			5	11	1.55	21000		17.4	
			5	4.7	.66	21500		17.8	BD
			10	19.2	1.36	25000		20.8	
			5	10	1.41	26000		21.6	
5 Oct	STD	35-35	5	7.6	1.07	19500	119600	16.2	OT
			4	10.5	1.85	12700		10.5	
			4	11	1.94	11000		9.1	
			7	18	1.82	16000		13.3	BD
			5	13.5	1.91	13000		10.8	
5 Oct	STD	62-35	4	6.6	1.16	23700	119600	19.7	OT
			10	16.8	1.19	26000		21.6	
			10	22.7	1.6	20800		17.3	
			4	5.8	1.02	14700		12.2	BD
			10	19	1.34	16300		13.5	
			5	12	1.76	17000		14.1	
5 Oct	STD	50-35	4	5	.88	19000	119600	15.8	OT
			10	21.9	1.55	19300		16	
			10	26.4	1.86	15500		12.9	
			5	7.5	1.06	13000		10.8	BD
			10	27	1.91	12800		10.6	
			10	26	1.84	14500		12.0	

Table 4-c. 50 K Rough Terrain Forklift Truck (cont'd)

[illegible]

Table A-4d. 50 K Rough Terrain Forklift Truck[illegible]

Table A-4c. 6 k Rough Terrain Forklift Truck[illegible]

Table A-4f. 20 Ton Rough Terrain Crane

Date	Type tire	Inflation F R	Time (secs)	Speed Check Count	Ground Speed (mph)	Force (lbs)	GVW	Force (%) (GVW)	Remarks
10 Sept	STD	55-55	20	3	.713	9500	64260	14.7	Undisturbed
			10	2	.95	9875		15.3	
			10	1	.475	7937.5		12.3	
			10	2	.95	8750		13.6	
			10	2	.95	18875		29.3	OT
			10	1	.475	18000		27.9	
			10	1	.475	17625		27.3	
			10	2	.95	17062.5		26.4	
			10	1	.475	8500		13.2	
			10	1	.475	11875		18.4	
			10	2	.95	13250		20.5	
			10	2	.95	13562.5		21	
			10	1	.475	11875		18.4	
			10	2	.95	9687.5		15	
			10	2	.95	9562.5		14.8	
			10	2	.95	10375		16.1	
			10	2	.95	8812.5		13.7	
12 Sept	STD	35-35	10	2	.95	9250	64260	14.3	OT
			10	4	1.9	9000		14	
			10	4	1.9	9562.5		14.8	
			10	4	1.9	6375		10	
			10	4	1.9	5375		8.3	
			10	4	1.9	6875		10.7	
			10	4	1.9	6375		10	
			10	4	1.9	6437.5		10	

Table A-4g. CAT D7E Tracked Vehicle[illegible]

A-5. VEHICLE CONTACT PRESSURES

The tire contact areas were taken by rolling the tires onto a large sheet of paper mounted on a firm, dry, level surface. A string was pulled tight around the tire to paper interface, and paint was sprayed around the contact region of the tire. The area within the string was measured and represents the overall tire contact area on a hard, level surface.

These areas were then used with the various axle loadings to give the ground contact pressures listed (Table A-5).

Table A-5. Vehicle Contact Pressure

Vehicle	Load Cond	Tire Press. P - R	Right Front Area	Left Front Area	Right Rear Area	Left Rear Area	GW	Front Axle Load	Rear Axle Load	Front Contact Press	Rear Contact Press	Ave Contact Press	Tire Type
6K RTFLT	6K	40-25	224	284	177	167	29280	20260	9020	39.8	26.2	33	Sand
"	No Load	35-25	147	187	241	245	23000	9820	13180	29.4	27.1	28	STD
"	6K	45-35	223	272	142	167	29280	20260	9020	40.9	29.1	35	Sand
"	6K	35-25	270	277	197	193	29280	20260	9020	37	23	30	STD
"	No Load	45-35	136	156	202	202	23000	9820	13180	33.6	32.6	33.1	STD
"	6K	45-35	230	242	172	160	29280	20260	9020	42.9	27.1	35	STD
10K RTFLT	No Load	50-45	172	203	233	200	33760	15320	18440	40.8	42.6	41.6	STD
"	Eq AX	30-30	273	258	277	290	35260	17630	17630	33.2	31.1	32.1	STD
"	No Load	35-30	231	246	308	312	33700	15320	18440	32.1	29.7	30.9	STD
"	10K	20-15	678	585	264	283	44100	32580	11520	25.8	21.1	23.4	STD
"	Eq AX	35-30	259	268	261	283	35260	17630	17630	33.5	32.4	32.9	STD
"	No Load	20-15	277	340	411	416	33700	15320	18440	24.8	22.3	23.5	STD
"	Eq AX	50-45	185	232	207	226	35260	17630	17630	42.2	40.7	41.5	STD
"	10K	35-35	426	419	191	184	44100	32580	11520	38.6	30.7	34.7	STD
"	Eq AX	40-40	236	253	230	234	35260	17630	17630	36.1	37.9	37	STD
"	Eq AX	50-50	206	237	216	190	35260	17630	17630	39.8	43.4	41.6	STD
"	10K	50-45	320	349	141	144	44100	32580	11520	48.7	40.4	44.6	STD
"	No Load	45-25L	223	226	358	342	35260	17630	17630	39.3	25.2	32.2	Radial
"	10K	45-25L	344	363	254	238	44100	32580	11520	46.1	23.4	34.8	Radial
"	Eq AX	40-30	236	253	261	283	35260	17630	17630	36.1	32.4	34.3	STD
"	Eq AX	30-40	273	258	230	234	35260	17630	17630	33.2	37.9	35.6	STD
"	Eq AX	30-50	273	258	216	190	35260	17630	17630	33.2	43.4	38.3	STD
"	Eq AX	40-50	236	253	216	190	35260	17630	17630	36.1	43.4	39.8	STD
"	Eq AX	50-30	206	237	277	290	35260	17630	17630	39.7	31.1	35.4	STD

Table A-5. Vehicle Contact Pressure (cont'd)

Vehicle	Load	Tire	Right	Left	Right	Left	GVW	Front	Rear	Front	Rear	Front	Rear	Ave	Type
	C-nd	F - R	Front Area	Front Area	Rear Area	Rear Area		AXle Load	AXle Load	Contact Press.	Contact Press.	Contact Press.	Contact Press.	Contact Press.	Tire
50K RTFLT	EQ AX	62-62	472	444	458	472	119600	59800	59800	65.3	64.3	64.8	64.8	64.8	STD
"	No Load	35-35	441	437	621	576	110350	44700	65650	50.9	54.8	52.9	52.9	52.9	STD
"	EQ AX	90-55	431	429	467	456	119600	59800	59800	69.5	64.8	67.1	67.1	67.1	STD
"	No Load	40-25	600	559	967	918	110350	44700	65650	38.6	34.8	36.7	36.7	36.7	Radial
"	No Load	62-35	498	421	805	813	110350	44700	65650	48.6	40.6	44.6	44.6	44.6	Radial
"	50K	62-35	986	899	466	465	160400	133000	27400	70.6	29.4	50	50	50	Radial
"	No Load	90-55	377	358	498	475	110350	44700	65650	60.8	67.5	64.1	64.1	64.1	STD
"	EQ AX	50-50	478	473	491	494	119600	59800	59800	62.9	60.7	61.8	61.8	61.8	STD
"	No Load	50-50	533	473	680	698	110350	44700	65650	44.4	47.6	46	46	46	Radial
"	EQ AX	35-35	564	527	530	532	119600	59800	59800	54.8	56.3	55.6	55.6	55.6	STD
"	50K	35-35	956	995	363	296	160400	133000	27400	68.1	41.6	55.3	55.3	55.3	STD
"	50K	50-50	1074	1018	390	386	160400	133000	27400	63.6	35.3	49.5	49.5	49.5	Radial
"	50K	80-35	877	835	466	465	160400	133000	27400	77.7	29.4	53.6	53.6	53.6	Radial
"	50K	40-25	1100	1199	527	505	160400	133000	27400	57.9	26.6	42.2	42.2	42.2	Radial
"	50K	90-55	736	681	247	250	160400	133000	27400	93.9	55.1	74.5	74.5	74.5	STD
"	No Load	80-35	408	385	805	813	110350	44700	65650	56.4	40.6	48.5	48.5	48.5	Radial
"	EQ AX	90-62	431	429	458	472	119600	59800	59800	69.5	64.3	66.9	66.9	66.9	STD
"	EQ AX	62-50	472	444	491	494	119600	59800	59800	65.3	60.7	63	63	63	STD
"	EQ AX	62-35	472	444	530	532	119600	59800	59800	65.3	56.3	60.8	60.8	60.8	STD
"	EQ AX	50-62	478	473	458	472	119600	59800	59800	62.9	64.3	63.6	63.6	63.6	STD
"	EQ AX	50-35	478	473	530	532	119600	59800	59800	62.9	56.3	59.6	59.6	59.6	STD
"	EQ AX	35-62	564	527	458	472	119600	59800	59800	54.8	64.3	59.6	59.6	59.6	STD
"	EQ AX	35-50	564	527	491	494	119600	59800	59800	54.8	60.7	57.8	57.8	57.8	STD
"	50K	50-35	1074	1018	466	465	160400	133000	27400	63.6	29.4	46.5	46.5	46.5	Radial

Table A-5. Vehicle Contact Pressure (cont'd)

[illegible]

03 Feb 1974

A-6. DRAWBAR TEST LANE CONE INDEX PROFILE

Cone Index strength readings were taken throughout the test using a standard cone penetrometer with a 0.2-in.² base. The readings are shown in terms of averages of a given number of profiles on a certain date (Tables A6a through A6d).

The beach strength is shown in graphical form in Fig. A6 for both the earliest and latest CI profiles. The 30 August data covers just the first 500 ft of the test lane, and the 16 October data covers the entire 1500-ft course. This coincides with the portion of the test lane in use at the time the profiles were taken.

Samples of the individual profiles are also shown to give some idea of the range of values. The profiles shown are denoted on the summary sheet (Table A6d) by *.

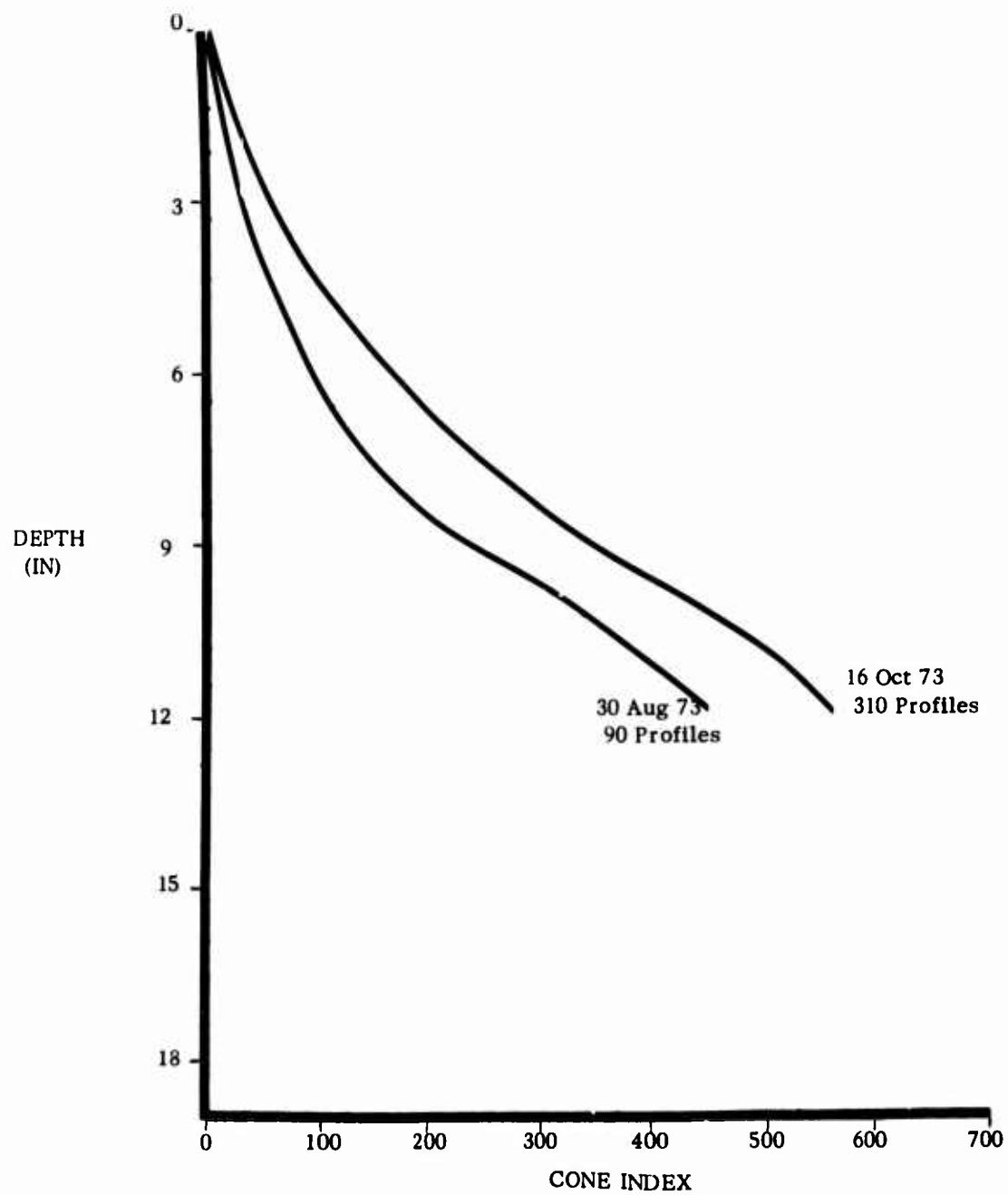


Fig. A6. Drawbar pull test lane cone index profile.

Table A-6a. Drawbar Test Lane Cone Index Profile

Date: 30 August 1973

[illegible]

Date: 20 September 1973

SMEFB Form 92

Date: 16 October 1973

Date: 16 October 1973

[illegible]

Table A-6d. Drawbar Pull Test Lane Cone Index Profiles 2 Cone

Date	Station	Average Cone Index Reading					0-6" ave	0-9" ave	0-12" ave	No. of Profiles	REMARKS
		SFC	3	6	9	12					
30 Aug *	0-5	9.7	38.1	98.1	245.4	443.6	50.7	106.8	175.4	90	Before Testing
7 Sept	0-5	7	36.8	119	271.8	497.7	56.5	111.3	183.3	78	20T RTO
10 Sept	0-8	20.3	49	111.8	205.5	361	60.4	96.6	149.5	16	20T RTO
10 Sept	5-10	16.9	53.5	123.5	229.8	423	64.6	105.9	169.3	80	20T RTO
11 Sept	0-5	22.5	53.8	125	252.8	514.5	62.1	114.1	196.1	45	20T RTO
13 Sept	0-6	29.8	67.3	148	308.8	609.4	64.6	138.5	196.1	39	10K RTFLT
17 Sept	0-6.5	13	64.3	124.5	223	519.8	69.8	116.7	196.1	42	10K RTFLT
18 Sept	0-6	16.3	61.5	124	228	498	76	136	213.7	39	10K RTFLT
19 Sept	0-6	13.5	76.5	181.8	373	634.5	90.5	151.5	243.2	39	10K RTFLT
20 Sept*	0-6	21.9	71.7	157.8	290.5	600.8	83.8	135.5	228.5	130	10K RTFLT
25 Sept	0-6.5	34.8	112.5	317.8	569.8	750	78.9	152	256.8	42	10K RTFLT
1 Oct	0-6	13.9	51.3	128.5	280.4	573.3	64.6	118.5	209.5	70	10K RTFLT
2 Oct	0-6	17.2	53.9	136	283.8	594.7	69.1	122.7	217.1	120	10K RTFLT
3 Oct	5-3	13	43.8	127.5	292.8	506.3	61.4	119.3	196.7	60	50 K RTFLT
3 Oct	0-5	13.8	45.3	106	212.5	430.9	55	94.4	161.3	110	50 K RTFLT
5 Oct	0-5	12.5	68.5	135	229.5	379.8	72	111.4	152.5	60	50 K RTFLT
12 Oct	0-5	13.8	47.3	124.5	259.3	464	61.8	111.2	181.7	55	50 K RTFLT
16 Oct *	0-4	12.6	58.3	165	325.3	538.8	78.6	140.2	220	210	End of Testing
10 Oct	10-15	20.3	67.3	159.5	326.5	534.5	82.3	143.4	221.6	45	50 K RTFLT
12 Oct	10-14	25	102	217.8	400	620.8	114.9	186.2	273.1	80	50 K RTFLT
16 Oct	10-15	14	71.5	179	362.5	588.8	88.2	166.8	243.1	100	End of Testing
16 Oct	0-15	13.3	64.9	172	343.9	563.8	83.4	148.5	231.6	310	End of Testing

A-7. SOIL MOISTURE AND DENSITY DATA

Table A7. Soil Moisture and Density Data

Station	Moisture Content (%)			Density (lb/cu ft)	Descriptive Moisture Classification	
	Surface	1 to 3 in.	6 to 9 in.	6 to 9 in.	Surface	Subsurface
A. Drawbar Lane						
0 + 00	0-1.0	0.5-1.0	1.0-3.0	91-98	Dry	Slightly Moist
1 + 00	0-1.0	0.0-0.5	1.0-3.0	90-96	Dry	Slightly Moist
2 + 00	0-1.0	0.4-1.6	1.5-3.0	87-97	Dry	Slightly Moist
3 + 00	0-1.5	0.6-2.0	1.5-3.0	88-96	Dry	Slightly Moist
4 + 00	0-1.0	1.0-3.0	1.0-3.0	87-95	Dry	Slightly Moist
5 + 00	0-1.2	1.0-2.7	1.0-4.0	82-98	Dry	Slightly Moist
10 + 00	0-0.5	1.3-1.8	3.0-4.0	98	Dry	Slightly Moist
11 + 00	0-0.5	1.1-1.7	1.0-3.0	92	Dry	Slightly Moist
12 + 00	0-0.5	1.0-2.0	1.0-3.0	95	Dry	Slightly Moist
13 + 00	0-0.5	2.0-2.4	2.5-2.9	88-97	Dry	Slightly Moist
14 + 00	0-0.5	1.0-3.0	2.0-4.0	91-98	Dry	Slightly Moist
B. Prepared Slopes						
Slope No.						
1	0-0.5	1.5-3.0	2.6-3.2	95-97	Dry	Moist
2	0-0.5	0.8-2.2	2.1-2.7	95-96	Dry	Moist
3	0-0.5	1.3-2.4	2.2-2.9	96-97	Dry	Moist
4	0-0.5	1.7-2.8	2.6-4.6	96	Dry	Moist
5	0-0.5	1.0-2.2	2.4-4.0	95-96	Dry	Moist
8	0-0.5	2.5-3.0	3.3-	-	Dry	Moist
9	0-0.5	1.5-2.7	1.9-3.1	95	Dry	Moist

A-8. GRAIN SIZE DISTRIBUTION

Table A8. Grain Size Distribution (Average Values)

Depth (in.)	Percent Fines by Weight for U. S. Standard Sieve Numbers					
	No. 10	No. 20	No. 40	No. 60	No. 100	No. 200
A. Station 0 + 00 thru 6 + 00						
1 to 3	99.7	94.3	50.0	4.8	0.4	0.2
6 to 9	99.7	94.6	52.2	5.4	0.5	0.2
B. Station 10 + 00 thru 14 + 00						
1 to 3	98.6	90.3	54.8	10.8	0.8	0.2
6 to 9	99.1	89.7	47.4	8.1	0.6	0.2

A-9. DRAWBAR PULL TEST LANE ELEVATION PROFILE

Drawbar pull test lane elevation data were taken to determine the percent of side slope present at the test site (Table A9). The data given cover a 35-foot-wide test lane, giving relative longitudinal elevations and the percent of side slope.

The area between the stations marked "Area not used for Drawbar Testing" was avoided because of excessive side slope.






The data under the heading " DBP_{adj} " on the master analysis sheets (Appendix A1) are drawbar force adjusted to side slope.

The side slope varied somewhat due to resurfacing of the test lane after each test. Resurfacing tended to decrease the side slope.

Table A-9. Drawbar Test Lane

Elevation Profile

Date: 11 Sept 1973

Station	Right Side	Center Lane 17.5	Left Side 17.5	Side Slope (%)					
0	6.3	6.1	6.6	.8					
50	6.6	6.2	6.1	1.4					
100	6.4	6.1	6	1.1					
150	6.3	6.0	6.8	1.4					
200	6.6	6.1	6.4	.6					
250	6.6	6.5	5.8	2.3					
300	6.8	6.5	5.6	3.4					
350	6.8	5.9	5.5	3.7					
400	6.9	5.6	5.2	5					
450	6.4	5.5	5.7	2					
500	6.5	5.5	4.8	4.9					
550	7.3	5.7	4.7	7.4	AREA NOT USED FOR DRAWBAR TESTING				
600	7.3	5.7	4.9	7.4					
650	7.3	5.9	5.0	6.6					
700	7.8	6.2	5.2	7.4					
750	8.0	6.5	5.1	8.3					
800	8.8	6.6	5.3	1.0					
850	8.9	6.7	4.4	12.9					
900	9.7	7.0	5.5	12					
950	9.5	6.7	5.5	11.4					
1000	7.5	5.1	5.2	6.6					
1050	7.2	6.1	5.3	5.4					
1100	5.8	5.4	5.8	0					
1150	6.1	5.6	4.1	5.7					
1200	5.7	5.3	4.8	2.6					
1250	6.0	5.7	4.9	3.1					
1300	6.4	6.2	4.2	6.3					
1350	5.2	6.1	5.5	.9					
1400	6.3	6.1	5.3	2.8					
1450	6.6	6.5	6.4	5.7					
1500	7.7	7.3	6.2	4.3					
NOTE: Right side is toward the shoreline.									

A-10. PREPARED SLOPE ELEVATION PROFILE

This section gives elevation profiles of the prepared slopes that were used in Appendix A-2. Given are coordinates going from 0 (at the bottom of the slope) to 75 ft, in intervals of 5 ft, and overall elevations (Table A-10). The average slope is calculated over the entire 75-ft length. Each slope was approximately 30-ft wide.

The slopes varied slightly due to resurfacing after each test (Section II-2). Because the top and bottom regions of the inclines tended to flatten out, the average slopes quoted here are generally less than those measured at the stall positions.

Table A-10. Prepared Slope Elevation Profile

[illegible]

Table A-10. Prepared Slope Elevation Profile (cont'd)

Slope No. 3				Slope No. 4			
	Station	Elev.	Average Slope		Station	Elev.	Average Slope
	0	3.8			0	1.7	
	5	4.1			5	3.1	
	10	4.7			10	3.7	
	15	5.0			15	4.1	
	20	5.4			20	4.5	
	25	5.7			25	4.8	
	30	6.1			30	5.2	
	35	6.6			35	5.6	
	40	7.0			40	6.1	
	45	7.4			45	6.4	
	50	7.7			50	6.7	
	55	8.2			55	7.1	
	60	8.6			60	7.4	
	65	9.1			65	7.6	
	70	9.6			70	7.9	
	75	10.0			75	8.2	
			8.3%				8.7%

Table A-10. Prepared Slope Elevation Profile (cont'd)

Slope No. 5				Slope No. 6			
	Station	Elev.	Average Slope		Station	Elev.	Average Slope
	0	3.2			0	2.6	
	5	3.3			5	2.8	
	10	3.4			10	2.9	
	15	3.6			15	3.1	
	20	3.8			20	3.3	
	25	4.0			25	3.6	
	30	4.2			30	3.7	
	35	4.5			35	3.8	
	40	4.8			40	4.0	
	45	5.1			45	4.3	
	50	5.4			50	4.6	
	55	5.6			55	4.7	
	60	5.9			60	5.0	
	65	6.2			65	5.3	
	70	6.4			70	5.6	
	75	6.7	4.7%		75	5.9	4.4%

Table A-10. Prepared Slope Elevation Profile (cont'd)

Slope No. 7				Slope No. 8			
	Station	Elev.	Average Slope		Station	Elev.	Average Slope
	0	3.5			0	3.2	
	5	3.6			5	3.6	
	10	3.7			10	4.1	
	15	4			15	4.7	
	20	4.2			20	5.2	
	25	4.5			25	5.8	
	30	3.9			30	6.4	
	35	5.15			35	7	
	40	5.4			40	7.8	
	45	6			45	8.6	
	50	6.2			50	9.6	
	55	6.3			55	10.5	
	60	6.7			60	11.4	
	65	7			70	12.2	
	70	7.4			75	13.2	
	75	7.9	5.8%				13.3%

A-11. VEHICLE AND TIRE PARAMETERS

Table A-11a. Vehicle Parameters

Vehicle	Load Cond	GVW (lb)	Front Axle Load (lb)	Rear Axle Load (lb)
50K RTFLT	Loaded	160,400	133,000	27,400
Caterpillar 824B	EQ AX	119,600	59,800	59,800
	Empty	110,350	44,700	65,650
10K RTFLT	Loaded	44,100	32,580	11,520
USA-109 69057	EQ AX	35,260	17,630	17,630
Model-A 3520-1, Serial No. -808	Empty	33,760	15,320	18,440
6K RTFLT	Loaded	29,280	20,260	9,020
Model-MLT 6-67 Serial No. LT-1-993	Empty	23,000	9,820	13,920
20T RTC USA 08B98567, Model A 134000, Serial No. 45891	Empty	64,260	32,340	31,920

Table A-11b. Tire Parameters

Vehicle	Tire	Tire Width (in.)	Rim Diameter (in.)	Ply Rating
20T RTC	Goodyear All-Weather	26.5	25	26
10K RTFLT	Goodyear Sure-Grip	20.5	25	16
10K RTFLT	Uniroyal Radial	20.5	25	12
6K RTFLT	Goodyear Sure-Grip	17.5	25	12
6K RTFLT	Goodyear R. 6-Sand Service	18	25	12
50K RTFLT	Goodyear Superhard Rock Lug	29.5	29	40
50K RTFLT	Michelin Steel Cord Radial	29.5	29	2-Star Rating

APPENDIX B

DRAWBAR PULL - MAXIMUM SLOPE EQUIVALENCY

The maximum DBP a vehicle can develop on a firm, level surface theoretically varies directly as the gross vehicle weight (Fig. B-1). The proportionality constant is defined as the static friction coefficient μ . Algebraically we have

$$\begin{aligned} \text{DBP} &\propto W \\ \text{or } \text{DBP} &= \mu W. \end{aligned} \quad (\text{B-1})$$

For a vehicle on an incline, the retarding force is the weight component which is directed down the slope (Fig. B-2). To insure a constant velocity up the slope, this force must be equal to the tractive force. Equating these forces results in

$$W \sin \theta = \mu W \cos \theta. \quad (\text{B-2})$$

For a tire operating in soft sand, the quantity μ cannot necessarily be viewed as a friction coefficient. It probably should be regarded as a sand traction factor of sorts. Nevertheless, if it is assumed that the tire-sand interaction is the same on inclines as on level, then μ is identically the same quantity in Equations (B-1) and (B-2). Eliminating μW between these equations results in

$$\begin{aligned} \text{DBP} &= W \frac{\sin \theta}{\cos \theta}, \\ \text{or } \frac{\text{DBP}}{W} &= \tan \theta = \text{slope } (\%). \end{aligned} \quad (\text{B-3})$$

Consequently, the maximum DBP (as percentage of the vehicle weight) is numerically equal to the maximum negotiable slope if the preceding assumption is valid.

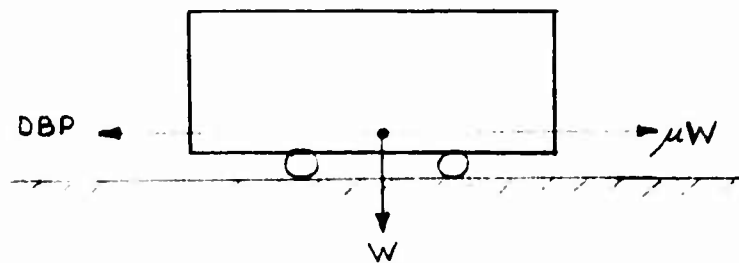


Fig. B-1. DBP - GVW Equivalency - Level Surface.

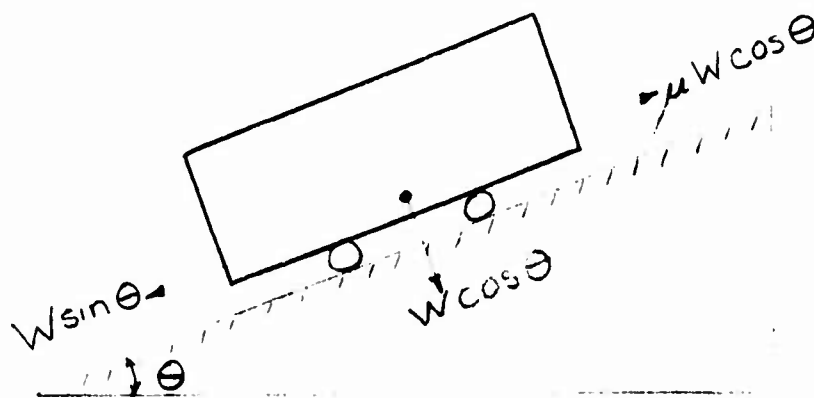


Fig. B-2. DBP - GVW Equivalency - Inclined Surface.

APPENDIX C

COMPUTER PROGRAM DESCRIPTION

This appendix contains the program listing, the input format, and an explanation of FORTRAN symbols.

A FORTRAN computer program was developed on the USAMERDC CDC 6600 machine for the analytical method proposed in Section II-3. The program computes vehicle performance quantities when vehicle characteristics and soil strength data are inputted. In particular, the input data required are tire width, rim diameter, number of powered wheels, tire ply rating, front and rear tire inflations, front and rear axle loads, and the soil CI. Computed quantities include maximum negotiable slope, S_{max} , or drawbar pull, DBP, vehicle cone index VCI, and S_{max}/DBP of a combination of prime mover and non-powered towed vehicles. The towed combination capability was obtained by curve fitting motion resistance data in the WES Report (Plate 23),³ and is not related to data gathered in the present work. The DBP was viewed as the excess towing capacity of the prime mover and was set equal to the sum of the motion resistance and down-slope weight component of the towed vehicle.

It should be pointed out that when operating this program for vehicles with gross weights in the 70,000 to 150,000 lb range, the CI input value or VCI calculation should be taken as that for the 0- to 9-inch depth average. The corresponding critical layer for smaller vehicles is 0 to 6 inches. This is a consequence of the manner in which the present data was used in deriving the adjustment terms for the CIMM. It occurred that the best DBP- S_{max} correlation was obtained for a 0- to 9-inch critical layer for the 50K RTFLT and for 0- to 6-inch layer for the 10K RTFLT. Measured CI profiles throughout the tests were generally linear in the 0- to 12-inch range with the surface value being about 5 to 10. Consequently, CI averages may be assumed to be directly proportional to the thickness of the critical layer. This approximation results in little loss of accuracy and provides a quick method to calculate CI averages for various critical layers.

³ U. S. Army Engineer Waterways Experiment Station, "Trafficability of Soils," Tech. Memo. No. 3-240, 17th Supplement, May 1973.

COMPUTER PROGRAM LISTING

PROGRAM BCH

74/74 OPT=1

FTN 4.0+P357

```

PROGRAM BCH(INPUT,OUTPUT,TAPE5=INPUT,TAPE6=OUTPUT)
INTEGER TT
S,TTIRE
5      DIMENSION TPRESS(100),CONEIN(100),GROSWT(100)
      S,X4(20),VCI(20,10),X1(20),X8(20)
      S,TPF(20),TPR(20),ALF(10),ALR(20)
      S,ADJ1(20),X5(20)
      S,
10     $X2(20,5),SLOPE(20,5,20),TOWR(20),P(20,5,20),SLOPEF(20,5,20)
C
C THIS PROGRAM COMPUTES THE VEHICLE CONE INDEX AND MAXIMUM SLOPE
C FOR LARGE WHEELED MHE VEHICLES ON SAND.
C PARAMETERS ARE INFLATION PRESSURE, GROSS VEHICLE WEIGHT, AND CONE
C INDEX
15     C
      TT=0
      WRITE(6,100)
100    FORMAT(1H1,30X,'MHE VEHICLE CHARACTERISTICS',//////)
      READ(5,35)TTIRE,TOWT
20     C
      C INPUT DATA
      C
      READ(5,25)TIREWD,RINDIA,PHRWHL,TIREPV
      READ(5,15)IMAX,JMAX,IIMAX
25     READ(5,25)(TPF(I),I=1,IMAX)
      READ(5,25)(TPR(I),I=1,IMAX)
      READ(5,25)(TPRESS(I),I=1,IMAX)
      READ(5,25)(CONEIN(J),J=1,JMAX)
      READ(5,25)(ALF(II),II=1,IIMAX)
30     READ(5,25)(ALR(II),II=1,IIMAX)
      READ(5,25)(GROSWT(II),II=1,IIMAX)
15     FORMAT(3I2)
25     FORMAT(8F10.2)
35     FORMAT(I2,8X,F10.2)
35     C
      C MAXIMUM SLOPE CALCULATION
      C
      DO 58 J=1,JMAX
      X1(J)=ALOG10(CONEIN(J))
40     58 CONTINUE
      IF(TT)67,67,68
      67 TTFAC=5.
      GO TO 69
      68 TTFAC=2.
45     69 XA=TTFAC*TIREWD+RINDIA
      DO 71 I=1,IMAX
      X8(I)=.607*TPRESS(I)+1.35*117.*TIREPV/XA-4.93
      X4(I)=TPRESS(I)
      DO 71 II=1,IIMAX
50     X2(I,II)=ALOG10(GROSWT(II)/X8(I))
      ADJ1(II)=-0.139*GROSWT(II)/1000.-8.93
      X5(II)=44.82-ADJ1(II)
71     CONTINUE
      X3=PHRWHL
55     DO 73 I=1,IMAX
      DO 73 II=1,IIMAX
      DO 73 J=1,JMAX

```

```

        SLOPE(I,II,J)=28.9*X1(J)+10.18*X2(I,II)
        S=-1.52*X3-.205*X4(I)-X5(II)
60      SLOPE(I,II,J)=SLOPE(I,II,J)+2.17*(TPF(I)
        S-TPR(I))/TPRESS(I)
        S+1.16*(ALF(II)-ALR(II))/GROSHT(II)
        IF(TTIRE) 81,81,80
        80 SLOPE(I,II,J)=SLOPE(I,II,J)+1.072E-4*GROSHT(II)-2.017
65      81 CONTINUE
      C TOWED COMBINATION
        TOWR(J)=207.44*CONEIN(J)*(-.6546)
        TOWR(J)=TOWR(J)/100.*TOWT
        P(I,II,J)=TOWT*SIN(ATAN(SLOPE(I,II,J)/100.))
70      SLOPEF(I,II,J)=SLOPE(I,II,J)-(TOWR(J)/GROSHT(II)+P(I,II,J)/
        S*GROSHT(II))*100.
        73 CONTINUE
      C
      C VEHICLE CONE INDEX CALCULATION
75      C
        DO 711 I=1,IMAX
        DO 711 II=1,IIMAX
        VCI(I,II)=10.0*((-10.1*X2(I,II)+1.52*X3
        S+.205*X4(I)+X5(II)
80      S-2.17*(TPF(I)-TPR(I))/TPRESS(I)
        S-1.16*(ALF(II)-ALR(II))/GROSHT(II))/28.9)
        711 CONTINUE
      C
      C OUTPUT
85      C
        WRITE(6,99)TIREWD,RINDIA,PWRWHL,TIREPY
        99 FORMAT(10X,*TIRE WIDTH =*,F5.1,10X,*RIM CIA =*,F5.1,10X,
        S*NO. PWR WHL = *,F4.0,10X,
        S*TIRE PLY = *,F4.0,/)
90      WRITE(6,175)
        175 FORMAT(17X,*PARAMETERS*,41X,*CALCULATIONS*,/)
        WRITE(6,200)
        200 FORMAT(1X,9HGROSS WT.,13X,10HTIRE PRESS,5X,10HCONE INDEX,
        S8X,3HVC I,8X,9HMAX SLOPE,13X,17HMAX SLOPE (TOWED))
95      WRITE(6,201)
        201 FORMAT(23X,1HF,4X,1HR,2X,3HAVE)
        DO 250 II=1,IIMAX
        WRITE(6,262)
        262 FORMAT(/)
100      DO 250 I=1,IMAX
        WRITE(6,261)
        261 FORMAT(/)
        DO 250 J=1,JMAX
        WRITE(6,300)GROSHT(II),TPF(I),TPR(I),TPRESS(I),CONEIN(J),
105      S*VCI(I,II),SLOPE(I,II,J)
        S,
        SSLOPEF(I,II,J)
        300 FORMAT(2X,F7.0,13X,3F4.0,6X,F4.0,11X,F4.0,8X,F7.2,10X,F7.2)
        250 CONTINUE
110      STOP
        END

```

INPUT FORMAT

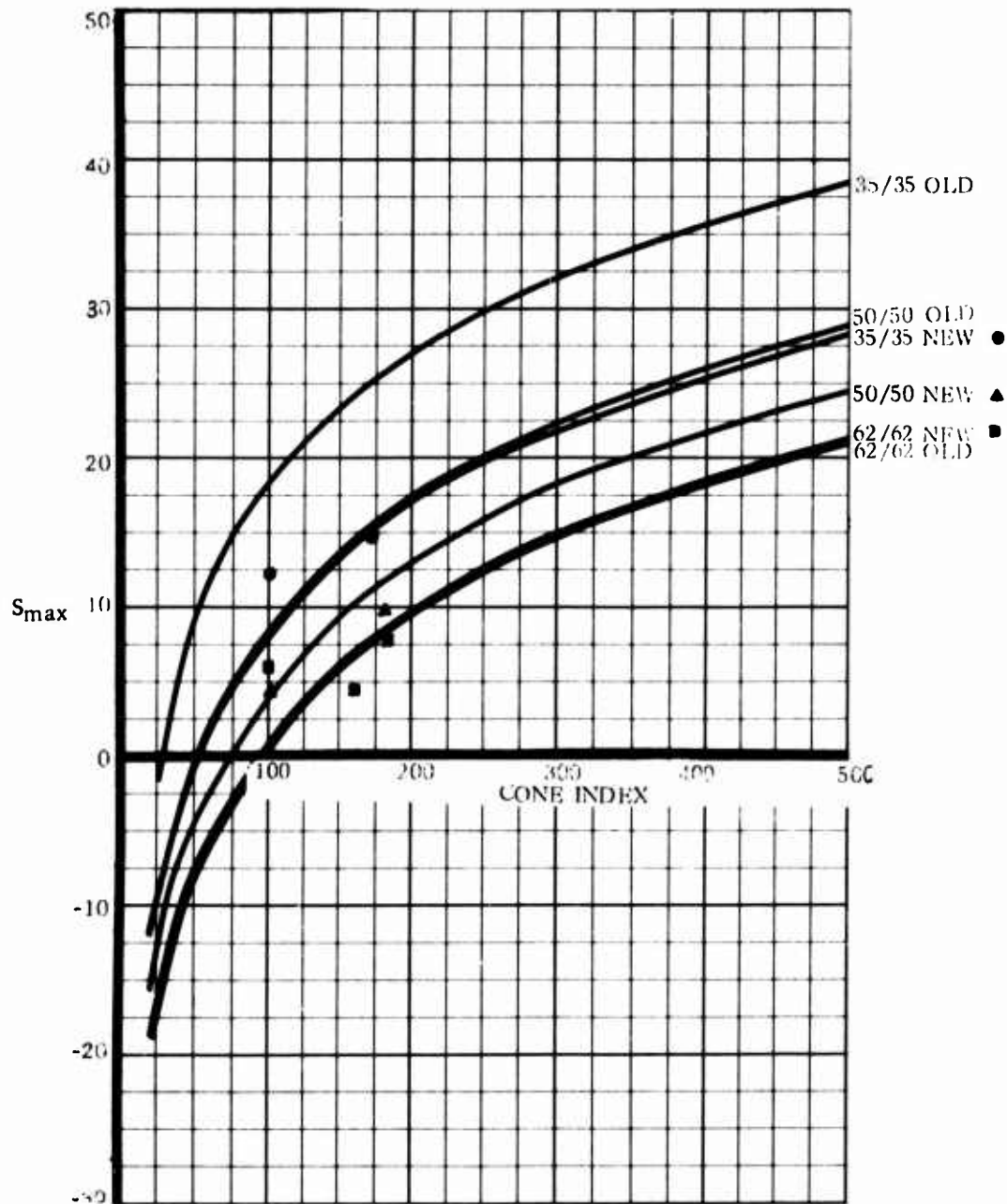
Input Card No.	Col. Nos.	Definitions
1	1-2	01—if Standard Tires, 02—if Radial Tires
1	11-20	Wt. of towed vehicle
2	1-10	Tire width-in.
2	11-20	Rim dia.-in.
2	21-30	No. of powered wheels
2	31-40	Tire ply rating
3	1-2	No. of inflation cases
3	3-4	No. of cone index cases
3	5-6	No. of axle loading cases
4	1-10, 11-20, ...71-80	Front tire inflation values
5	1-10, 11-20, ...71-80	Rear tire inflation values
6	1-10, 11-20, ...71-80	Ave. tire inflation values
7	1-10, 11-20, ...71-80	Cone index values
8	1-10, 11-20, ...71-80	Front axle load values
9	1-10, 11-20, ...71-80	Rear axle load values
10	1-10, 11-20, ...71-80	Gross veh. wt. values

FORTRAN SYMBOLS

<u>FORTRAN</u>	<u>DEFINITION</u>
ADJ1	Gross wt adjustment to floating constant
ALF	Front axle load-lbs.
ALR	Rear axle load-lbs.
CONEIN	Cone index
GROSWT	Gross vehicle weight
I	Index for tire inflation cases
II	Index for axle loading cases
I MAX	No. tire inflation cases
II MAX	No. axle load cases
J	Index for cone index cases
JMAX	No. cone index cases
P	Down-slope component of towed vehicle weight
PWRWHL	No. of powered wheels
SLOPE	Maximum negotiable slope
SLOPEF	Max. negotiable slope of towed combination
TIREPY	Tire ply rating
TIREWD	Tire section width
TOWR	Motion resistance
TOWT	Wt of towed vehicle
TPF	Front tire inflation-psi
TPR	Rear tire inflation-psi
TPRESS	Average tire inflation-psi
TT	Terra tire index
TTFAC	Constant for terra/standard tire
VCI	Vehicle cone index
XA	Intermediate quantity in contact area
XB	Contact area
X1	Soil strength term, Log_{10} of cone index
X2	Log_{10} of contact area factor
X3	Same as PWRWHL
X4	Same as TPRESS
X5	"Floating" constant in performance formula

APPENDIX D

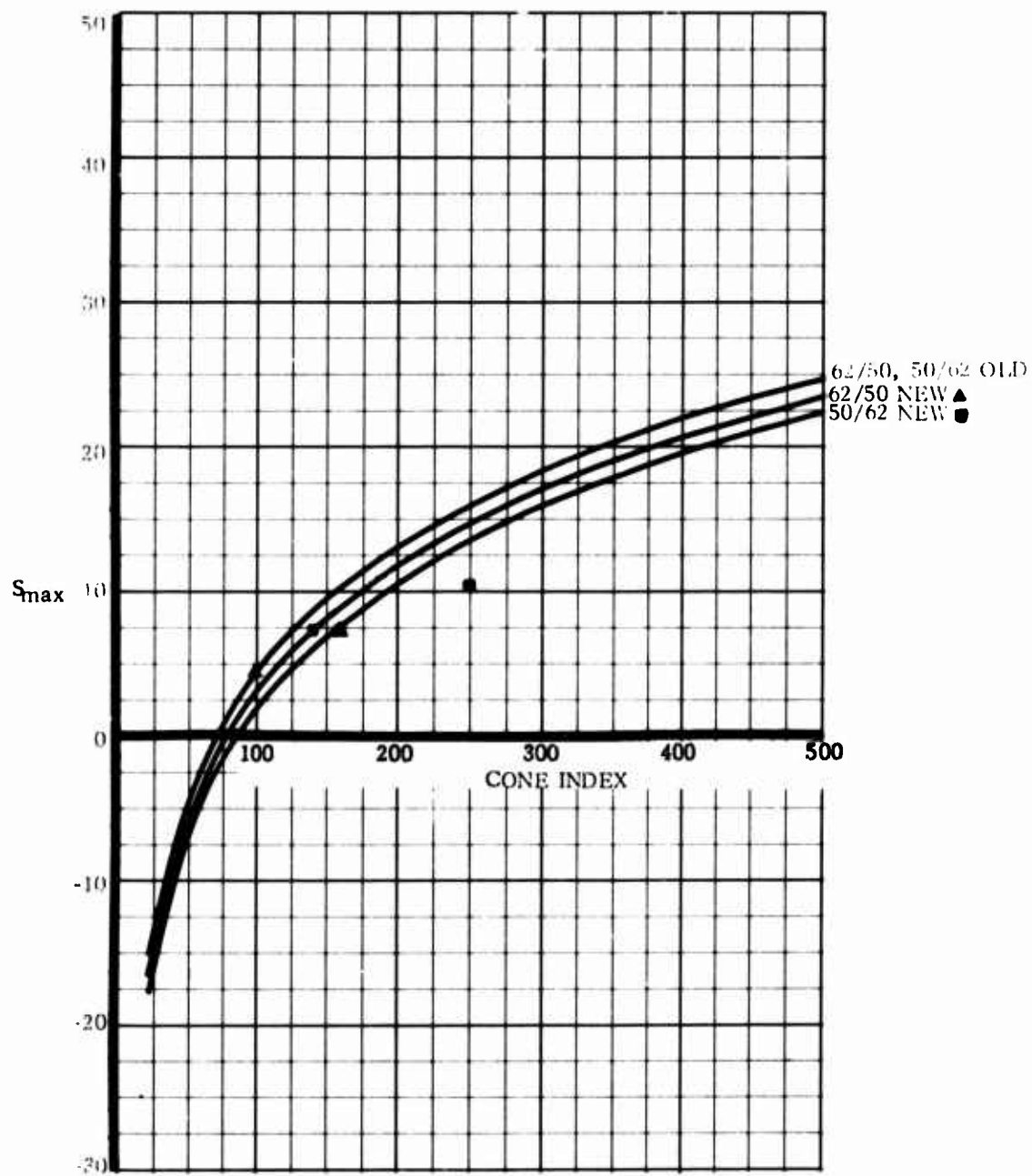
GRAPHICAL REPRESENTATION OF COMPUTER PROGRAM CALCULATIONS



Graph 1

Standard Tires
Equal axle load

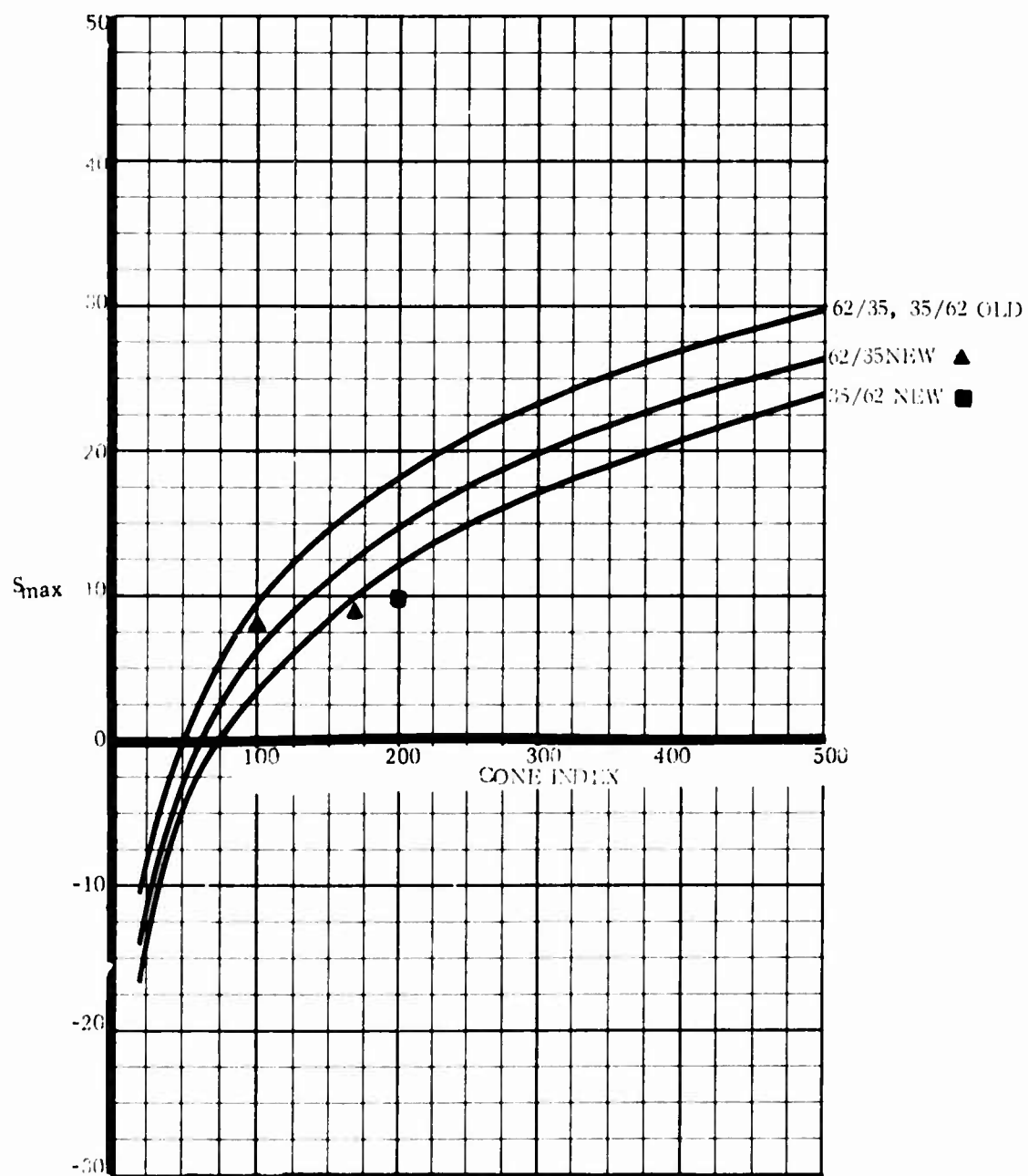
50K RTFLT



Graph 2

Standard Tires
Equal axle load

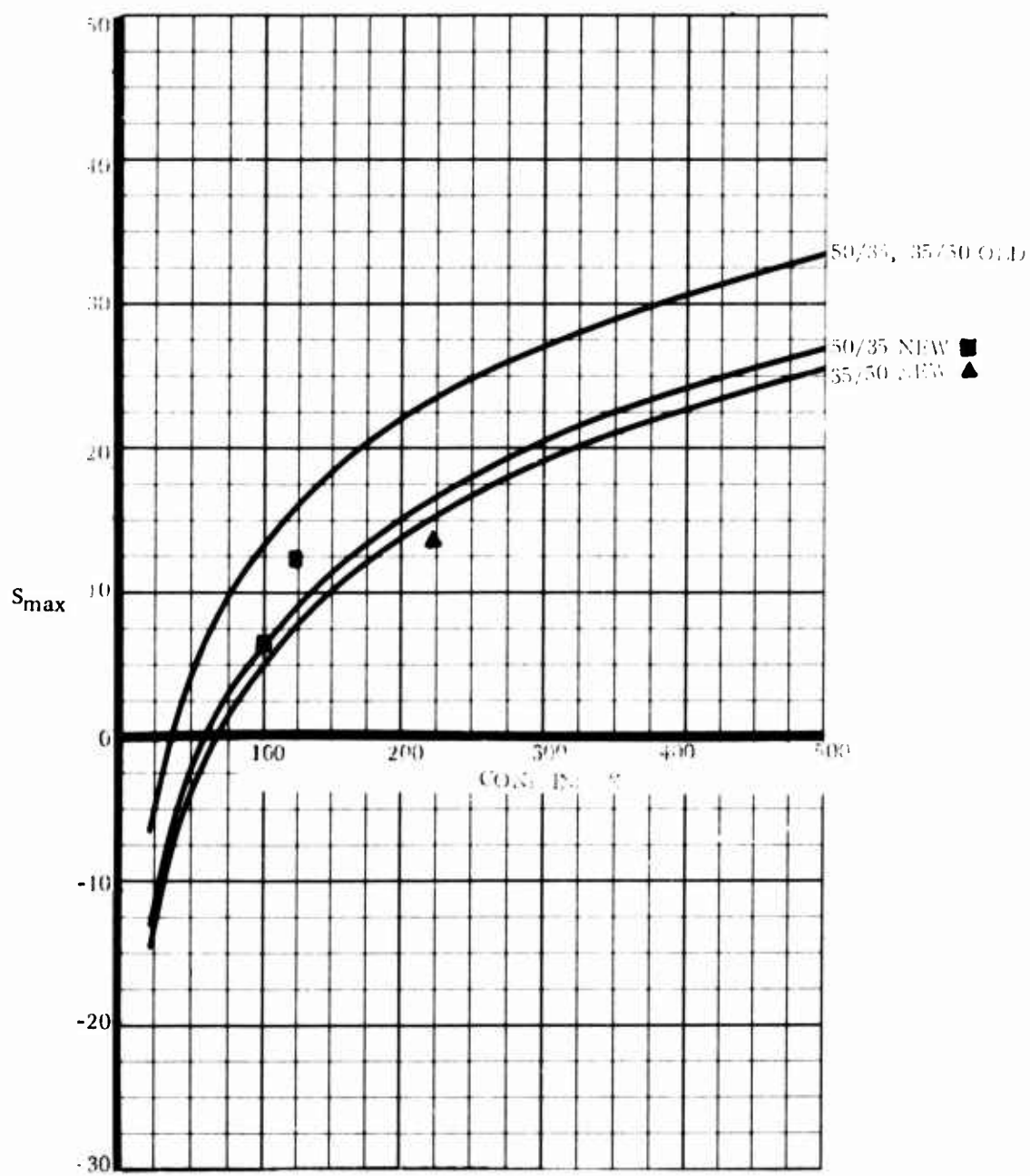
50K RTFLT



Graph 3

Standard Tires
Equal axle load

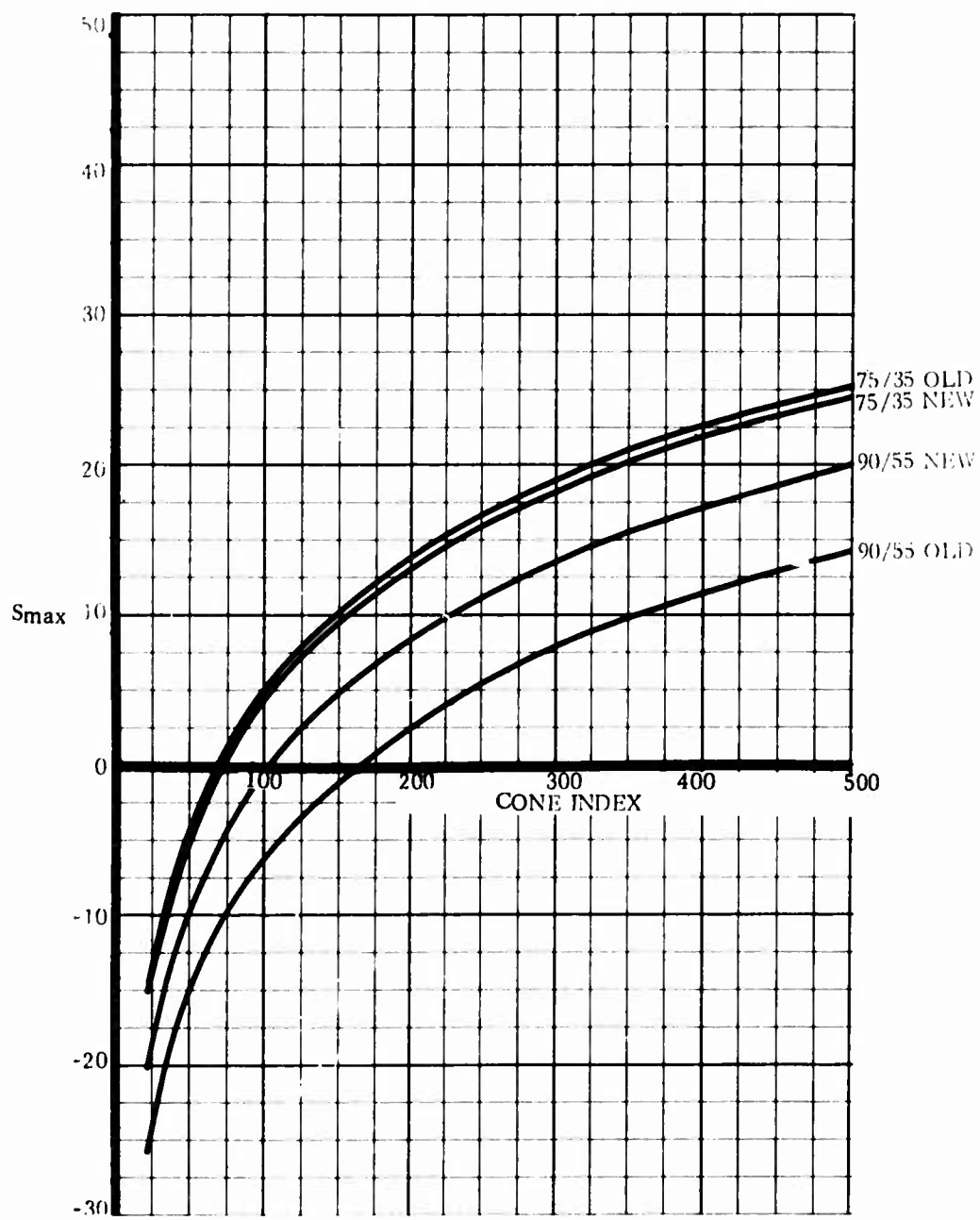
50K RTFLT



Graph 4

Standard Tires
Equal axle load

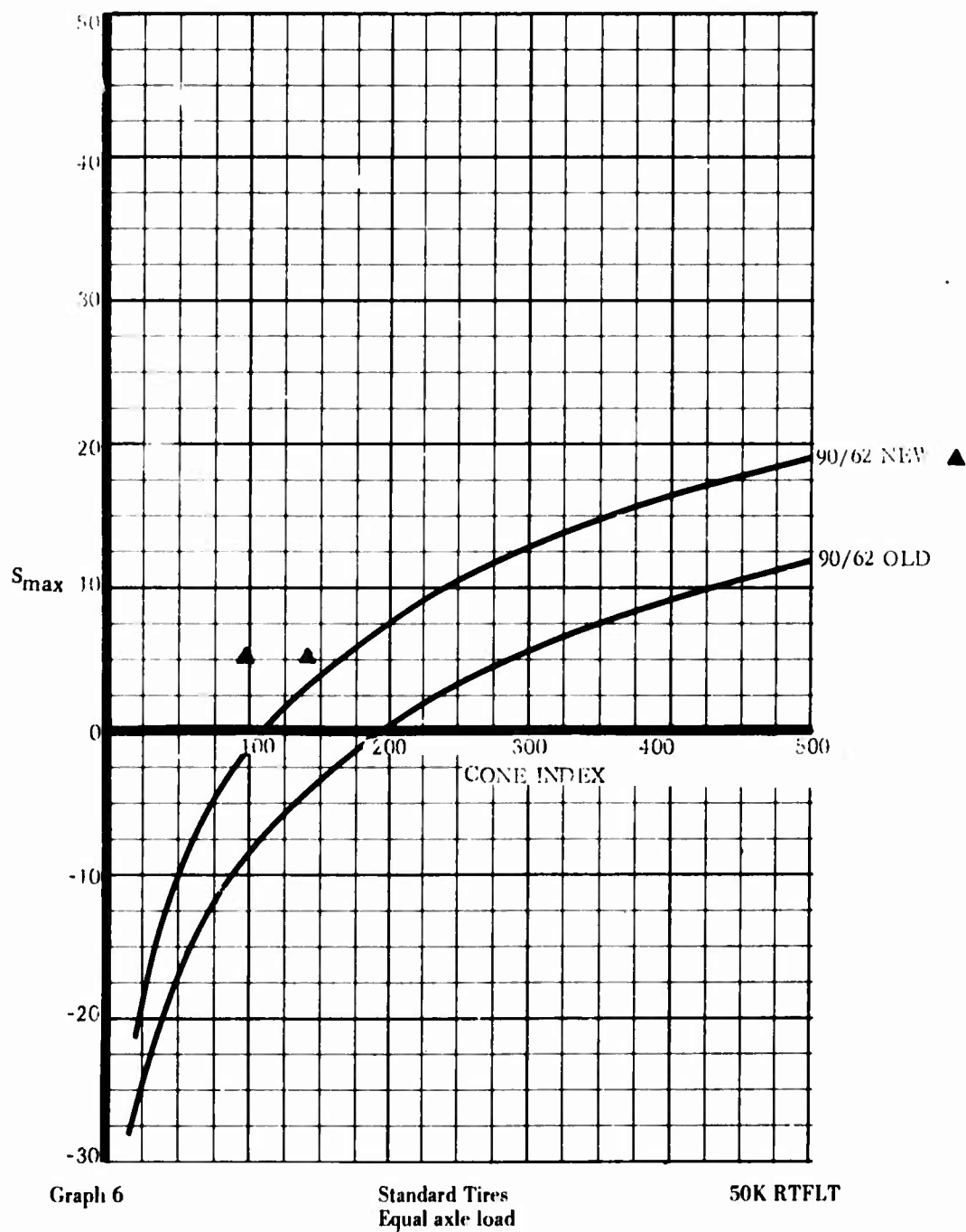
50K RTFLT

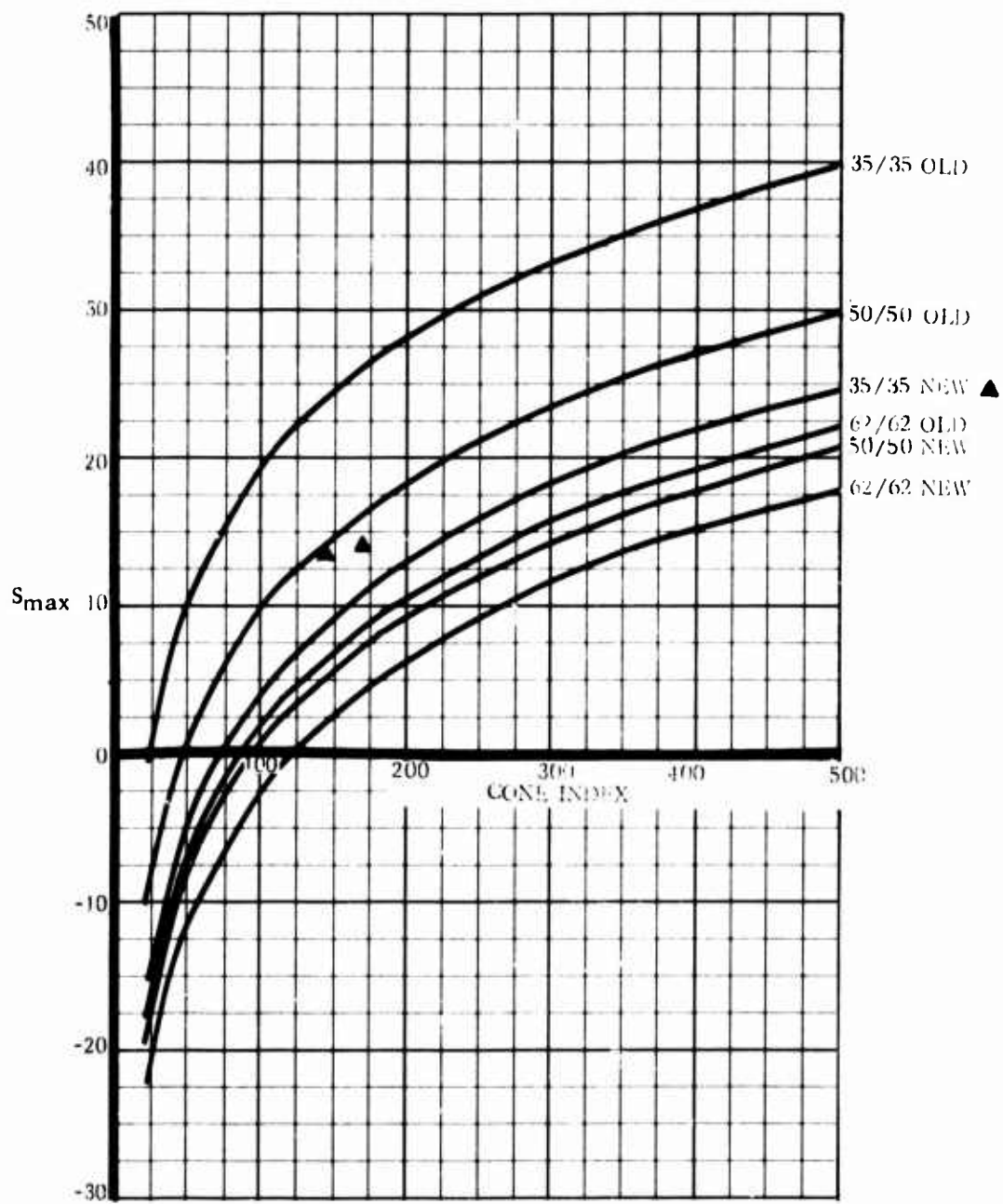


Graph 5

Standard Tires
Equal axle load

50K RTFLT

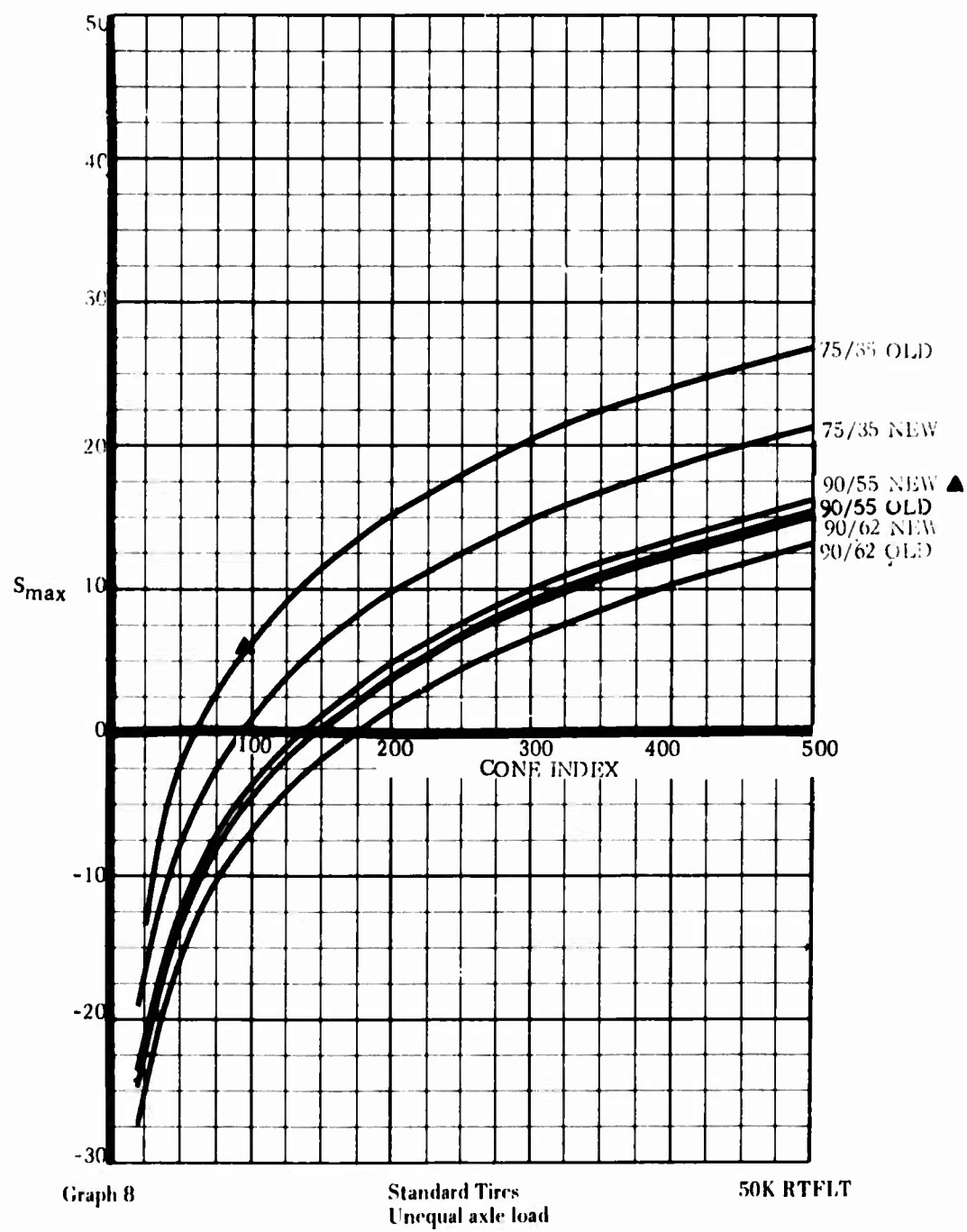


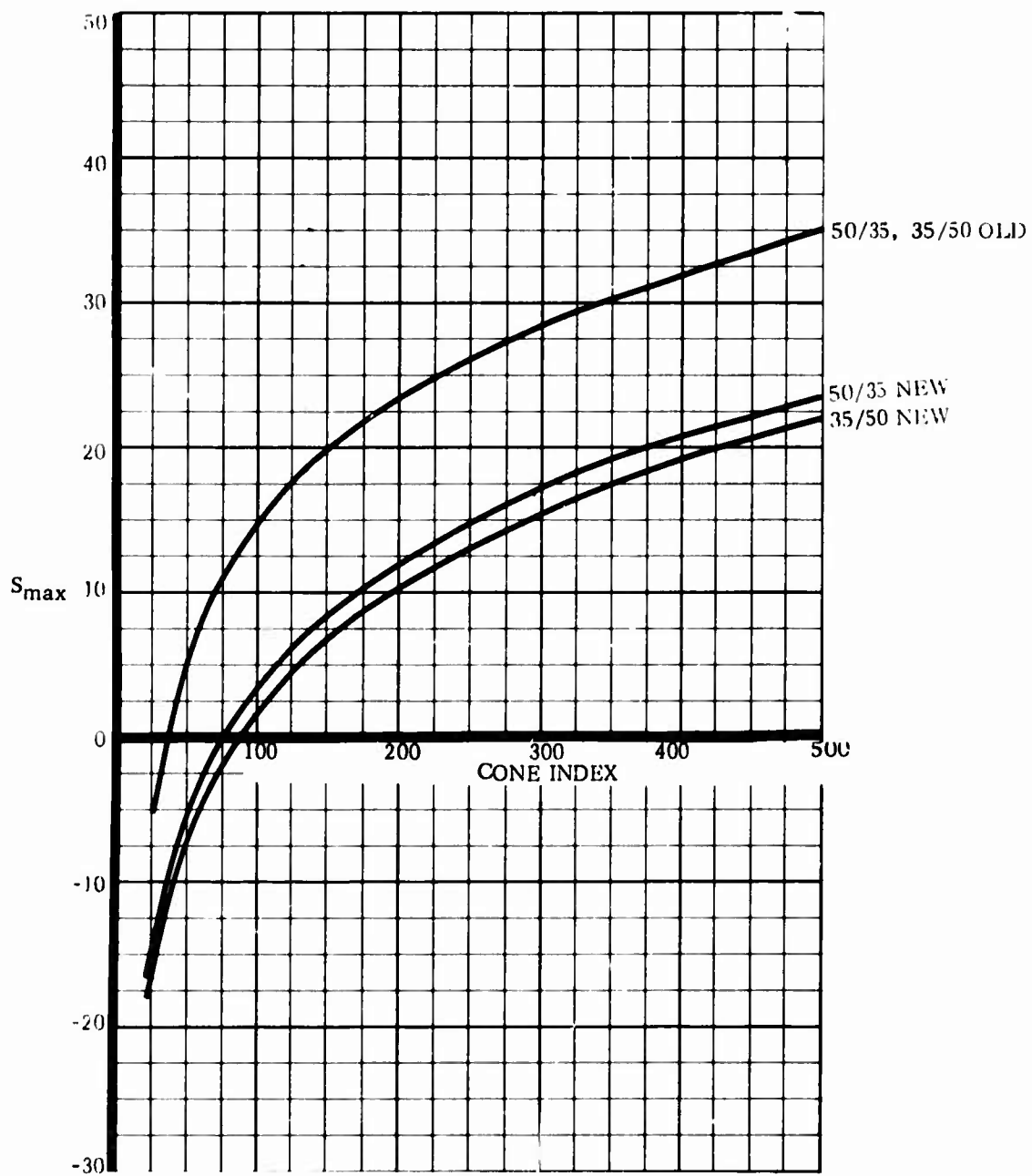


Graph 7

Standard Tires
Unequal axle load

50K RTFLT

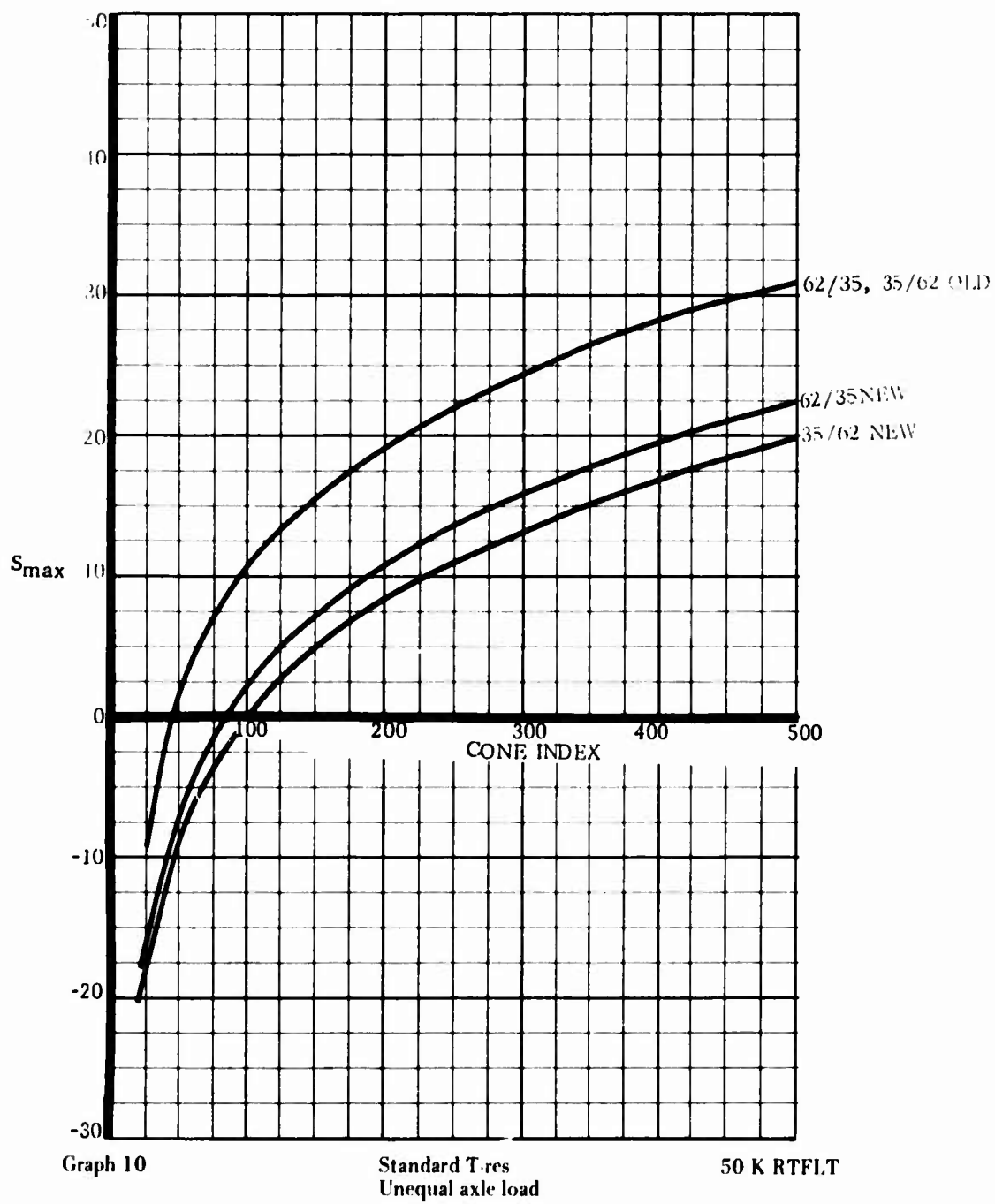


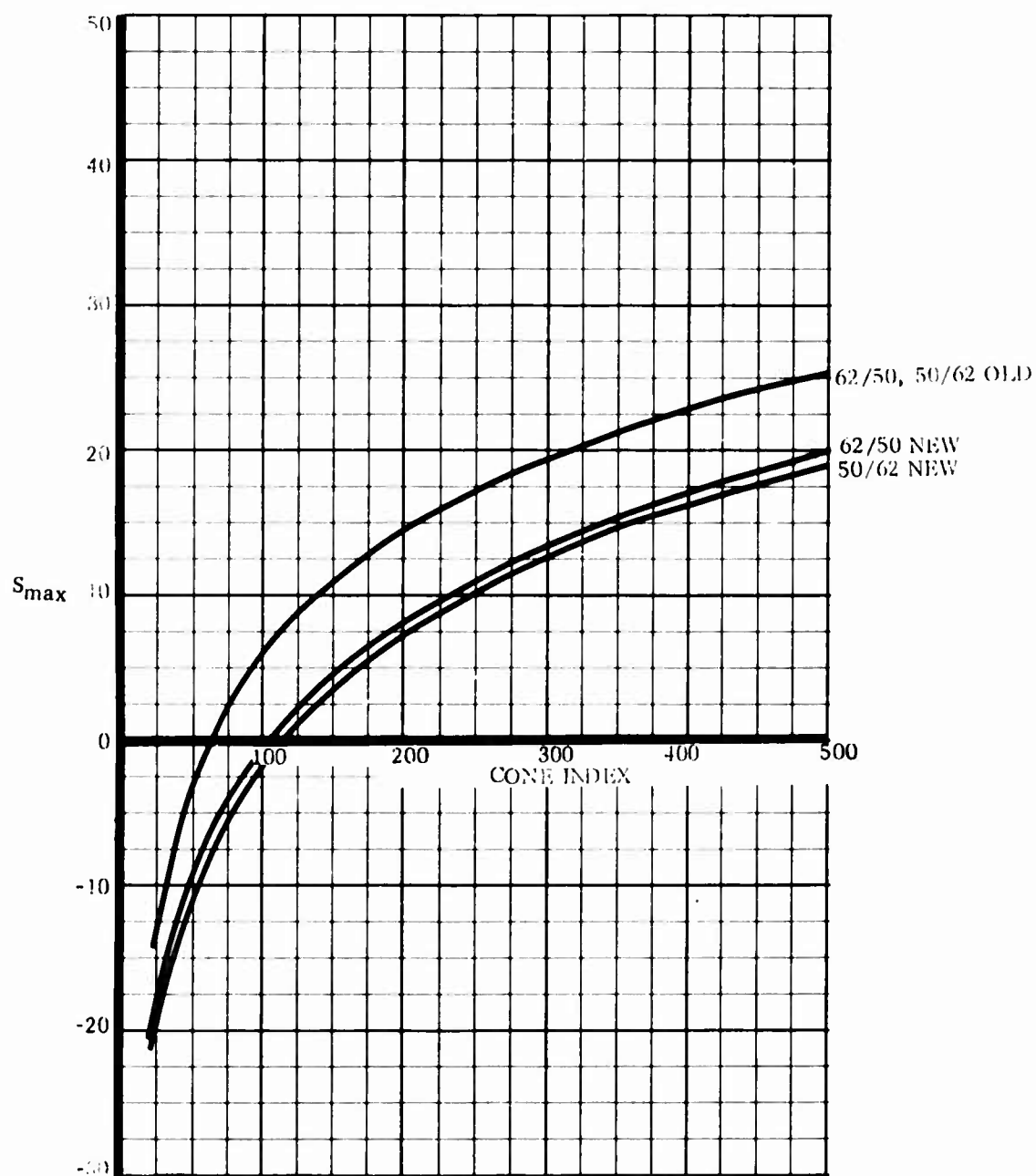


Graph 9

Standard Tires
Unequal axle load

50K RTFLT

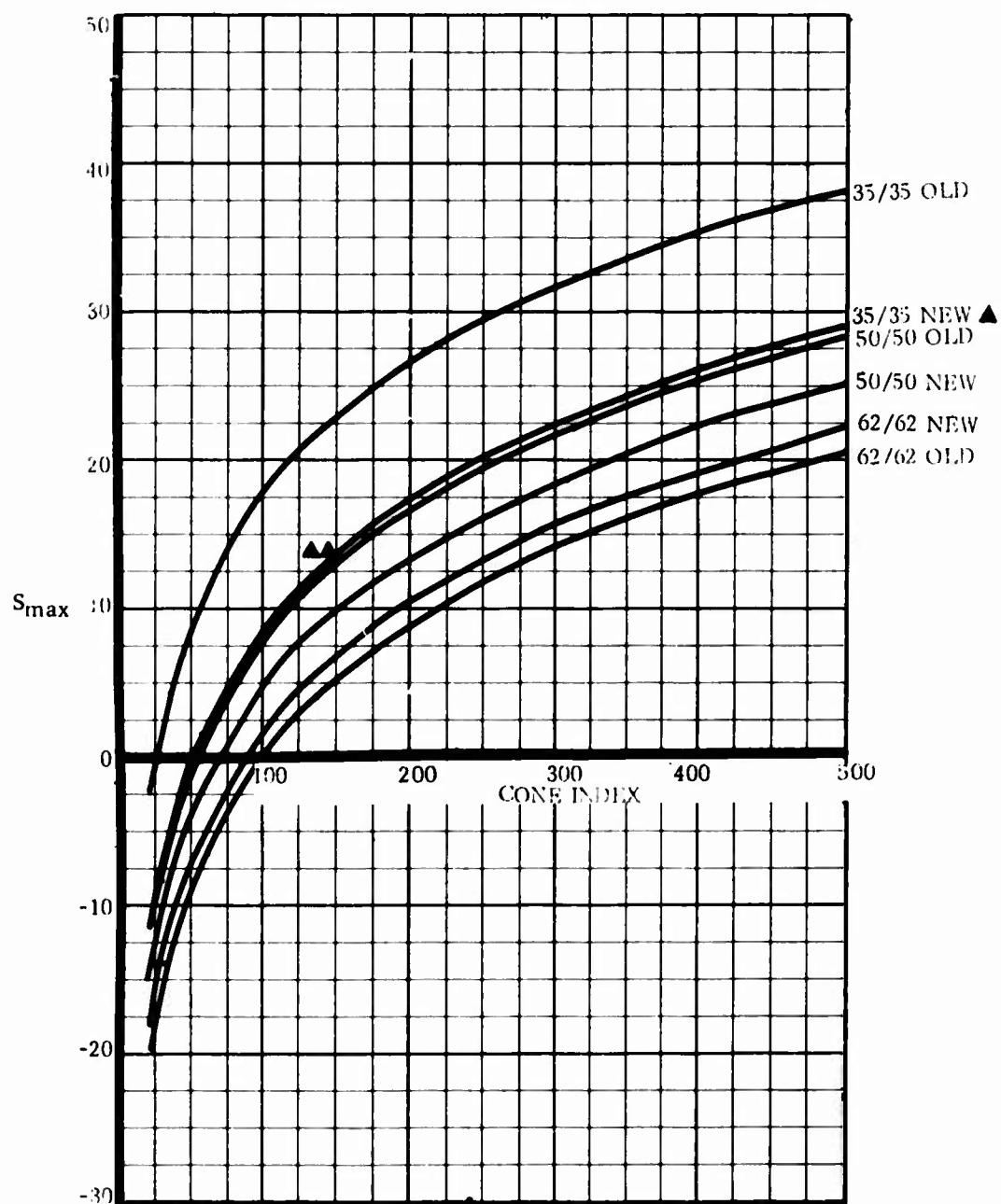




Graph 11

Standard Tires
Unequal axle load

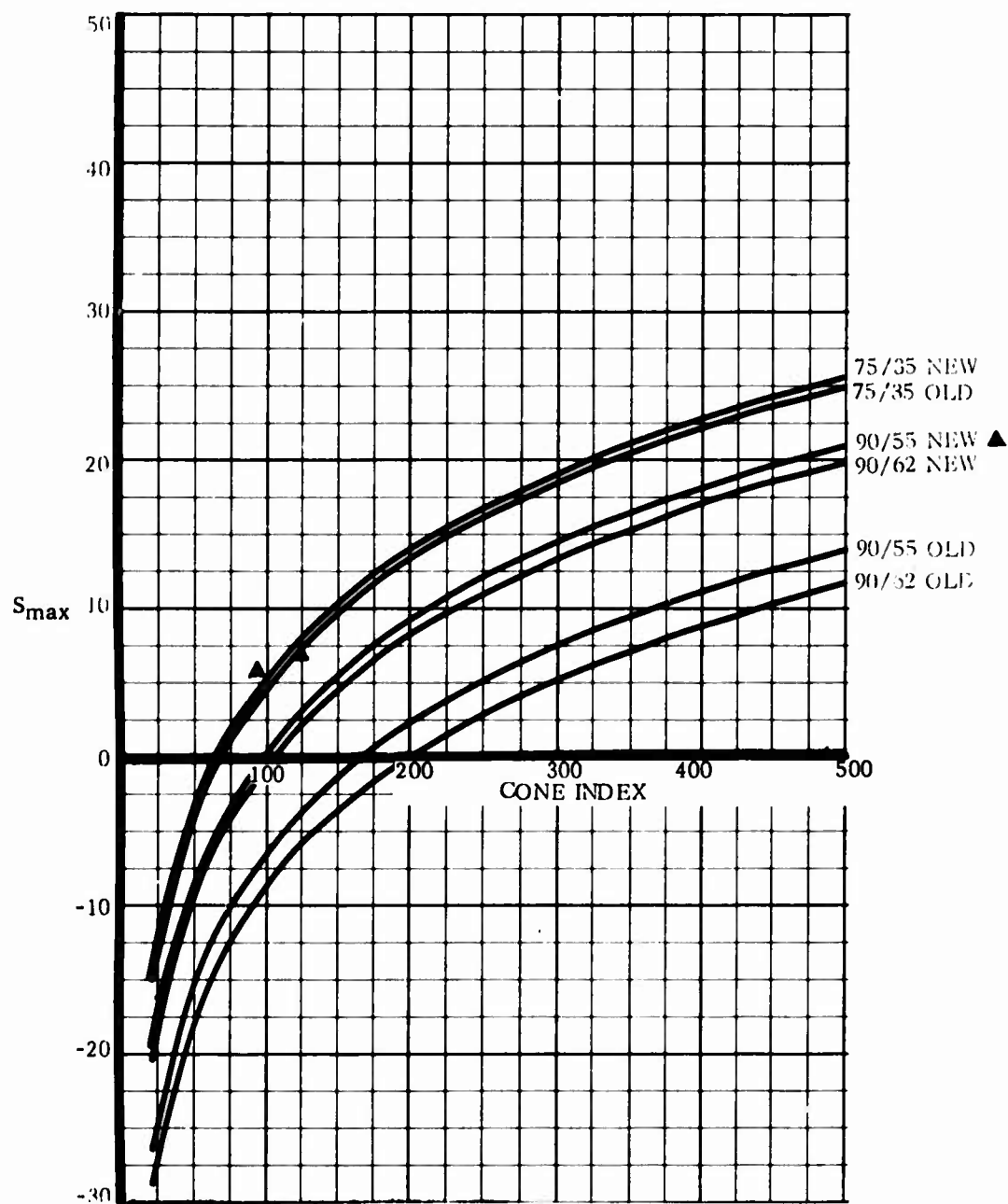
50K RTFLT



Graph 12

Standard Tires
No axle load

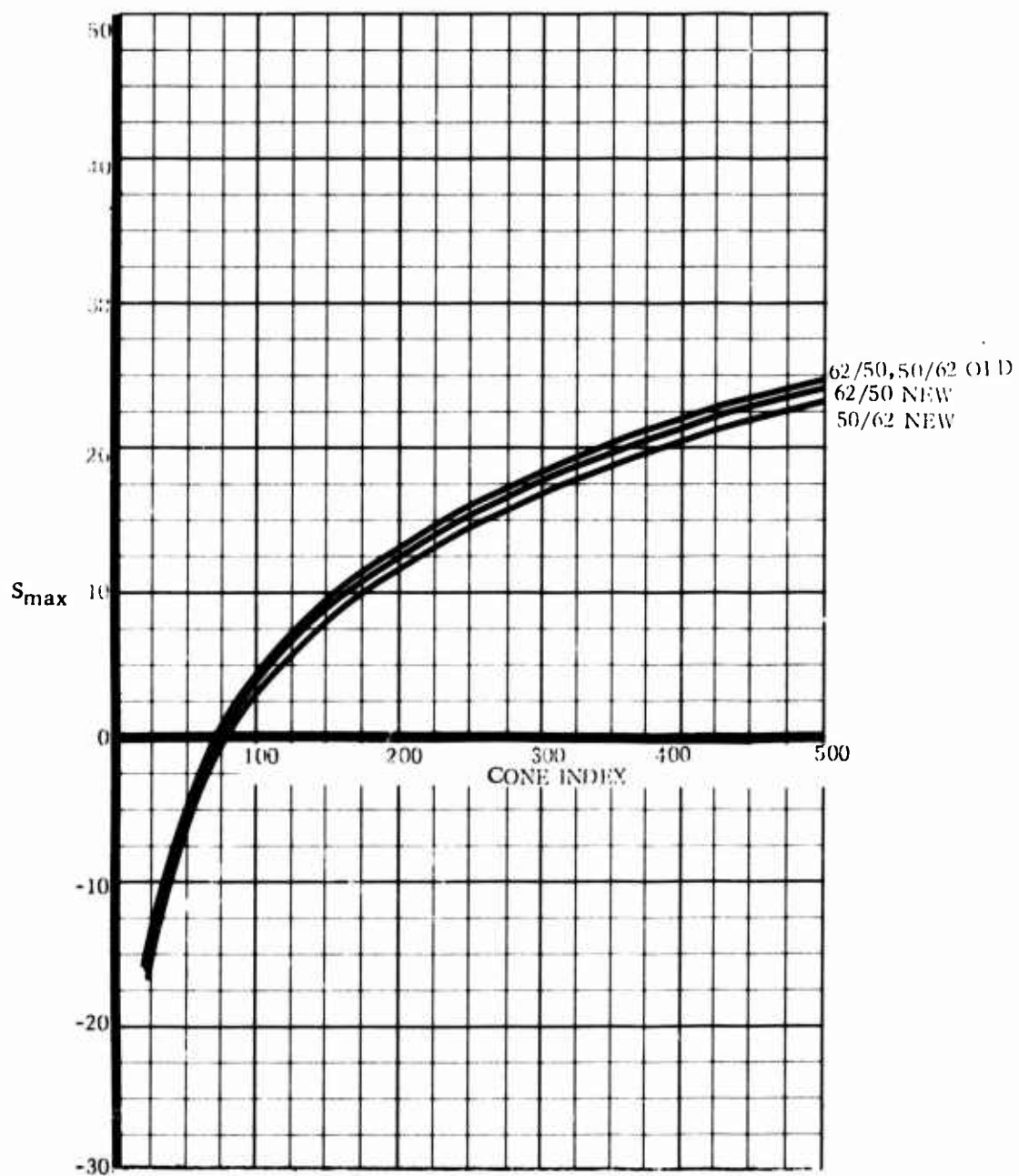
50K RTFLT



Graph 13

Standard Tires
No axle load

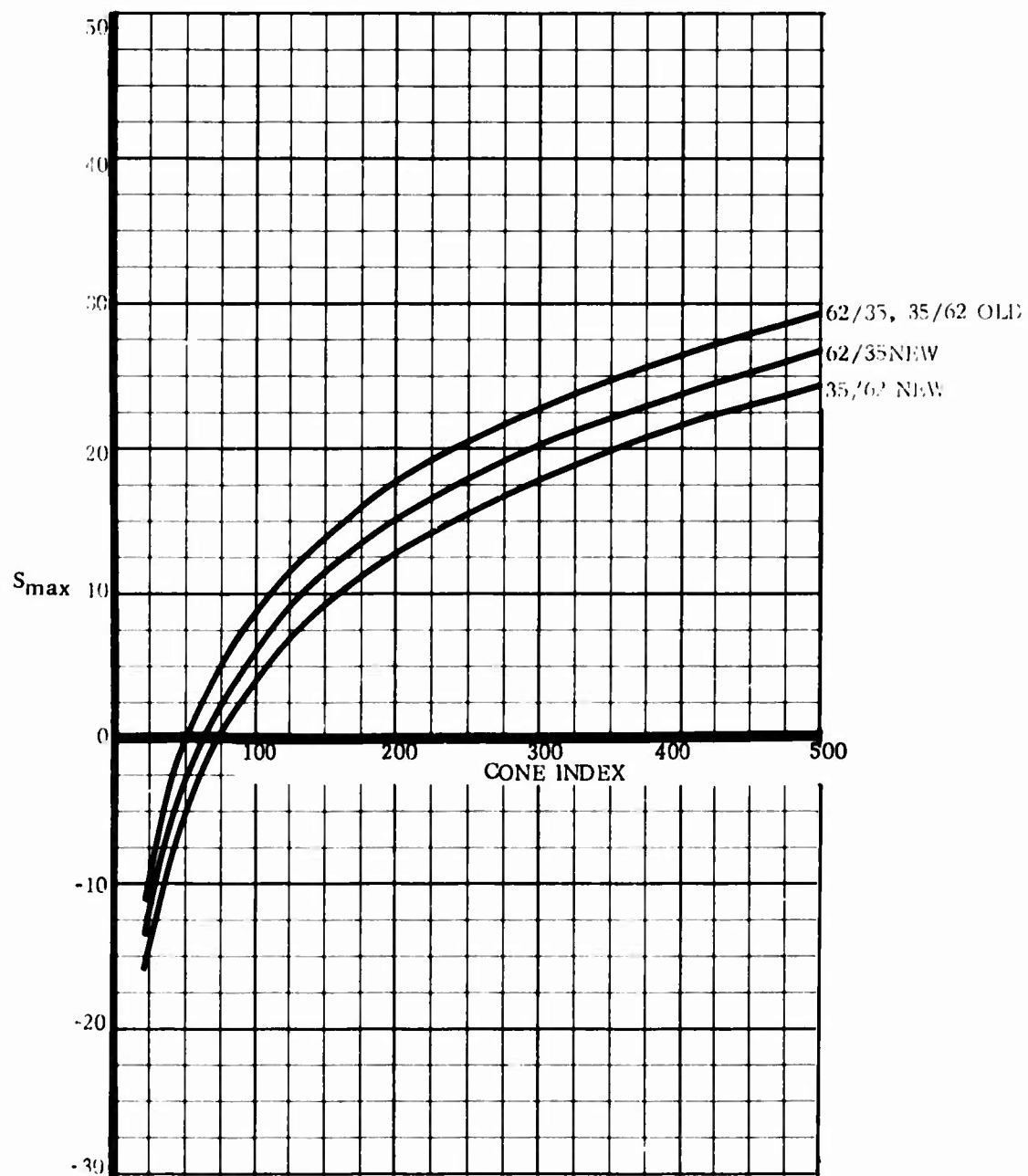
50K RTFLT



Graph 14

Standard Tires
No axle load

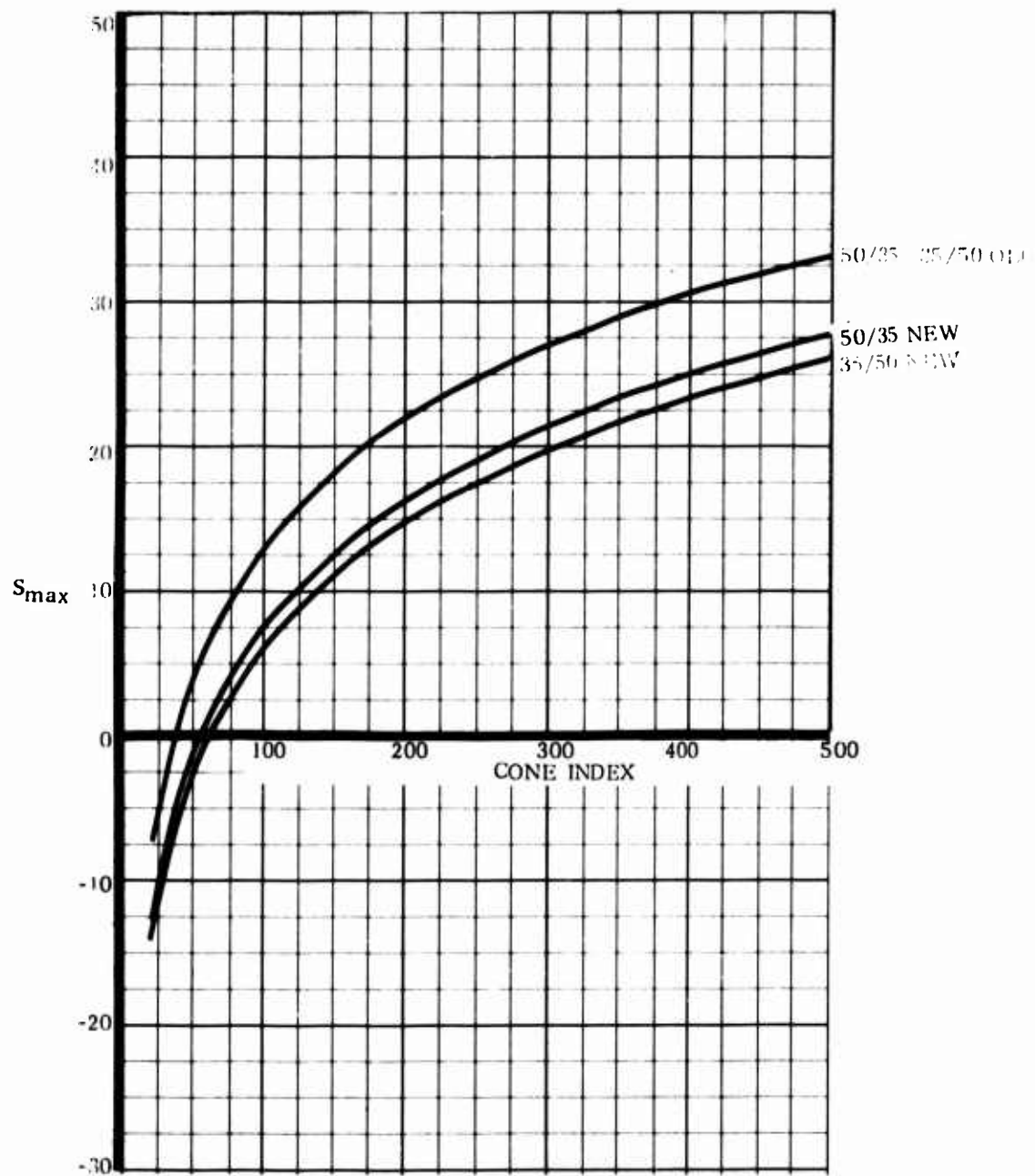
50K RTFLT



Graph 15

Standard Tires
No axle load

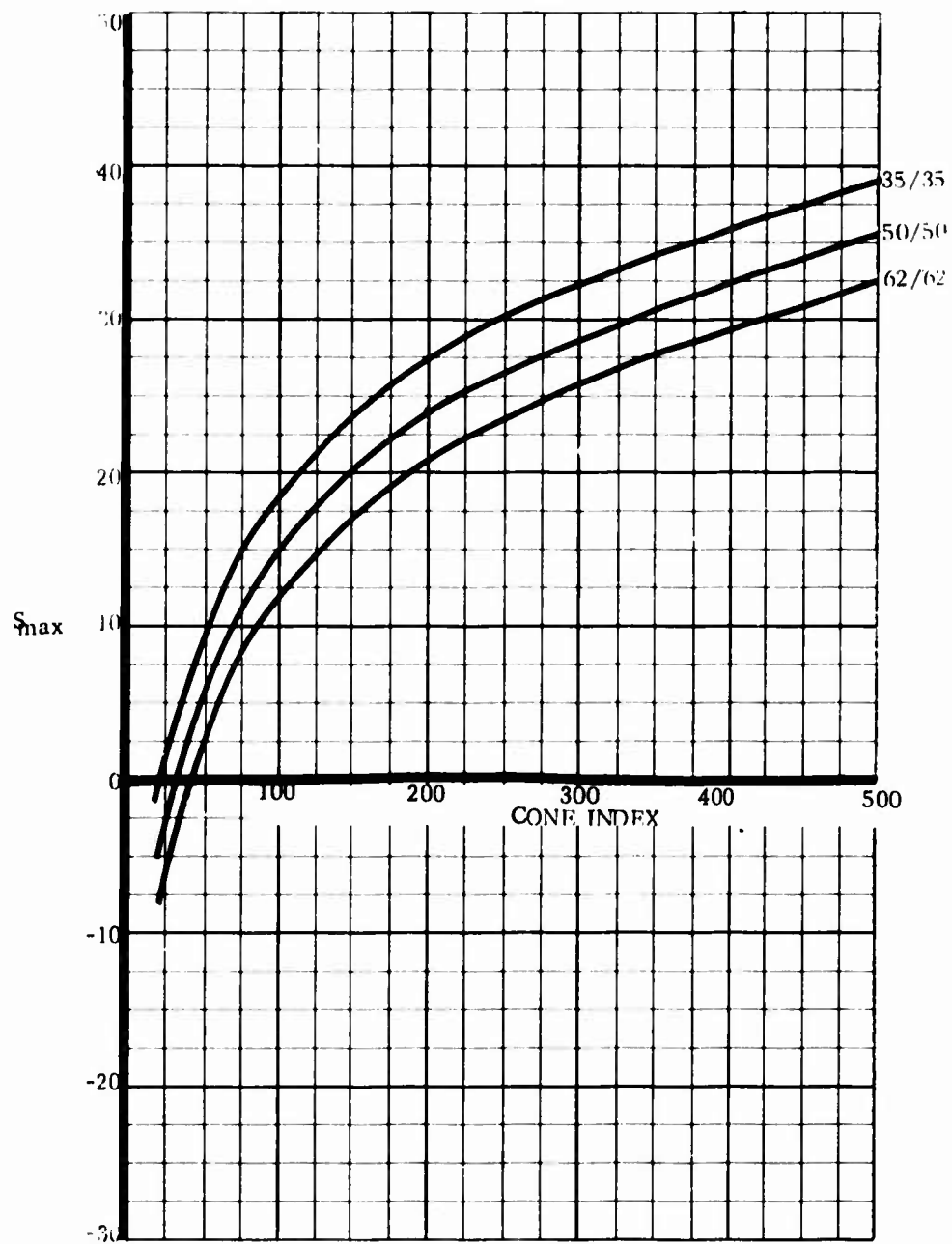
50K RTFLT



Graph 16

Standard Tires
No axle load

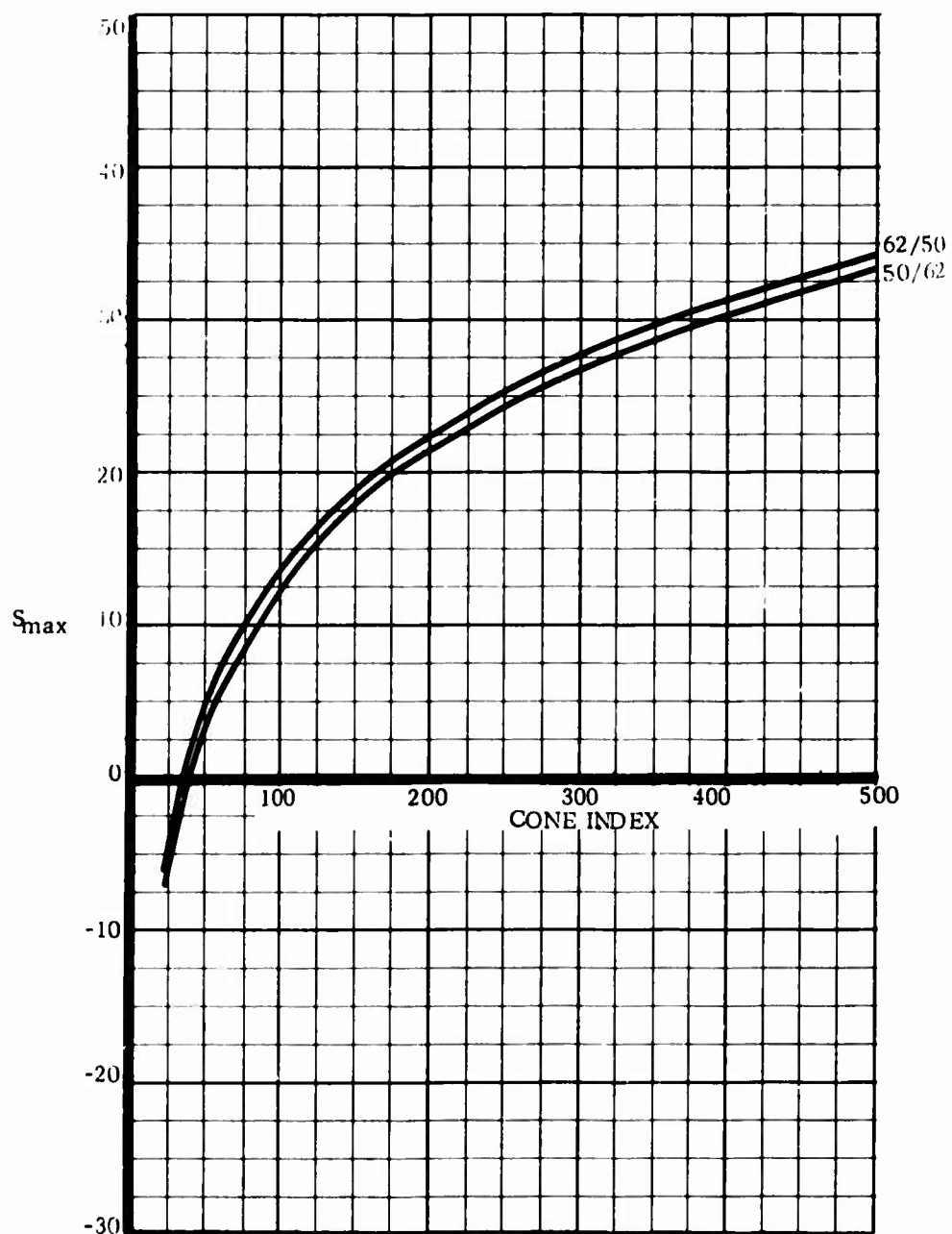
50K RTFLT



Graph 17

Radial Tires
Equal axle load

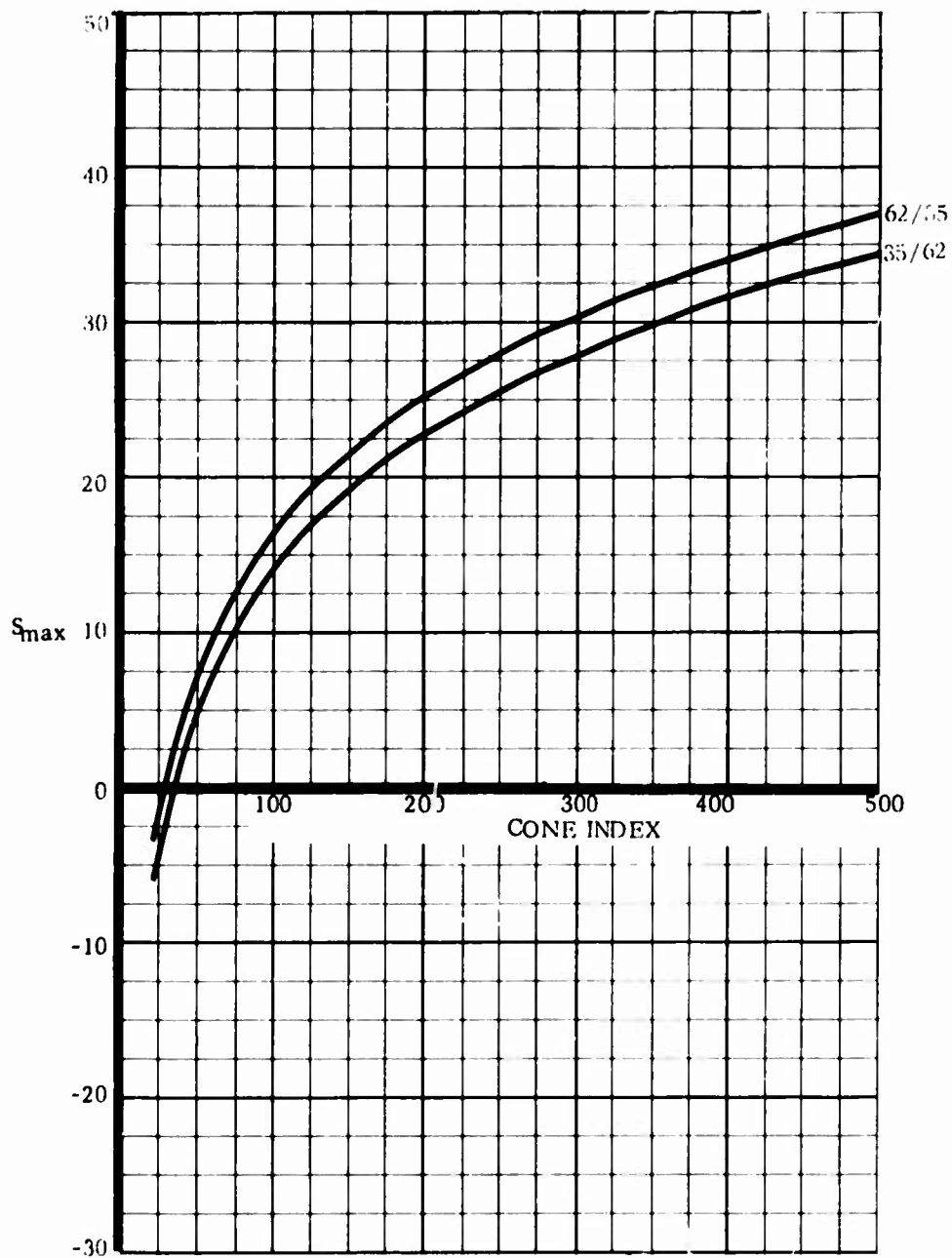
50K RTFLT



Graph 18

Radial Tires
Equal axle load

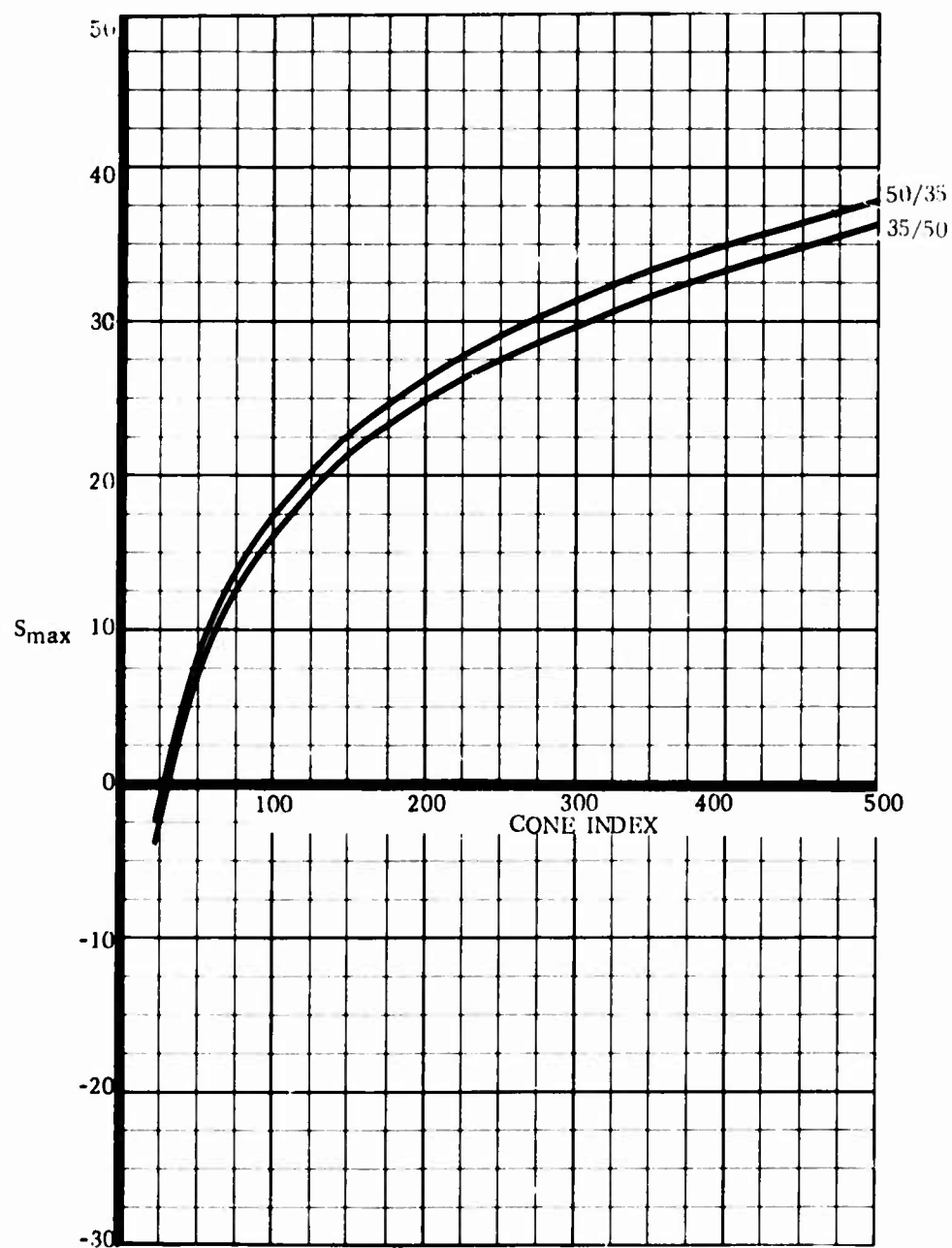
50K RTFLT



Graph 19

Radial Tires
Equal axle load

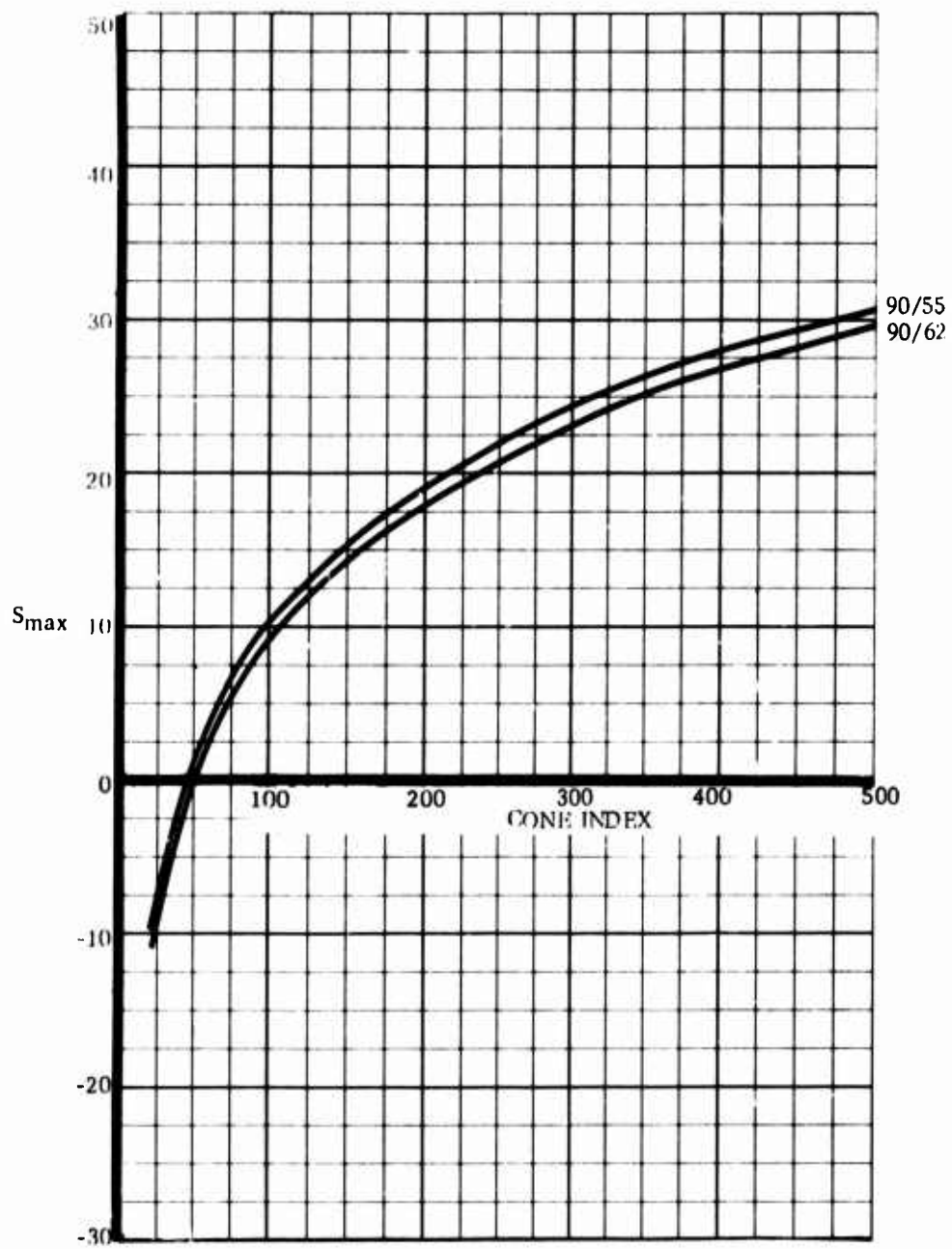
50K RTFLT



Graph 20

Radial Tires
Equal axle load

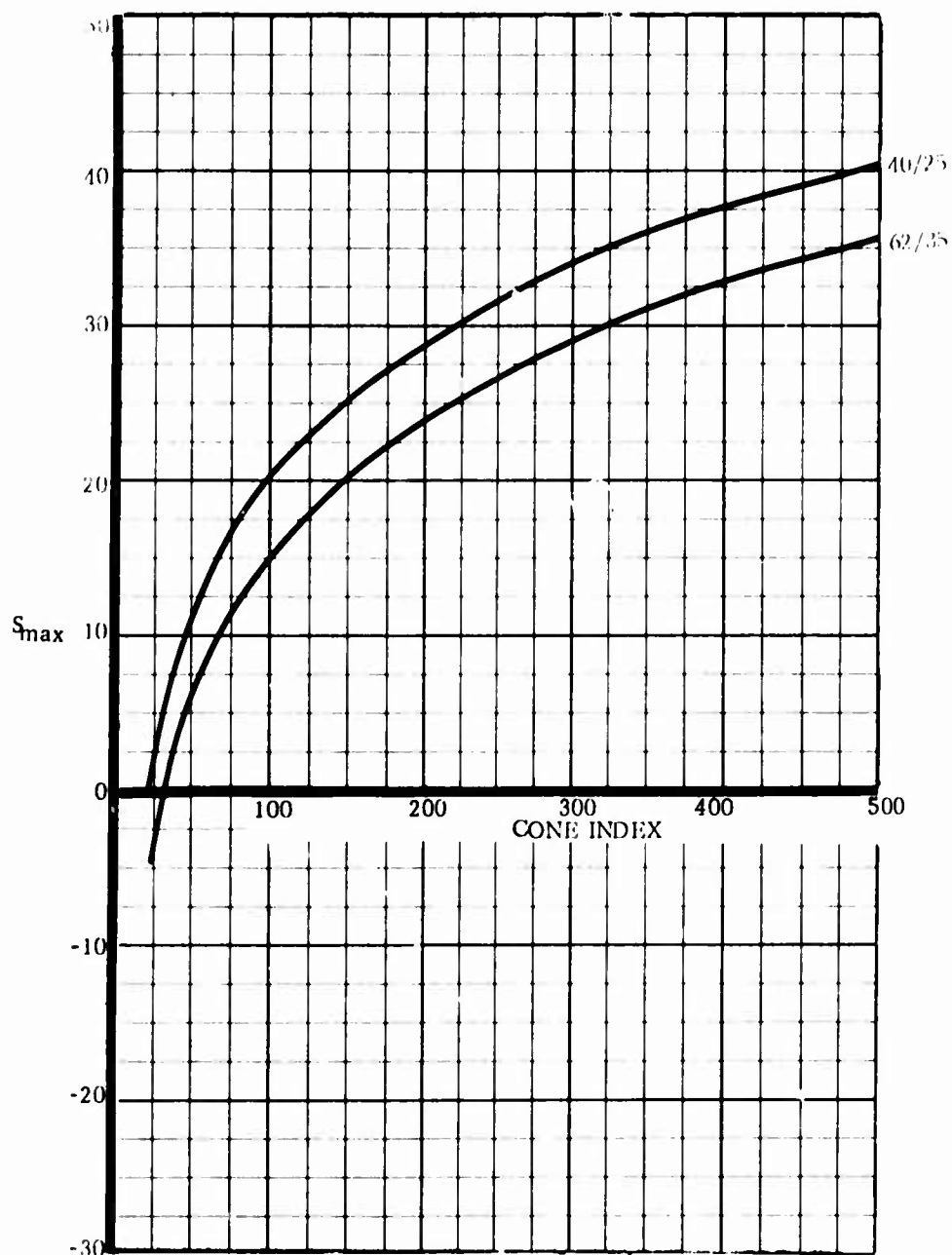
50K RTFL/T



Graph 21

Radial Tires
Equal axle load

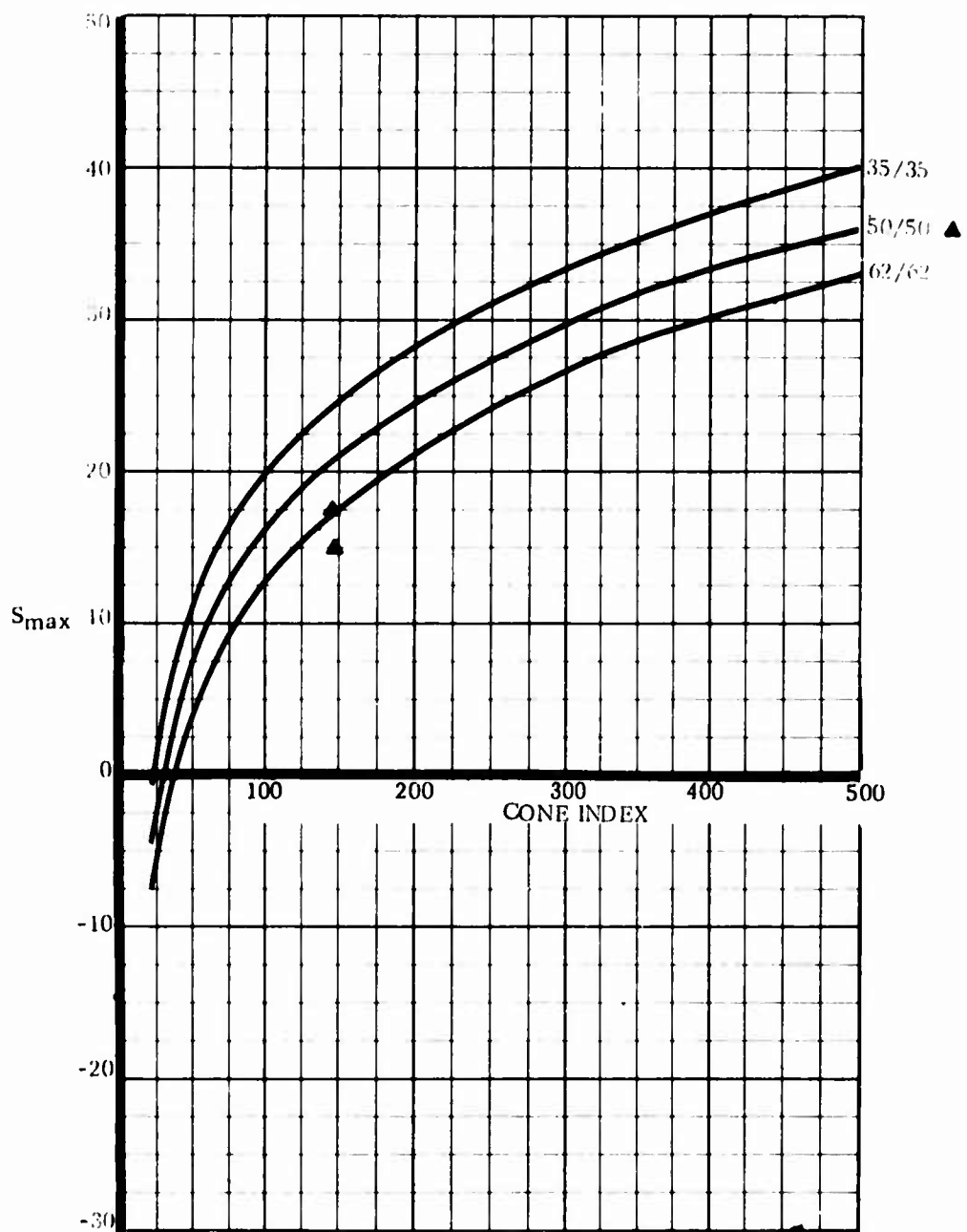
50K RTFLT



Graph 22

Radial Tires
Equal axle load

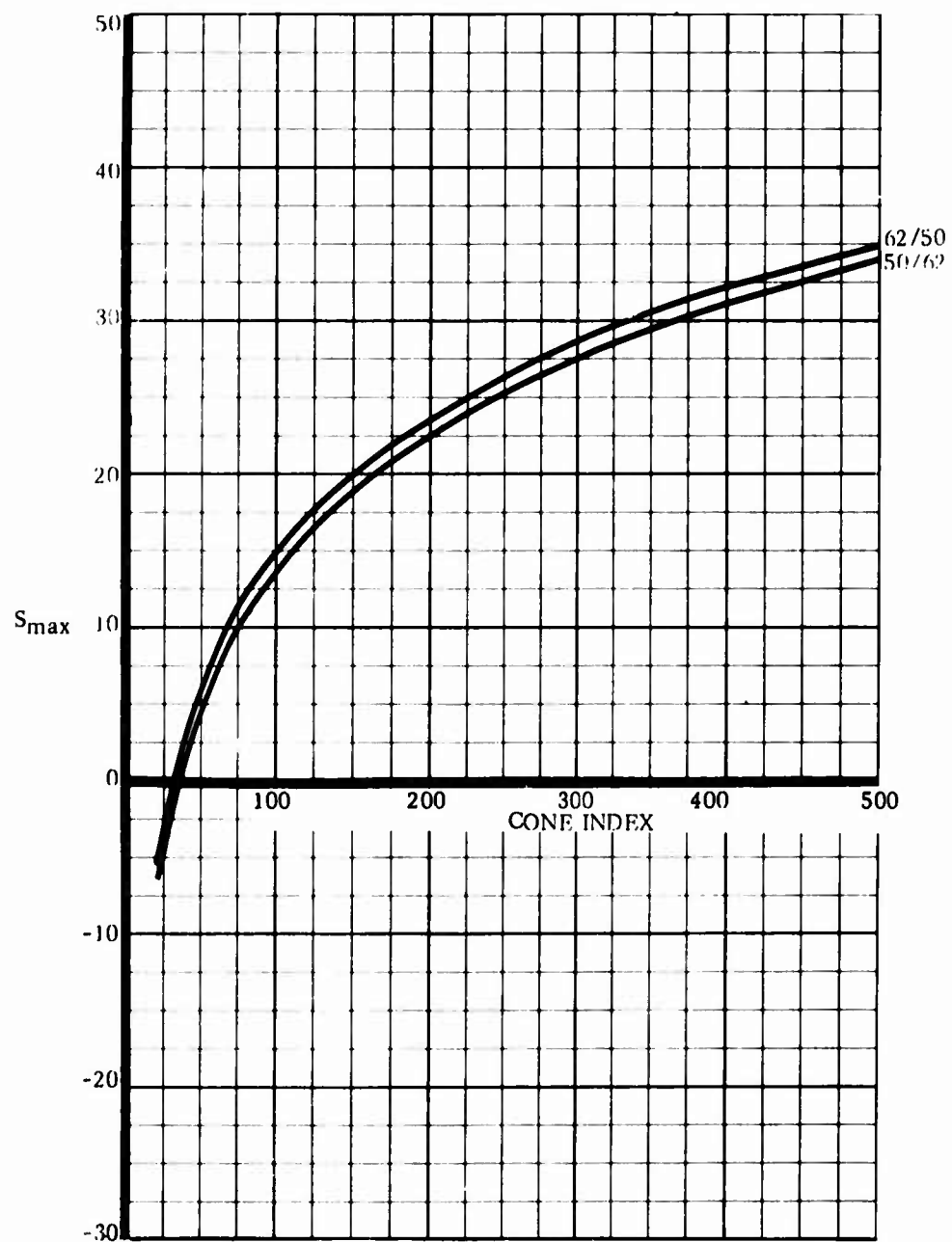
50K RTFLT



Graph 23

Radial Tires
Unequal axle load

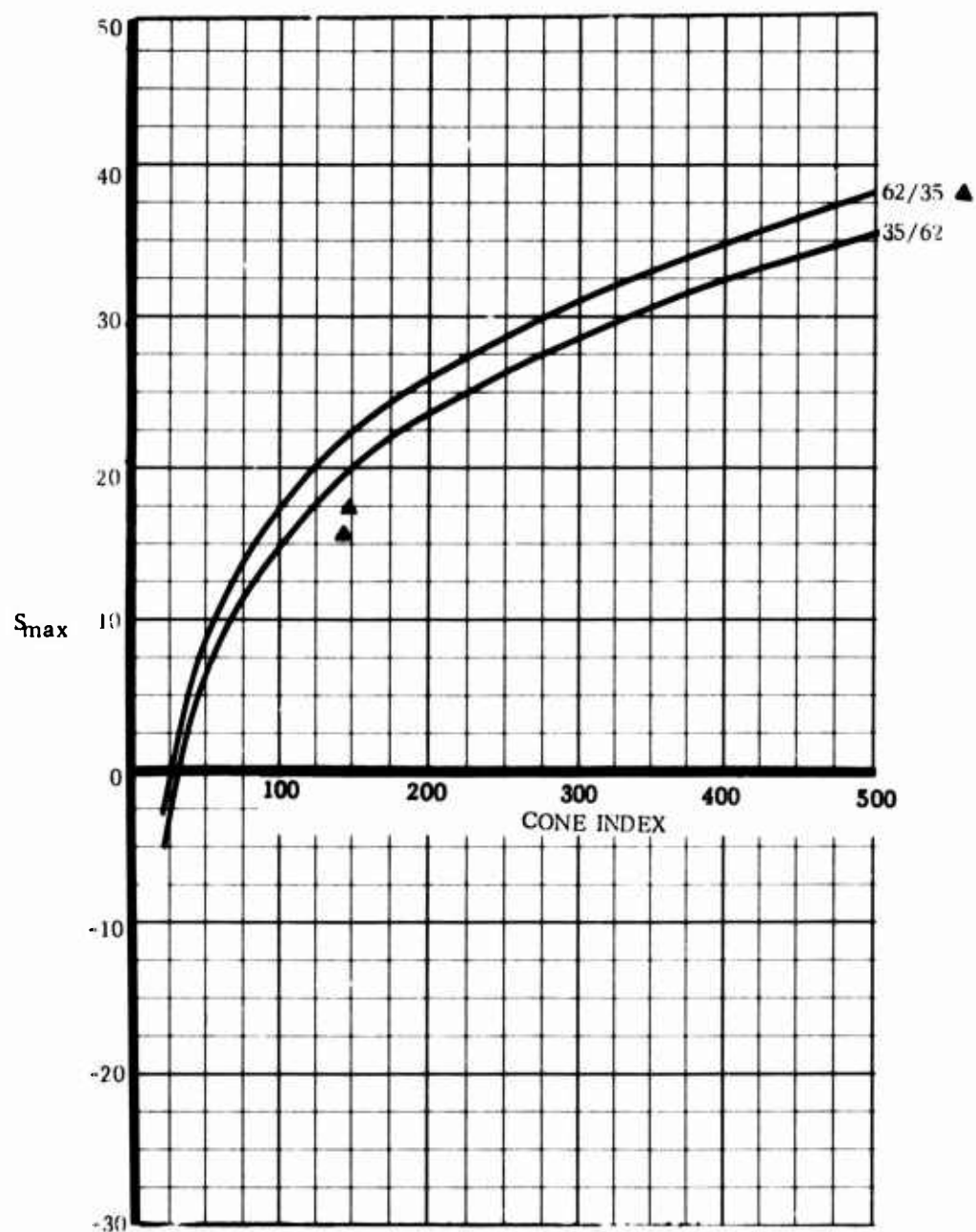
50K RTFLT



Graph 24

Radial Tires
Unequal axle load

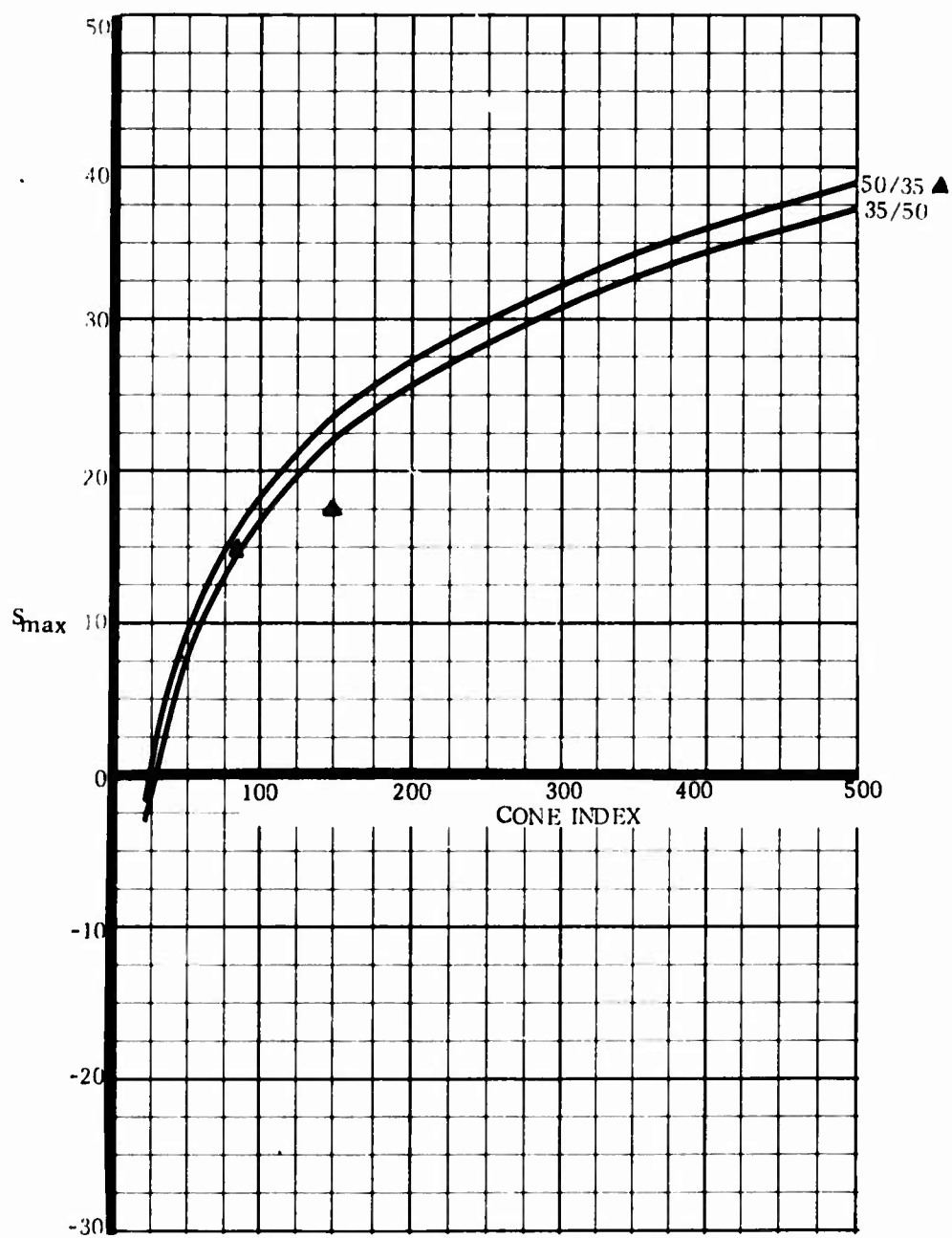
50K RTFLT



Graph 25

Radial Tires
Unequal axle load

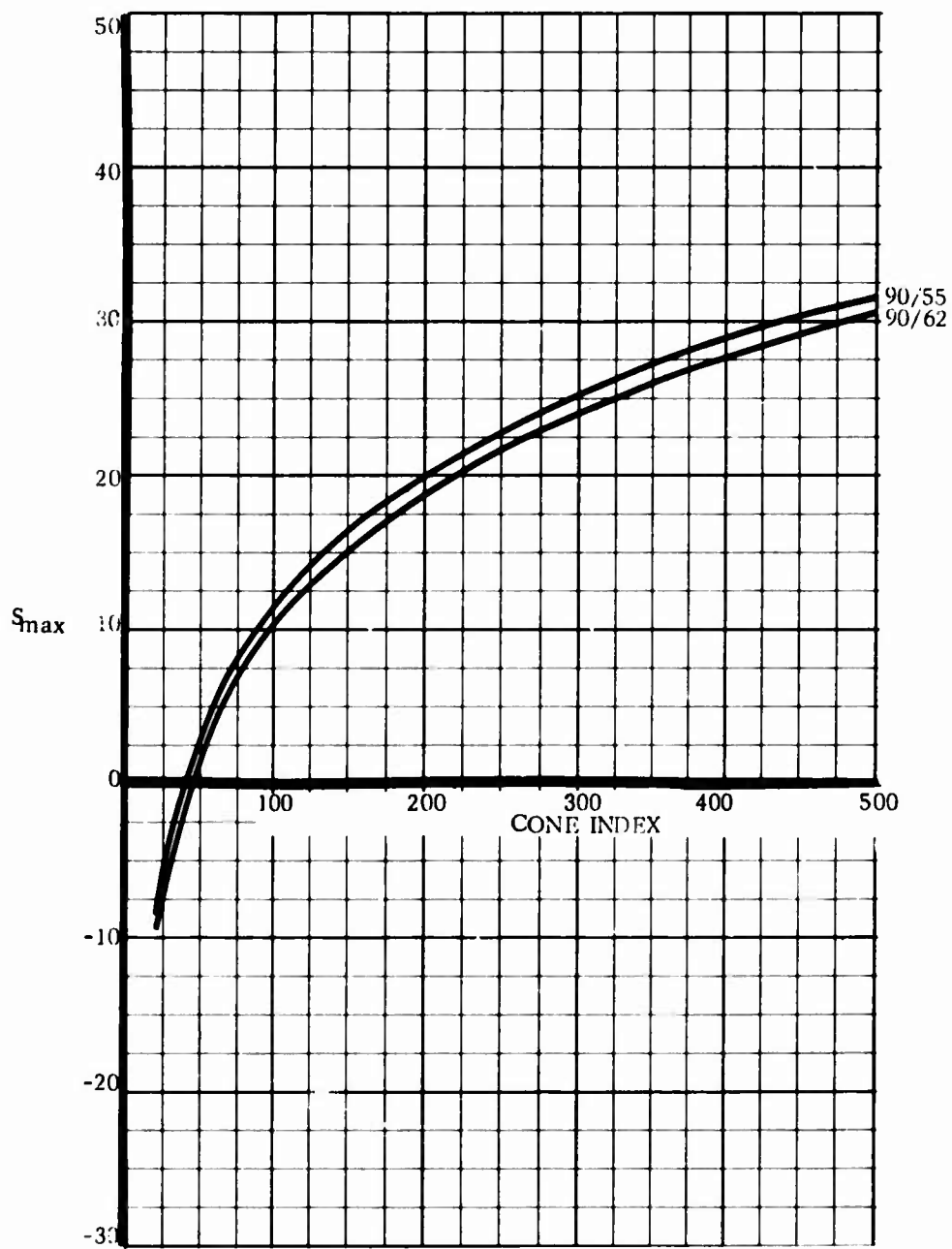
50K RTFL/T



Graph 26

Radial Tires
Unequal axle load

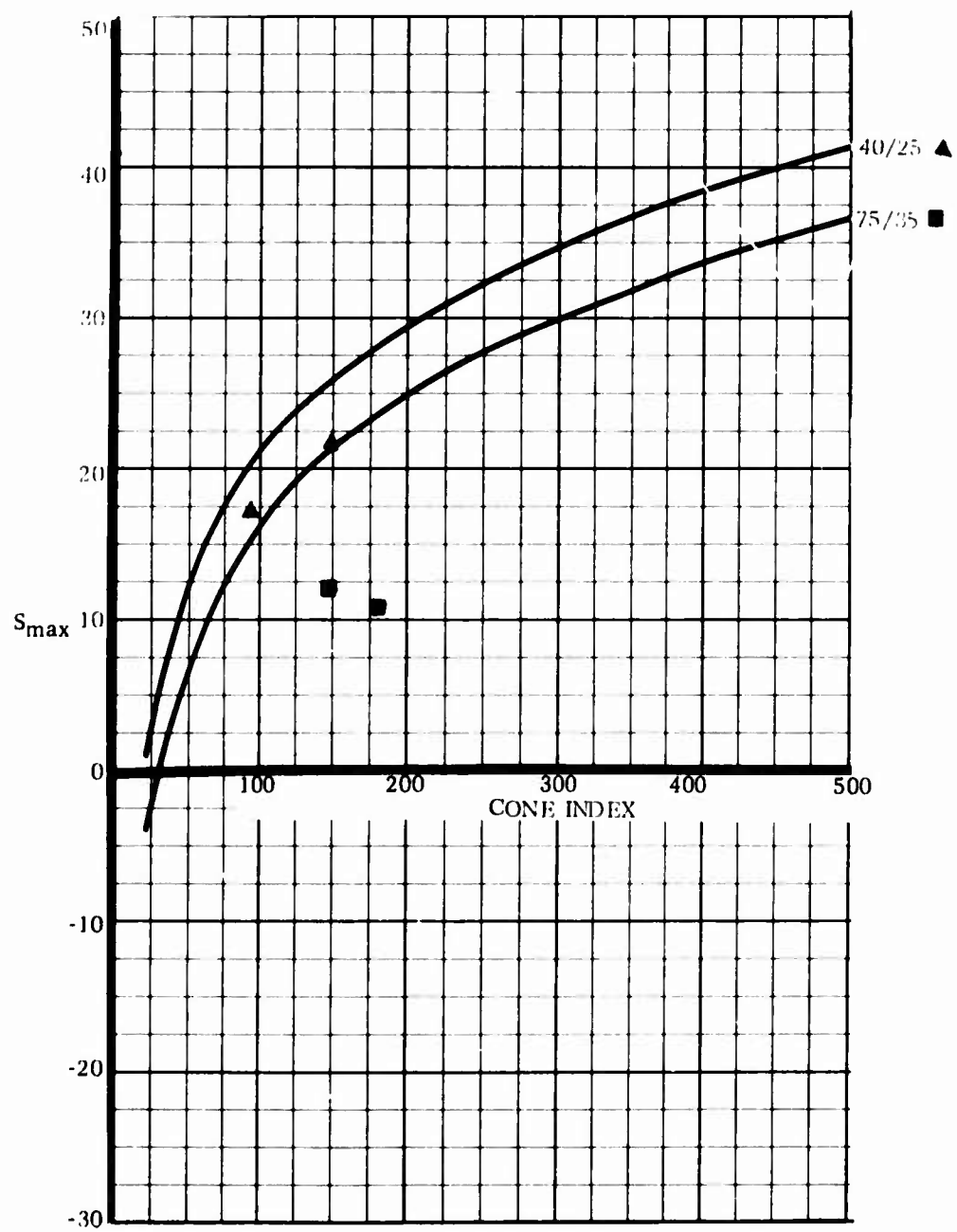
50K RTFLT



Graph 27

Radial Tires
Unequal axle load

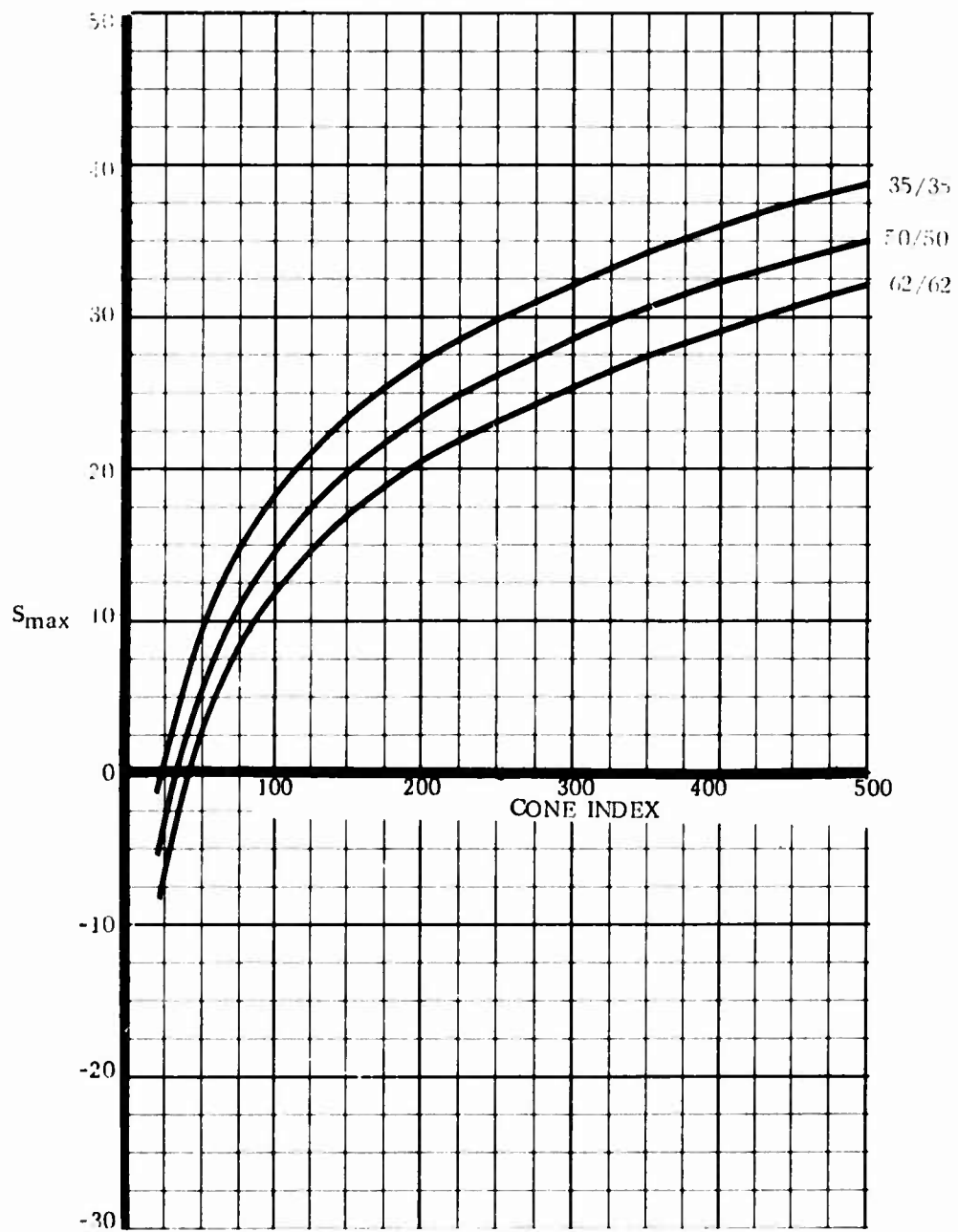
50K RTFLT



Graph 28

Radial Tires
Unequal axle load

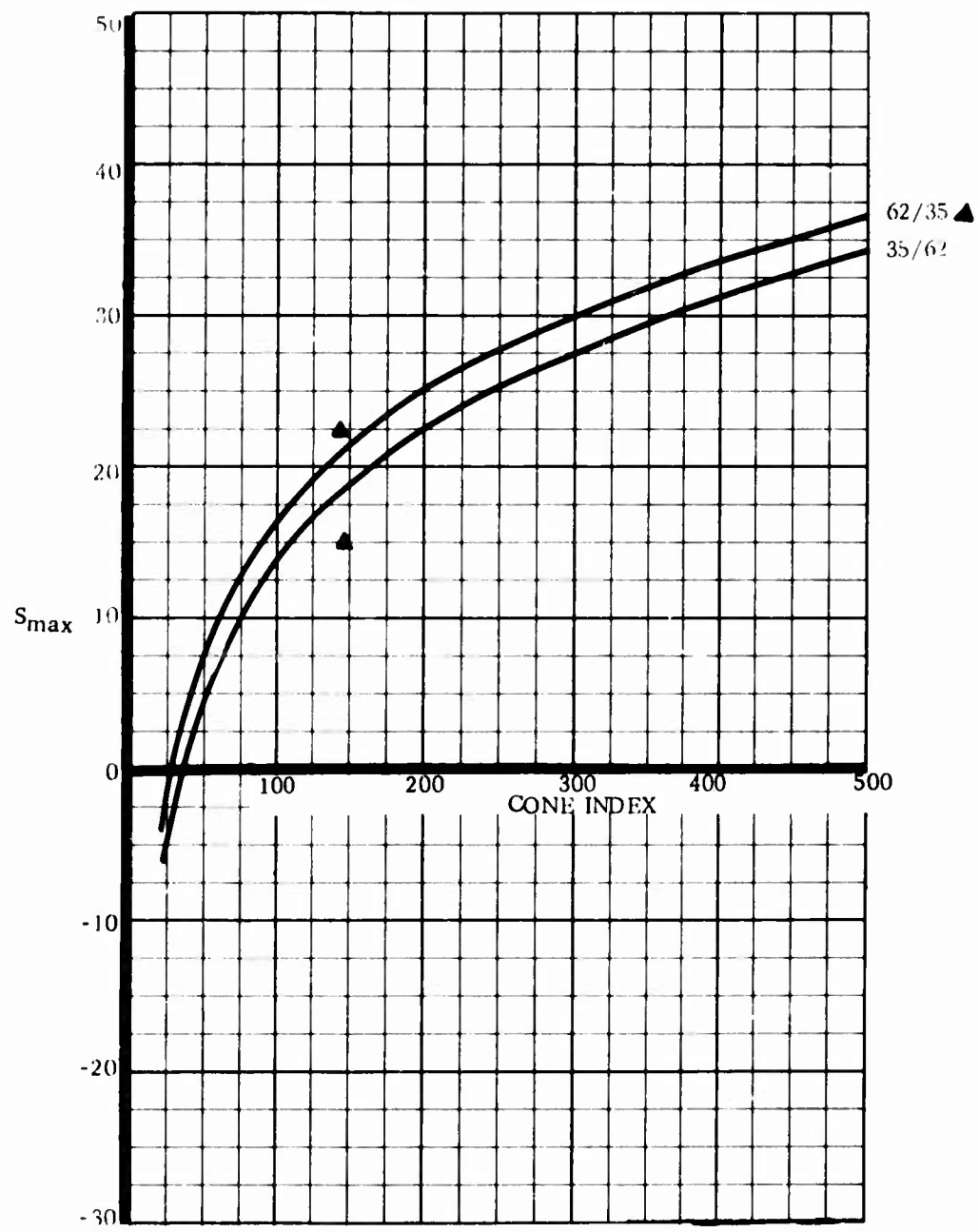
50K RTFLT



Graph 29

Radial Tires
No axle load

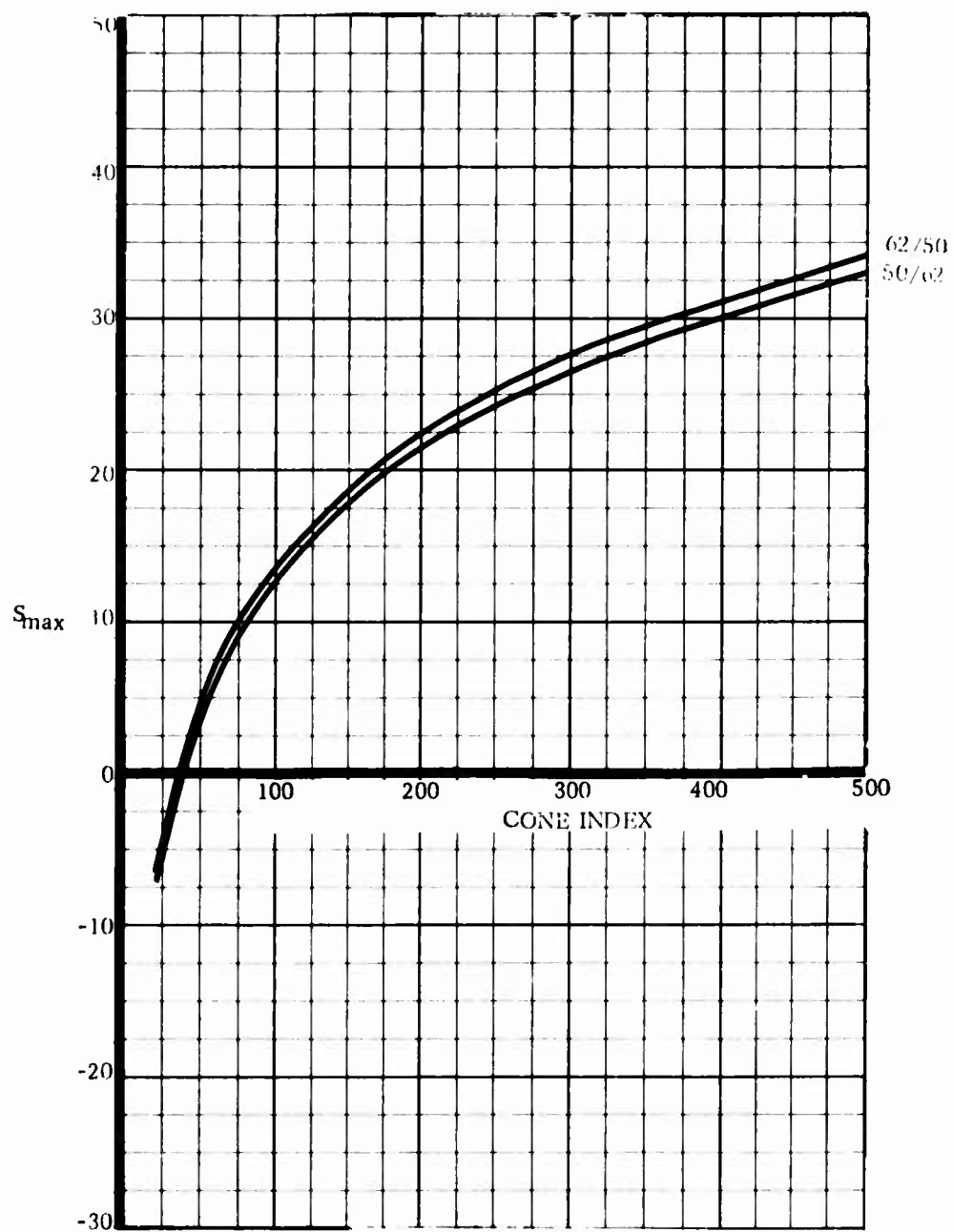
50K RTFLT



Graph 30

Radial Tires
No axle load

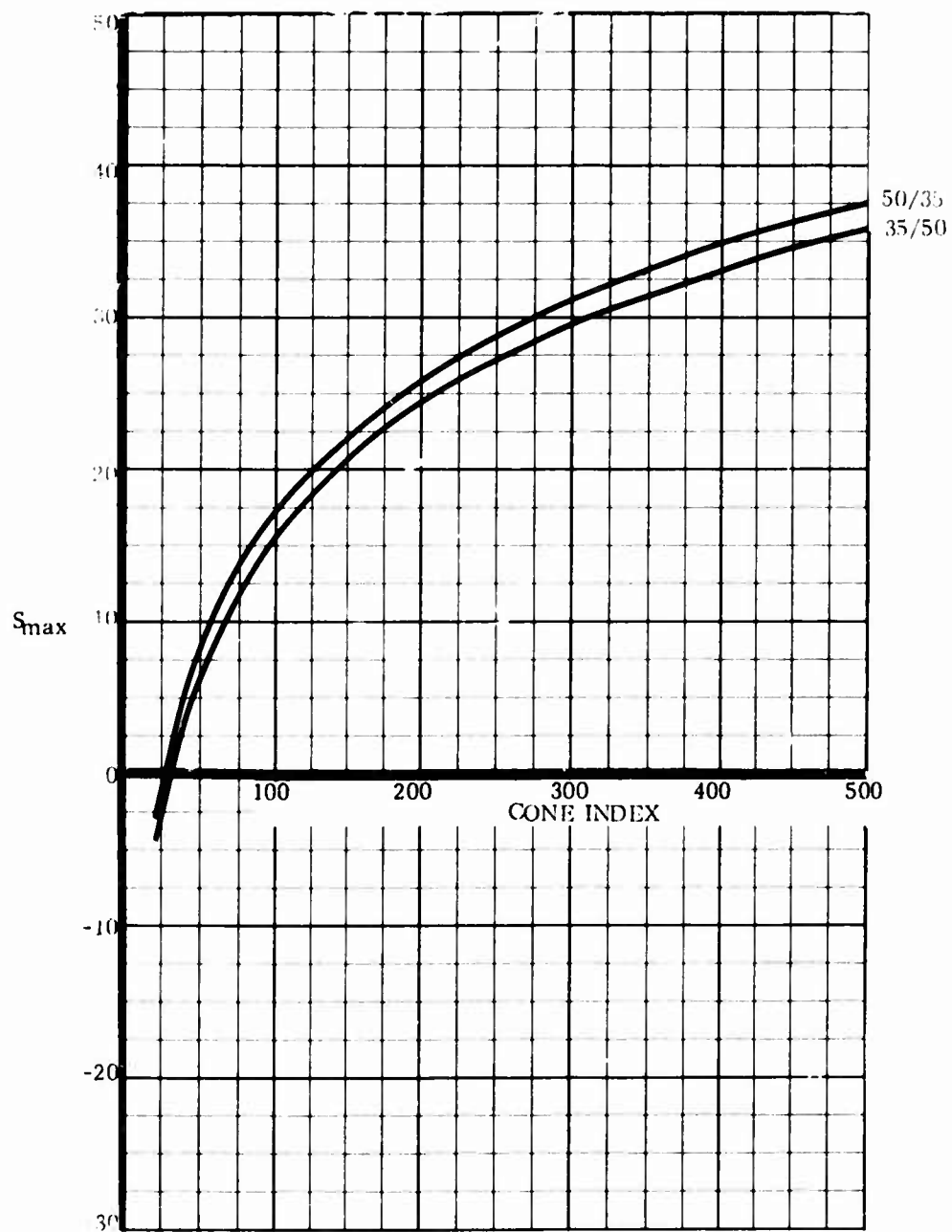
50 K RTFLT



Graph 31

Radial Tires
No axle load

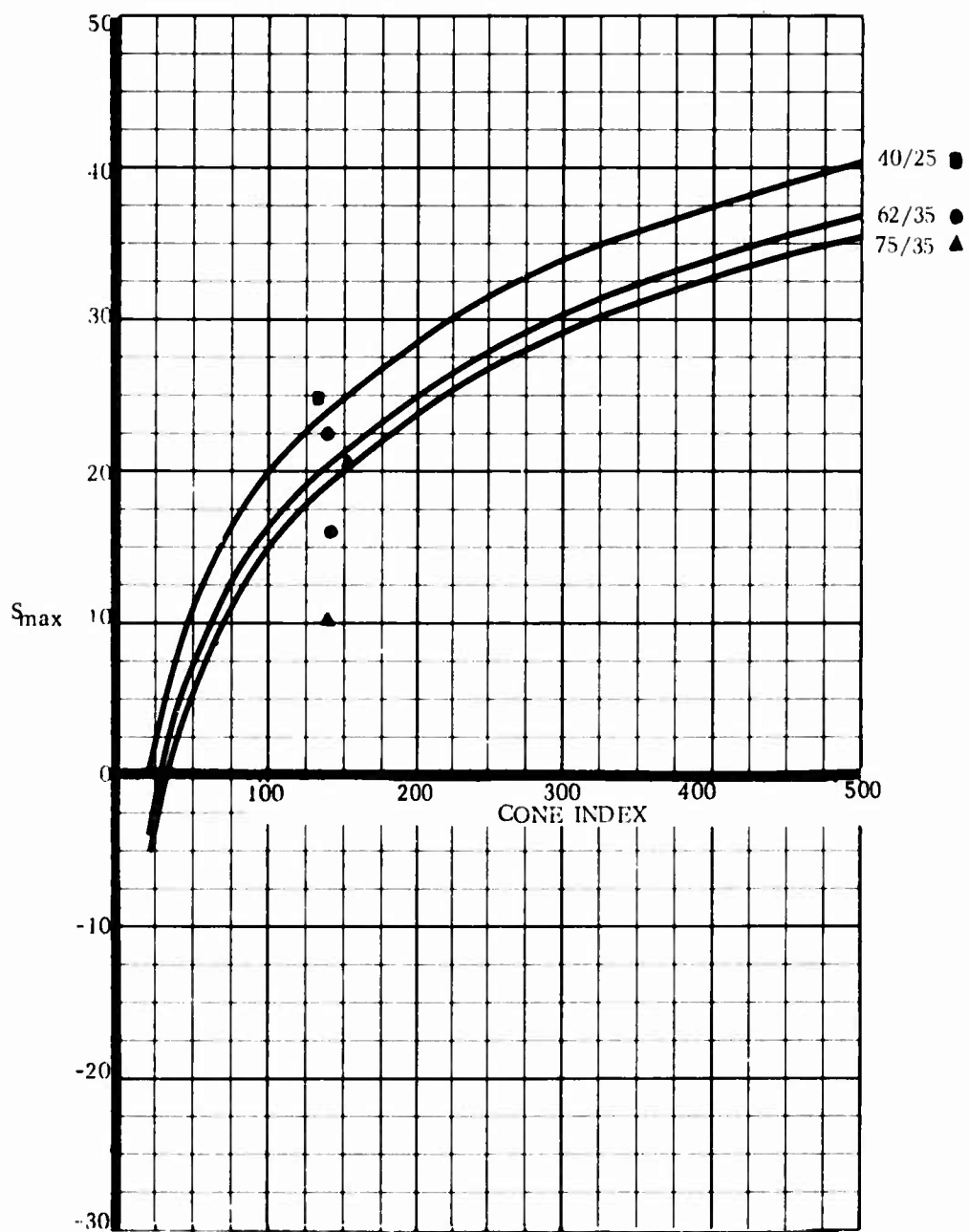
50 K RTFLT



Graph 32

Radial Tires
No axle load

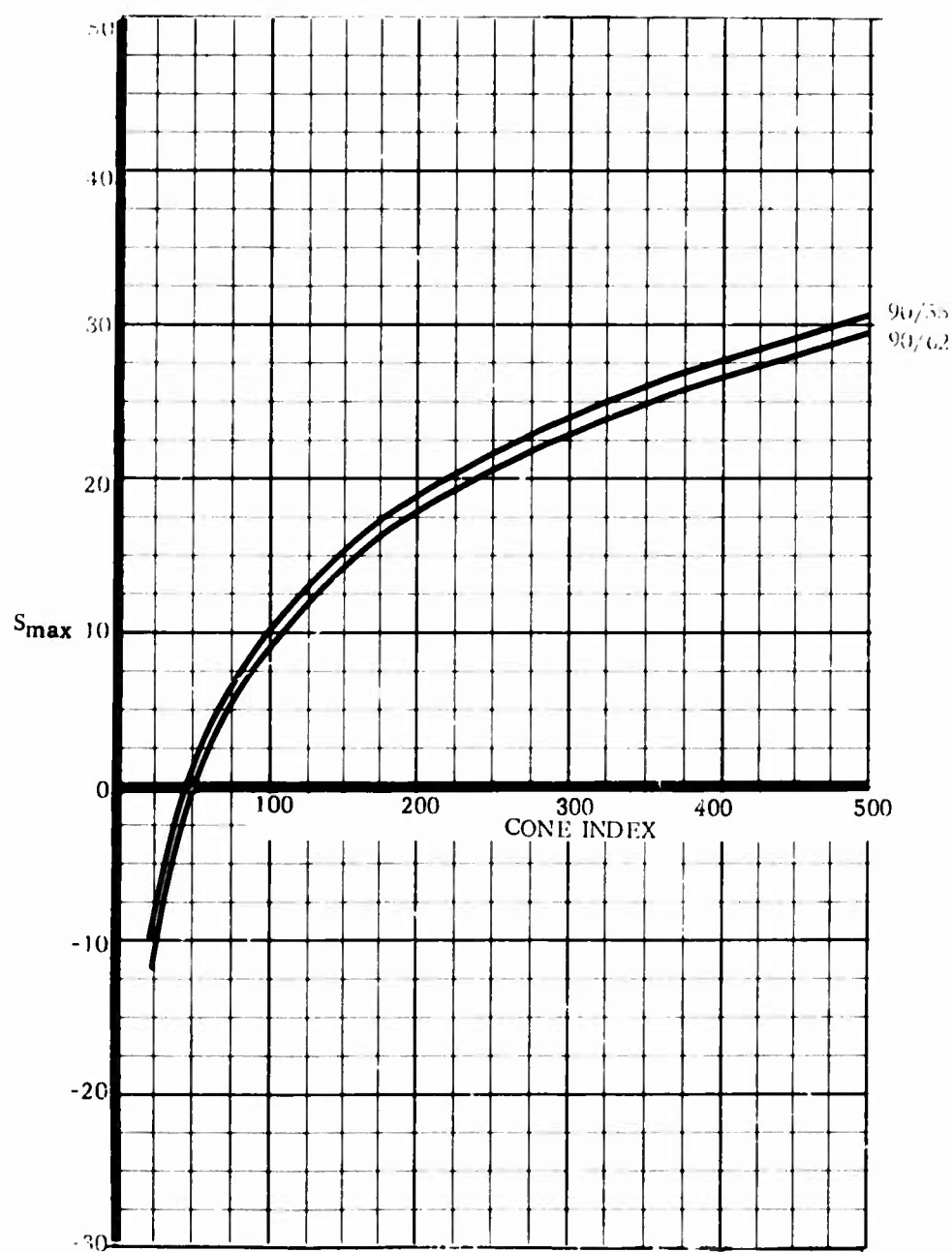
50K RTFLT



Graph 33

Radial Tires
No axle load

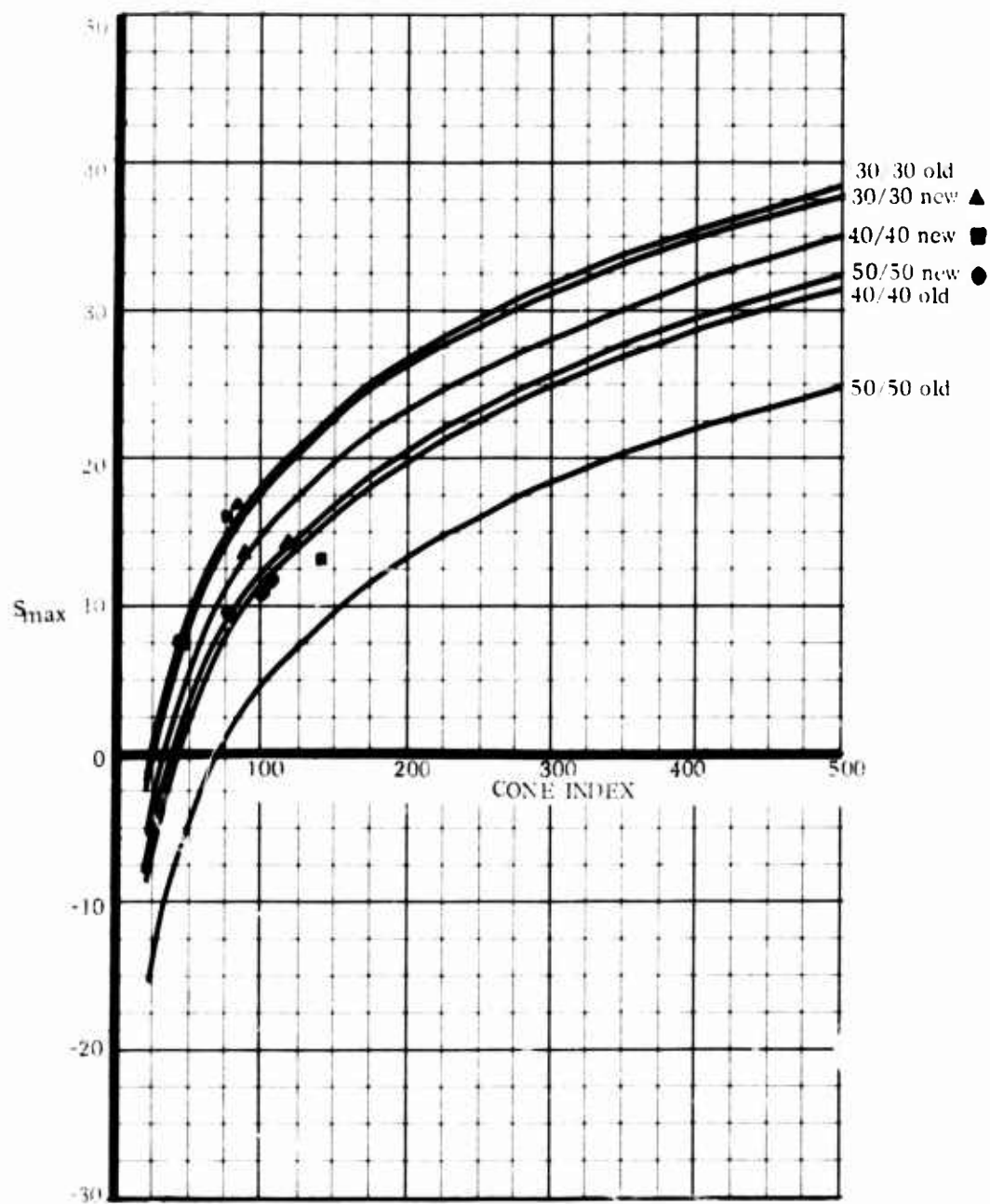
50K RTFLT



Graph 34

Radial Tires
No axle load

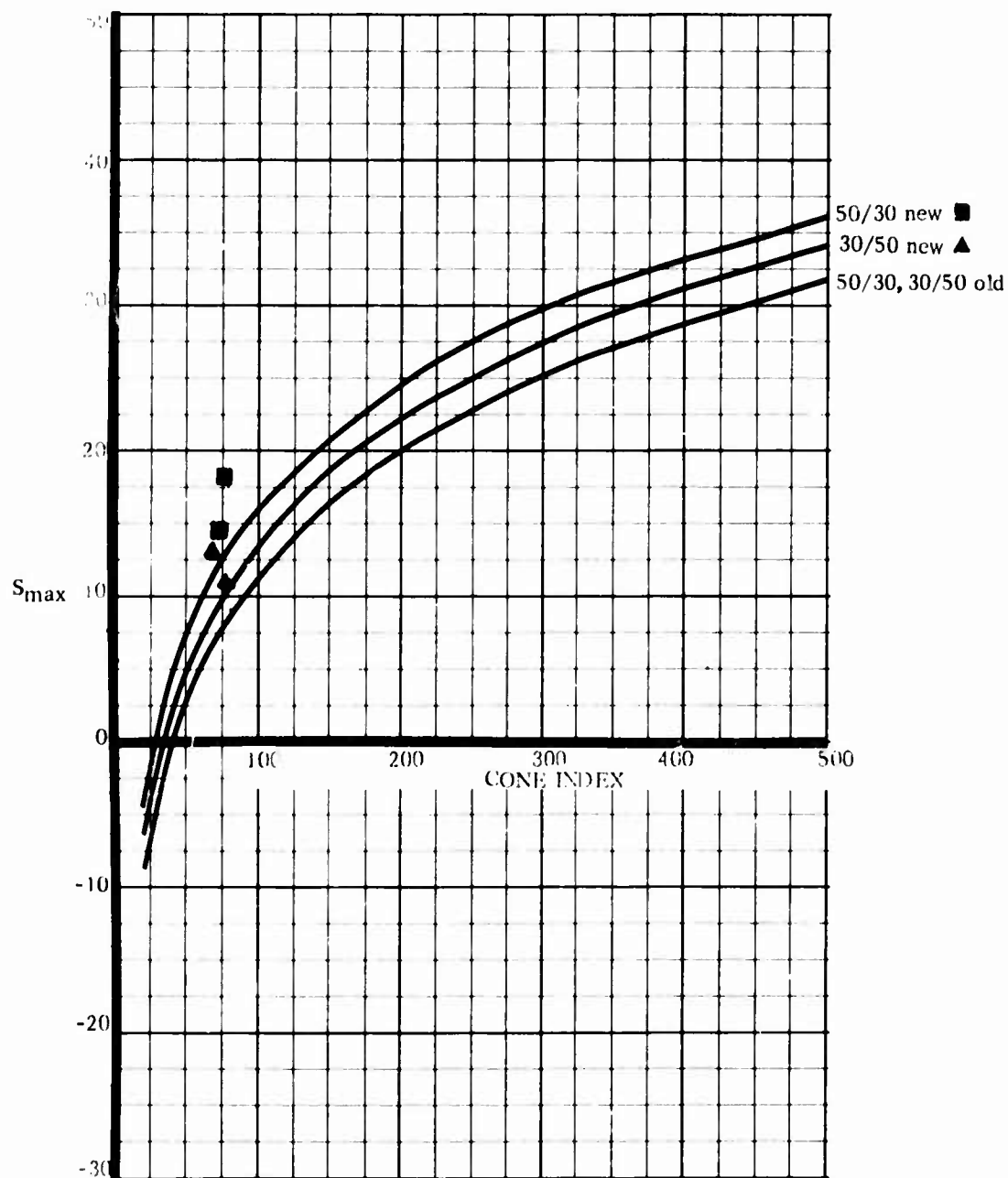
50K RTFLT



Graph 35

Standard Tires
Equal axle load

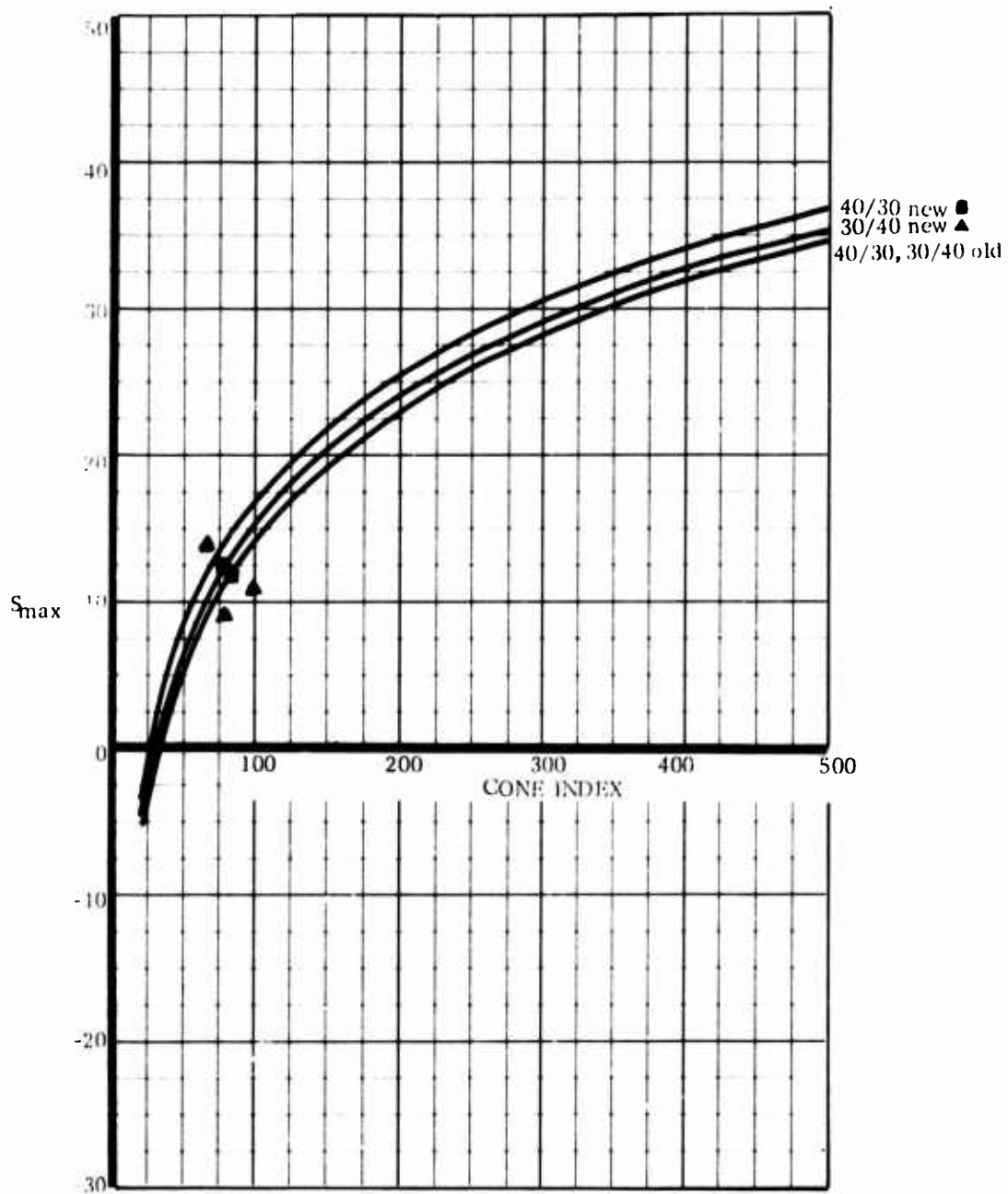
10K RTFLT



Graph 36

Standard Tires
Equal axle load

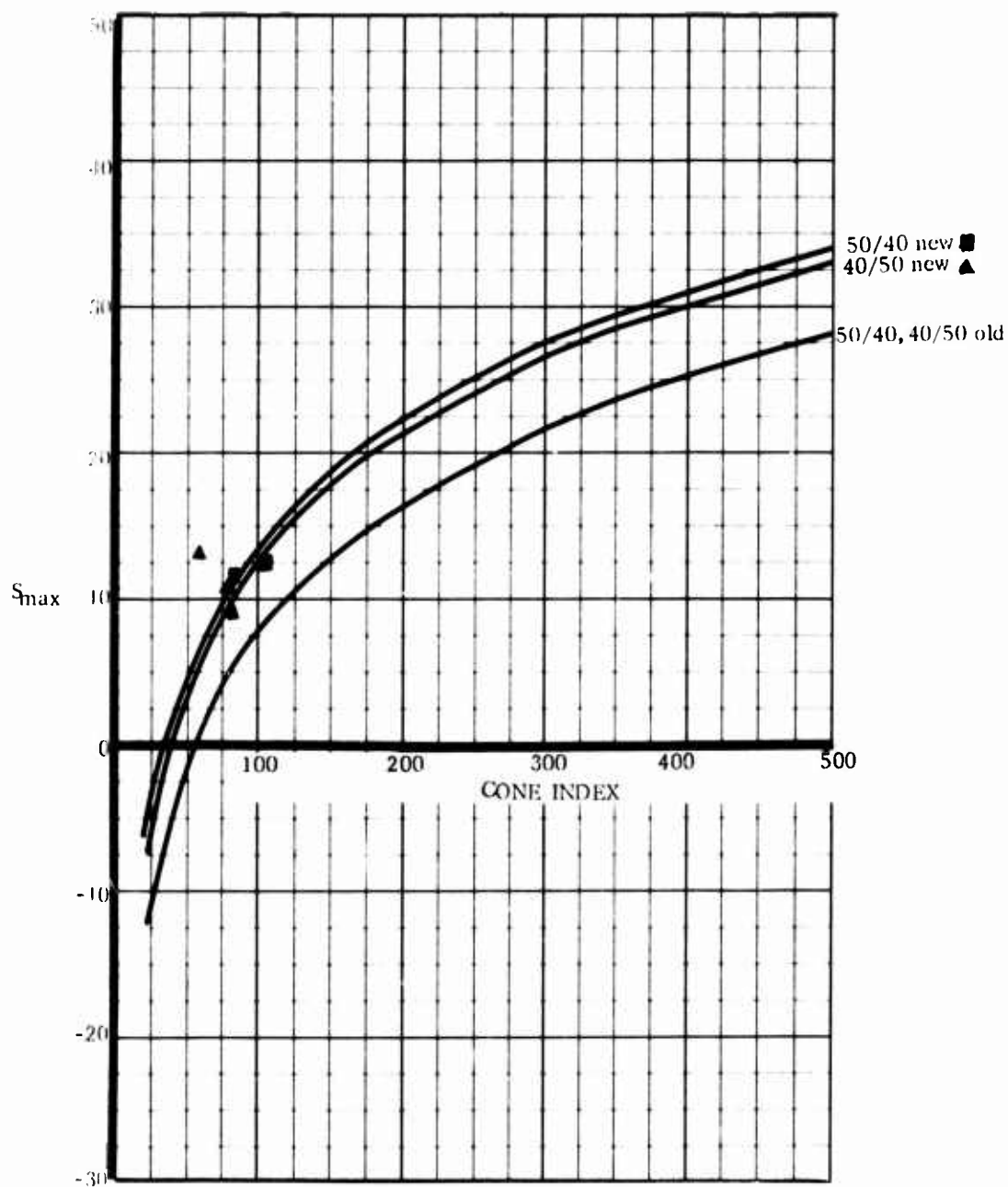
10K RTFLT



Graph 37

Standard Tires
Equal axle load

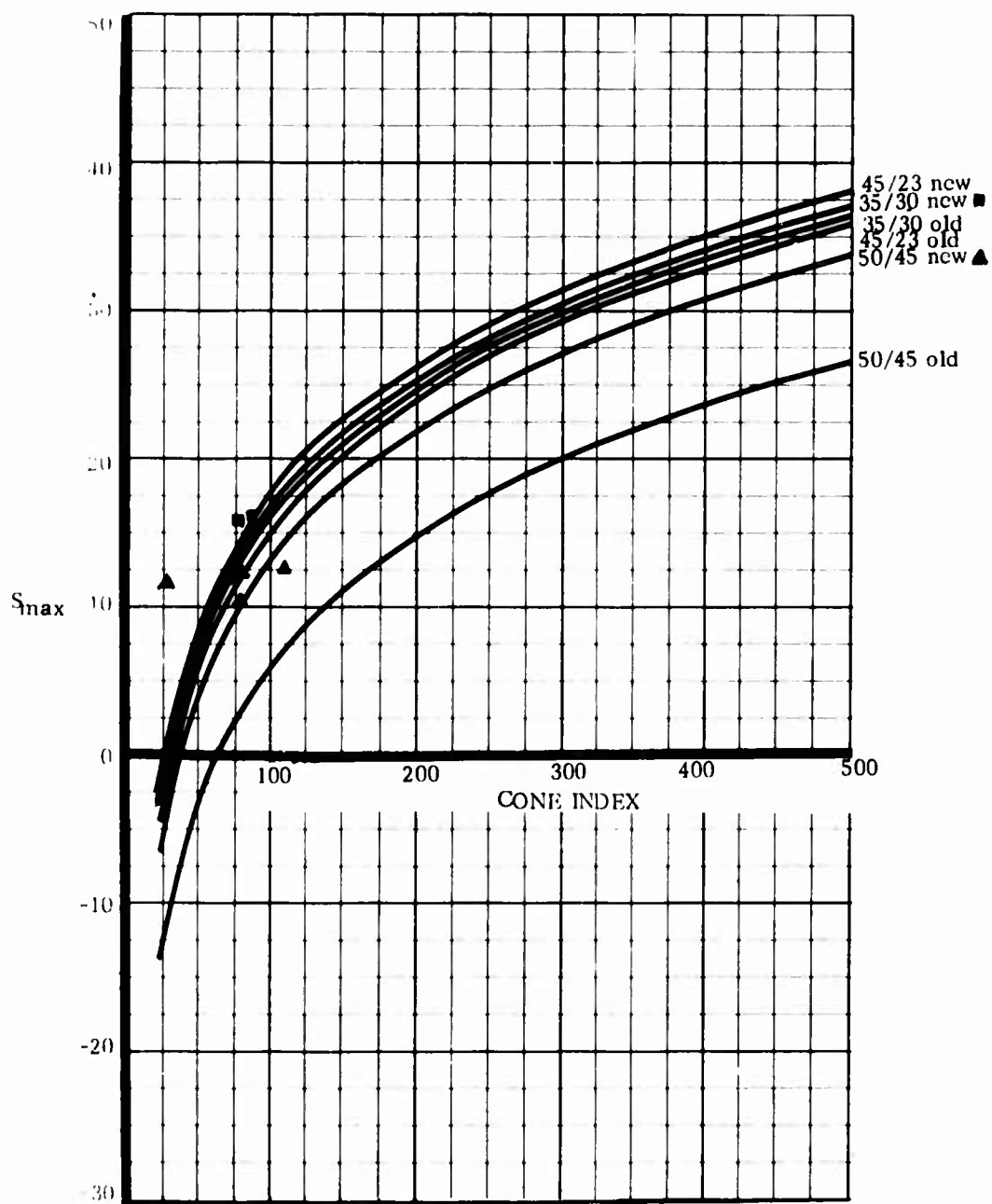
10K RTFLT



Graph 38

Standard Tires
Equal axle load

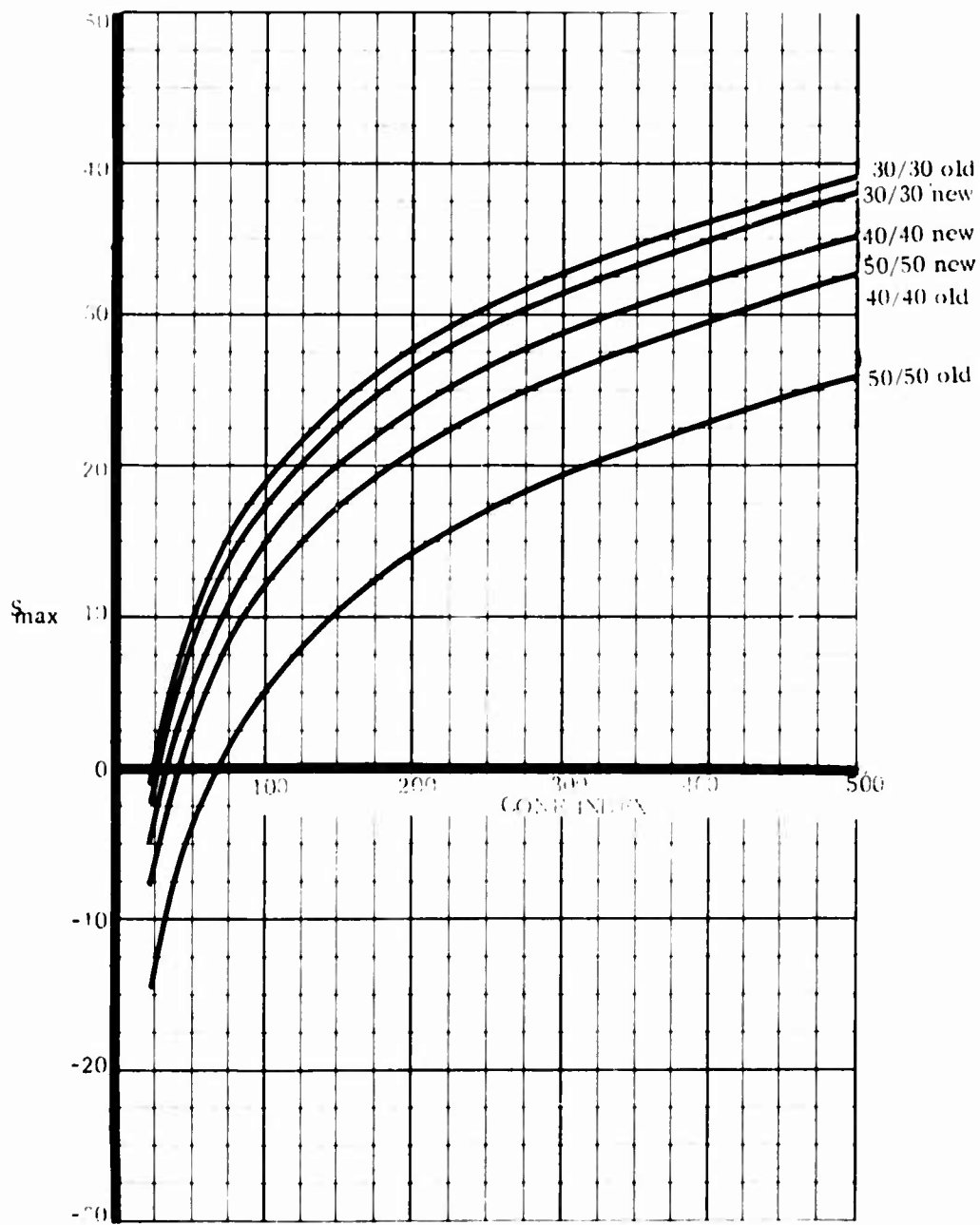
10K RTFL/T



Graph 39

Standard Tires
Equal axle load

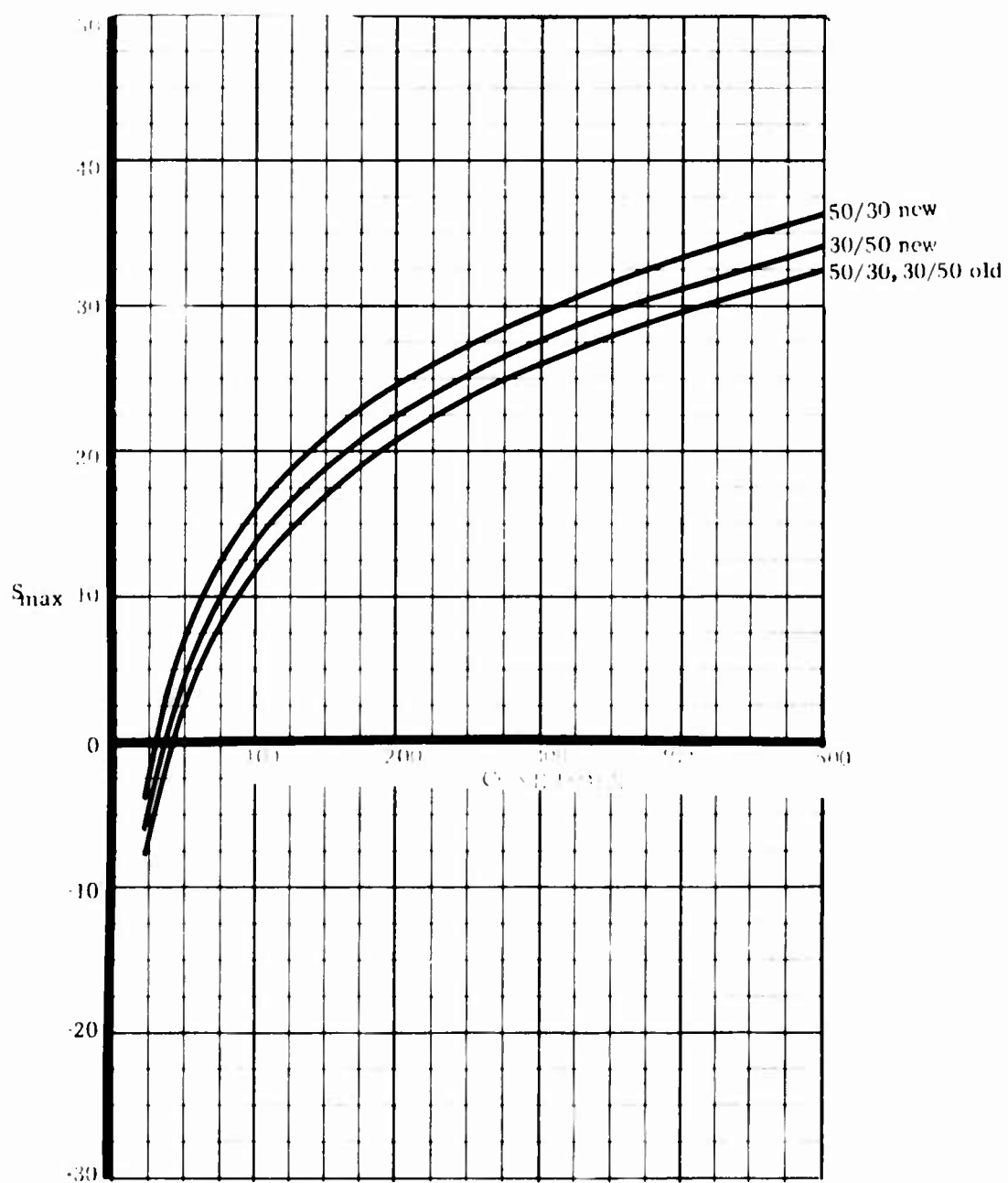
10K RTFLT



Graph 40

Standard Tires
Unequal axle load

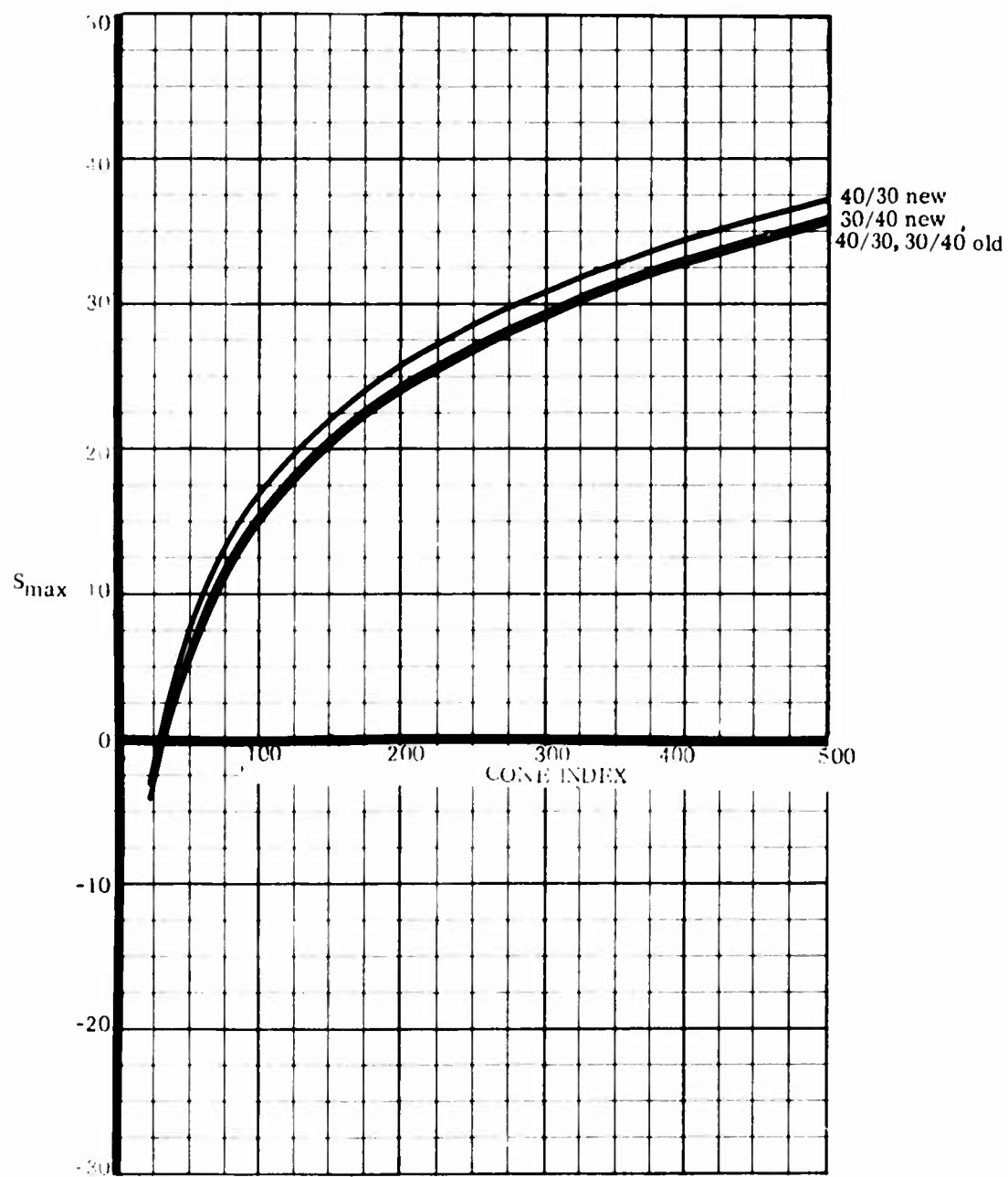
10K RTFLT



Graph 41

Standard Tires
Unequal axle load

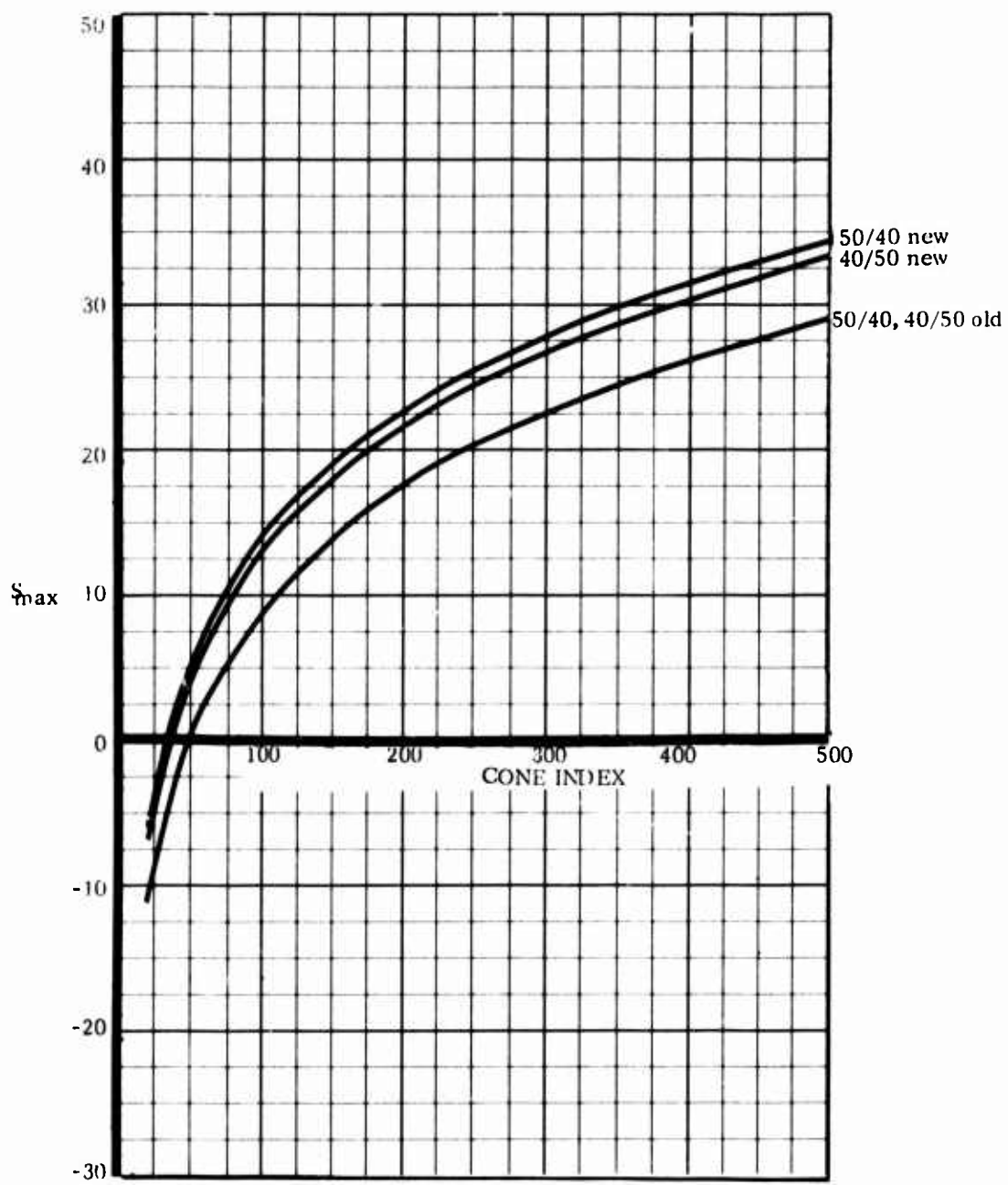
10K RTFLT



Graph 42

Standard Tires
Unequal axle load

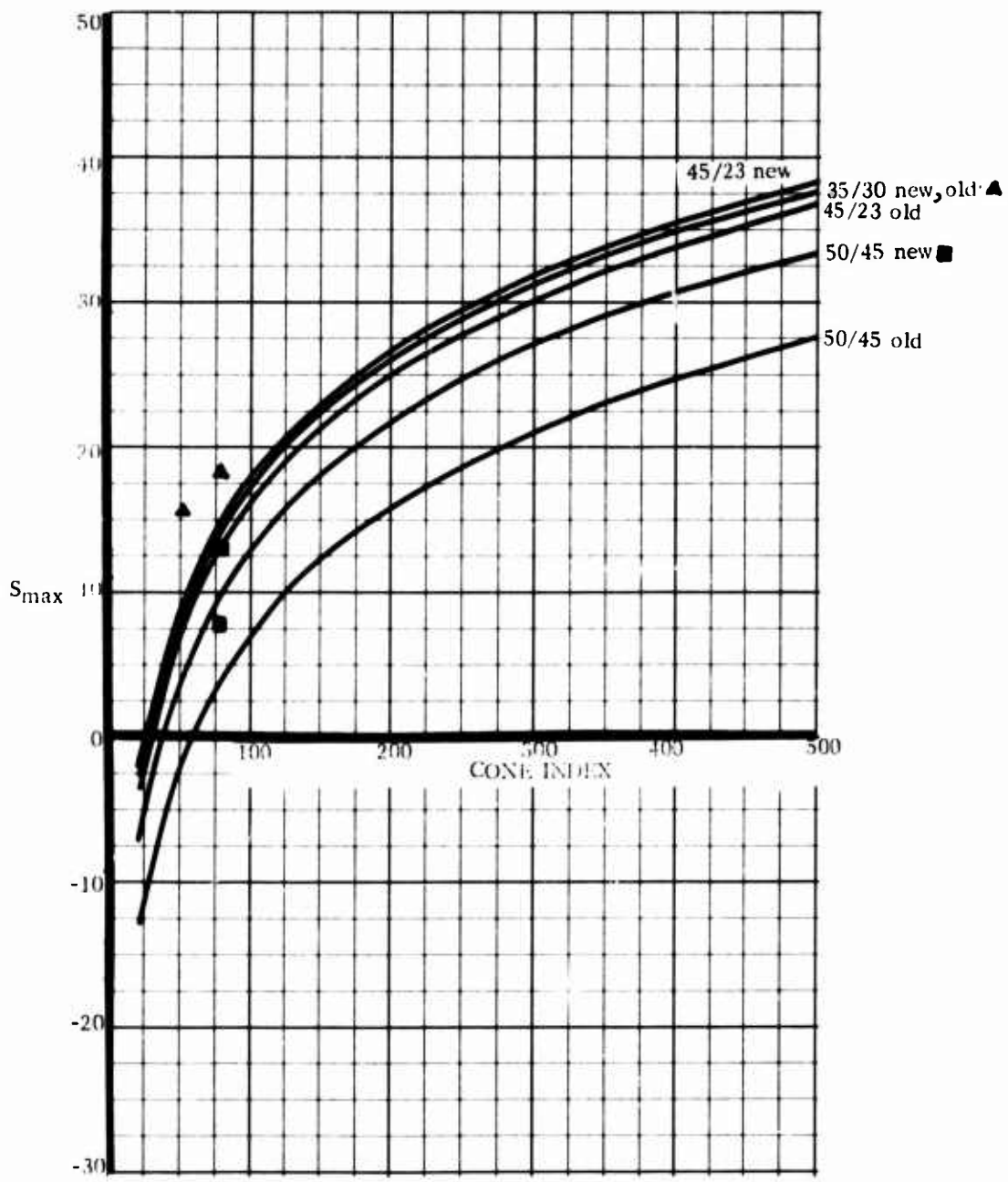
10K RTFLT



Graph 43

Standard Tires
Unequal axle load

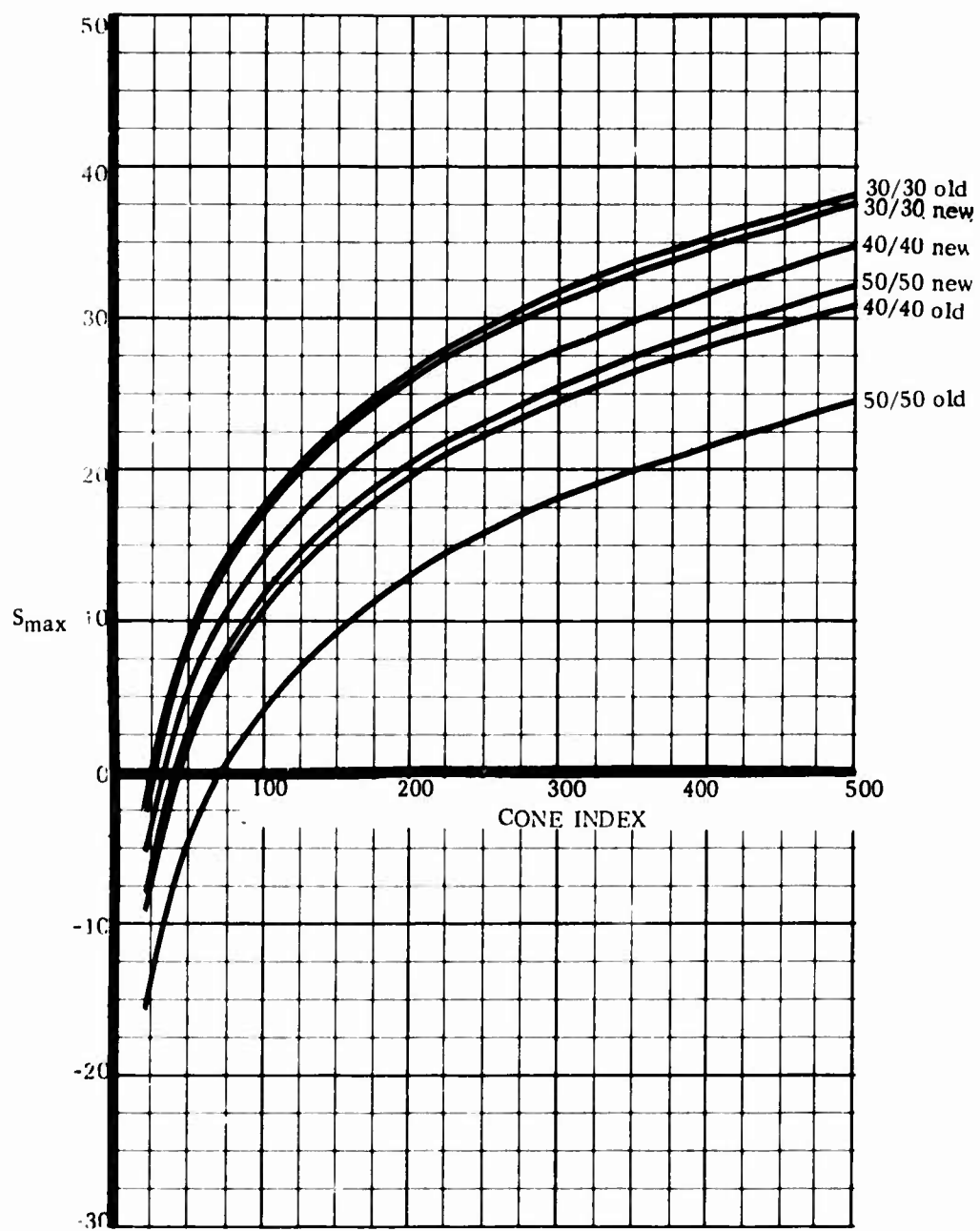
10K RTFLT



Graph 44

Standard Tires
Unequal axle load

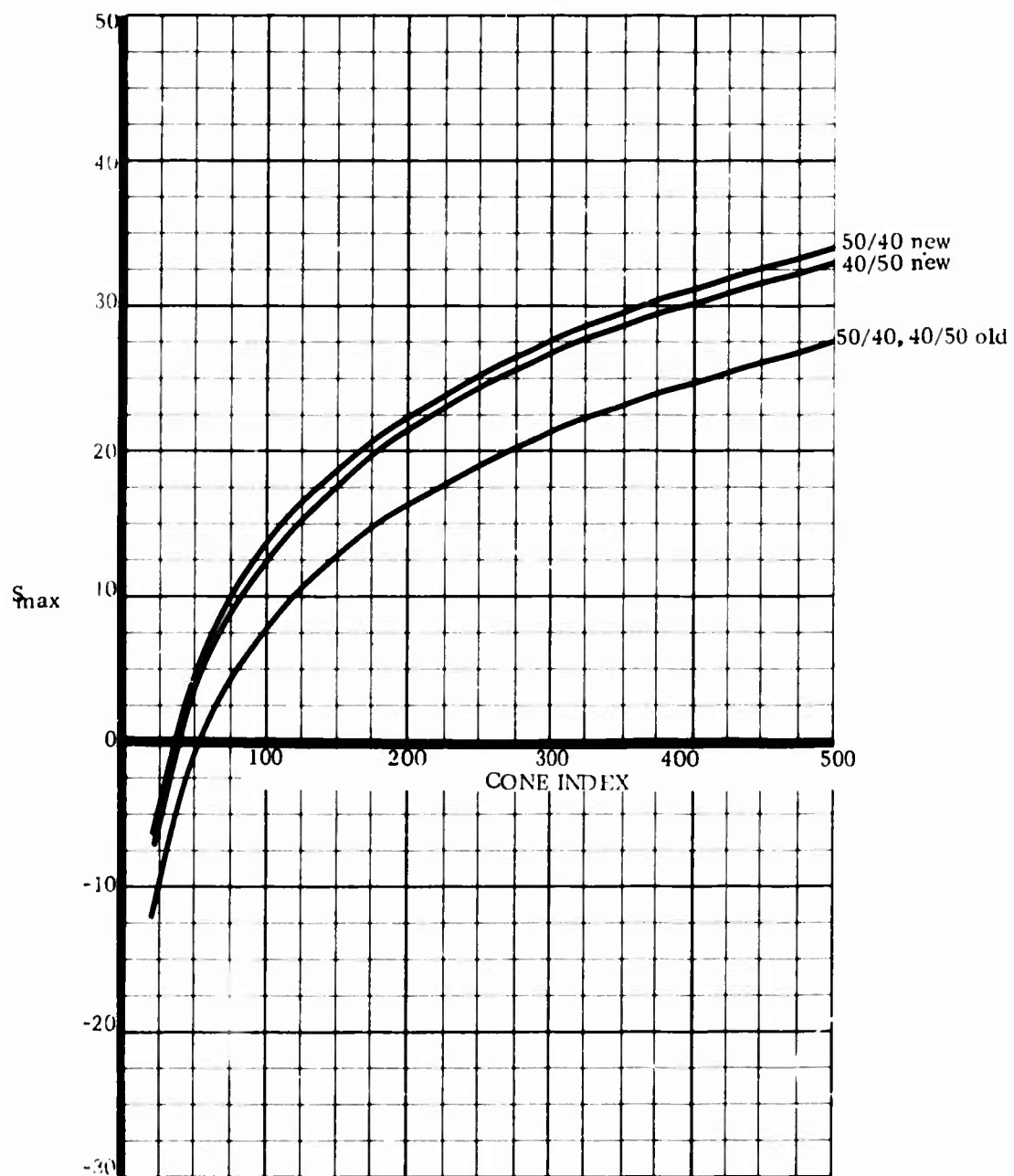
10K RTFLT



Graph 45

Standard Tires
No axle load

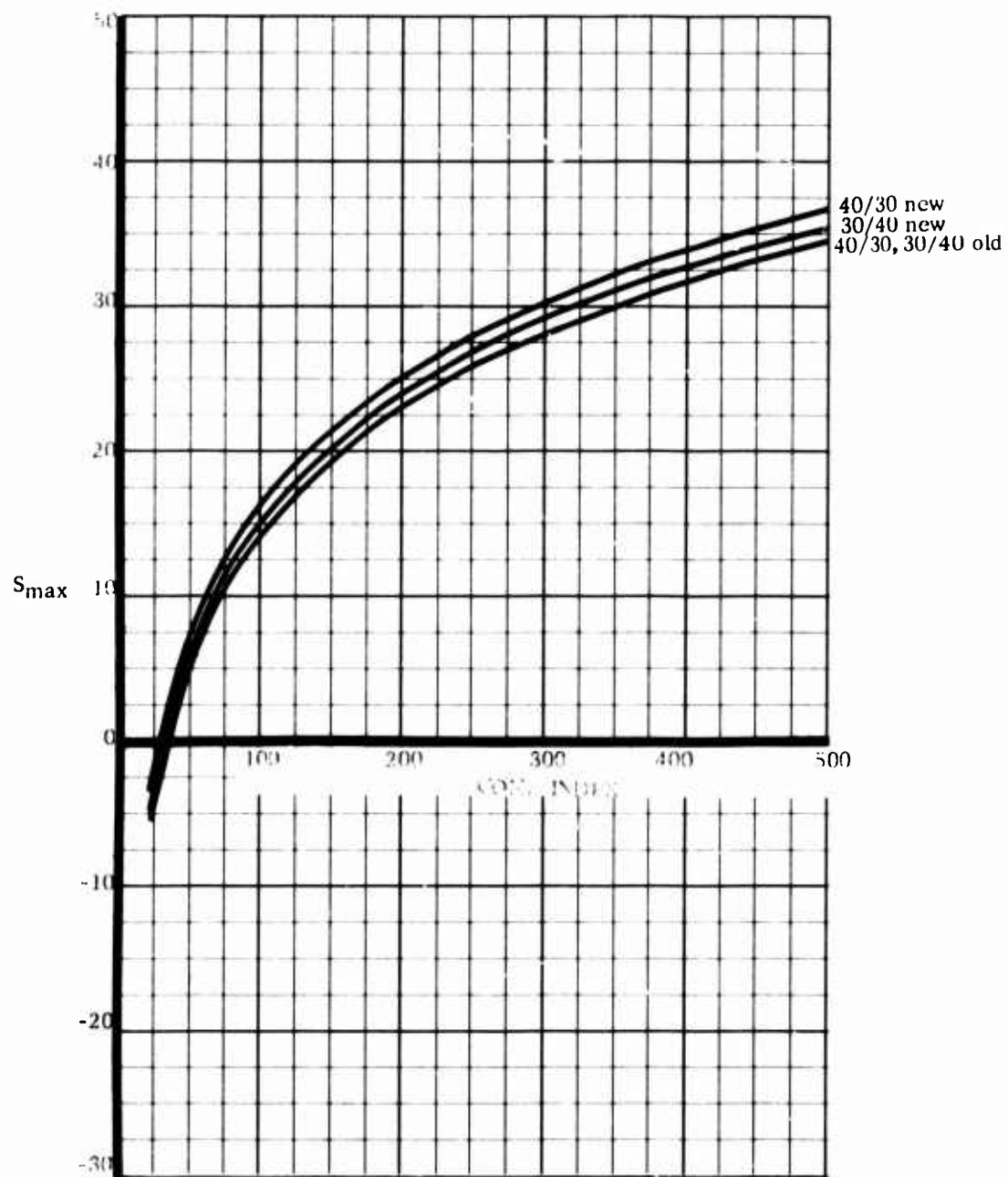
10K RTFLT



Graph 46

Standard Tires
No axle load

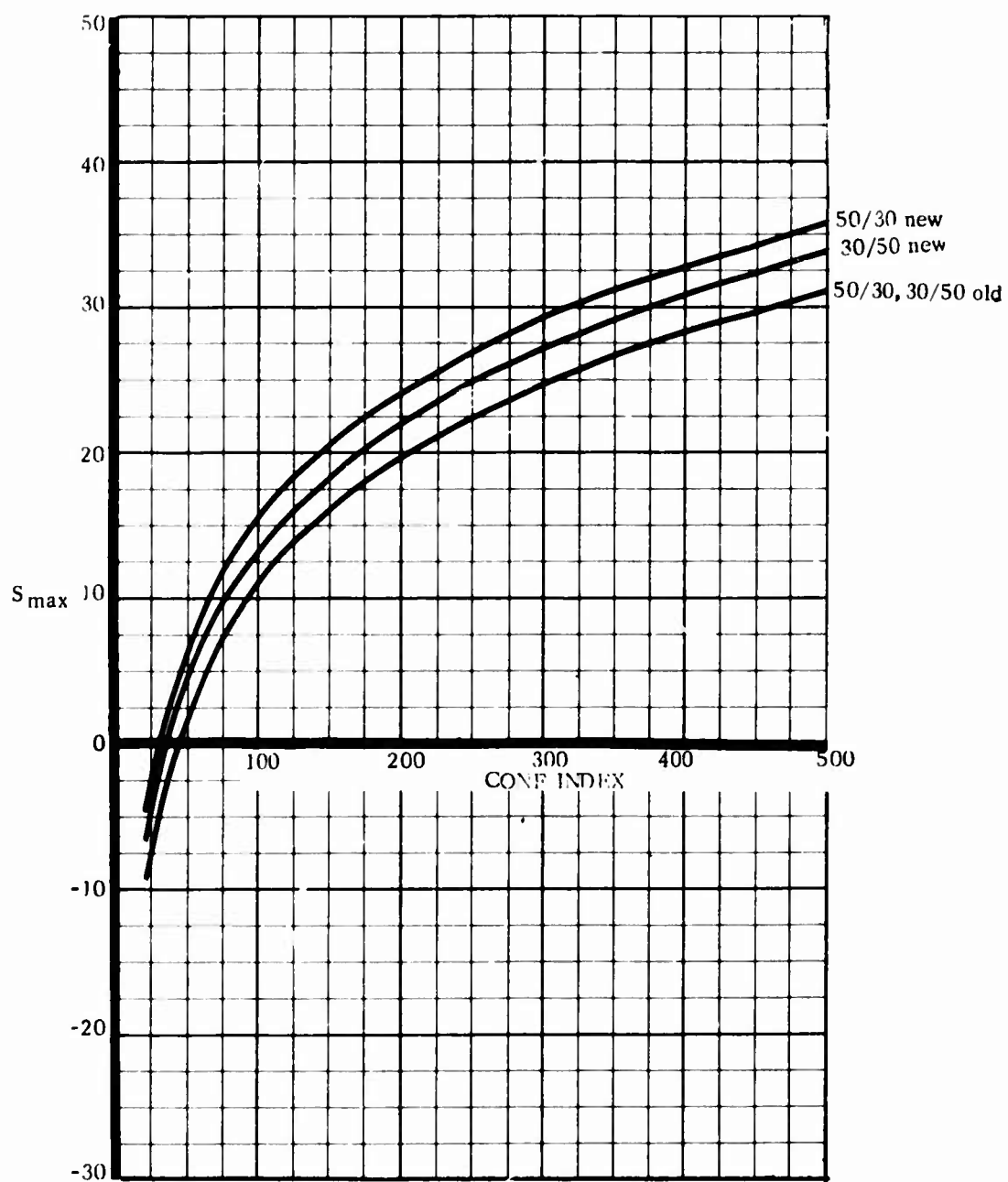
10K RTFLT



Graph 47

Standard Tires
No axle load

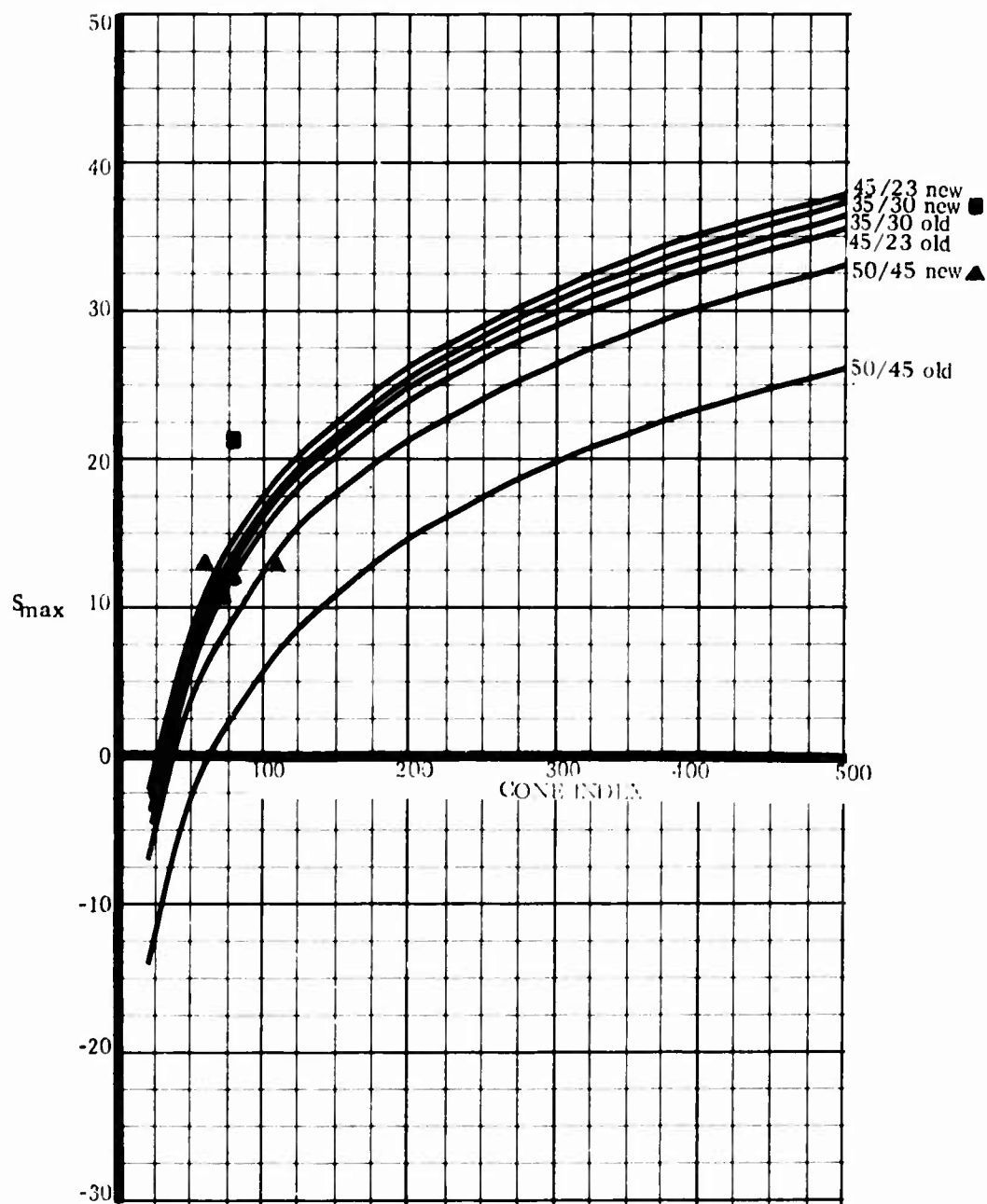
10K RTFLT



Graph 48

Standard Tires
No axle load

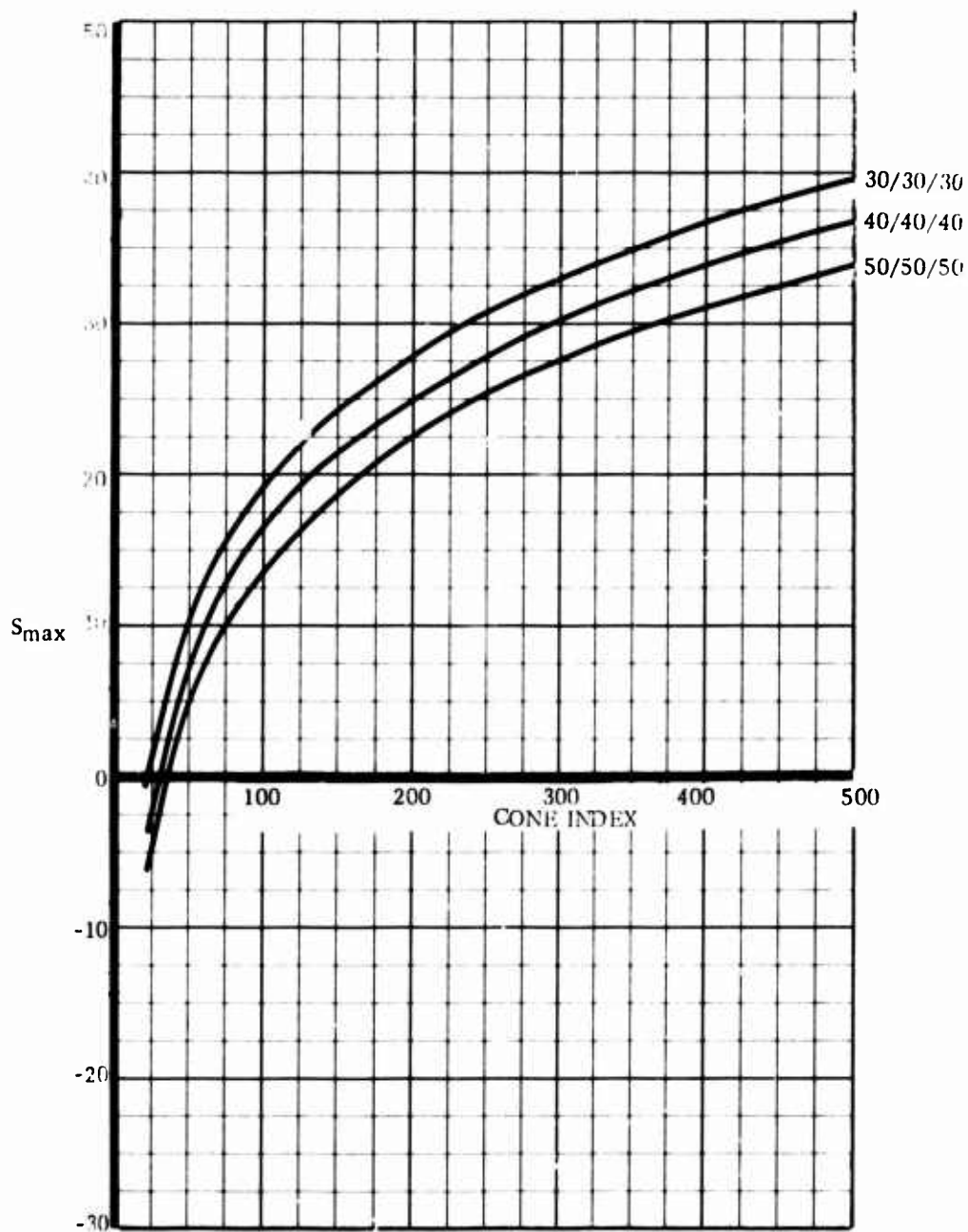
10K RTFLT



Graph 49

Standard Tires
No axle load

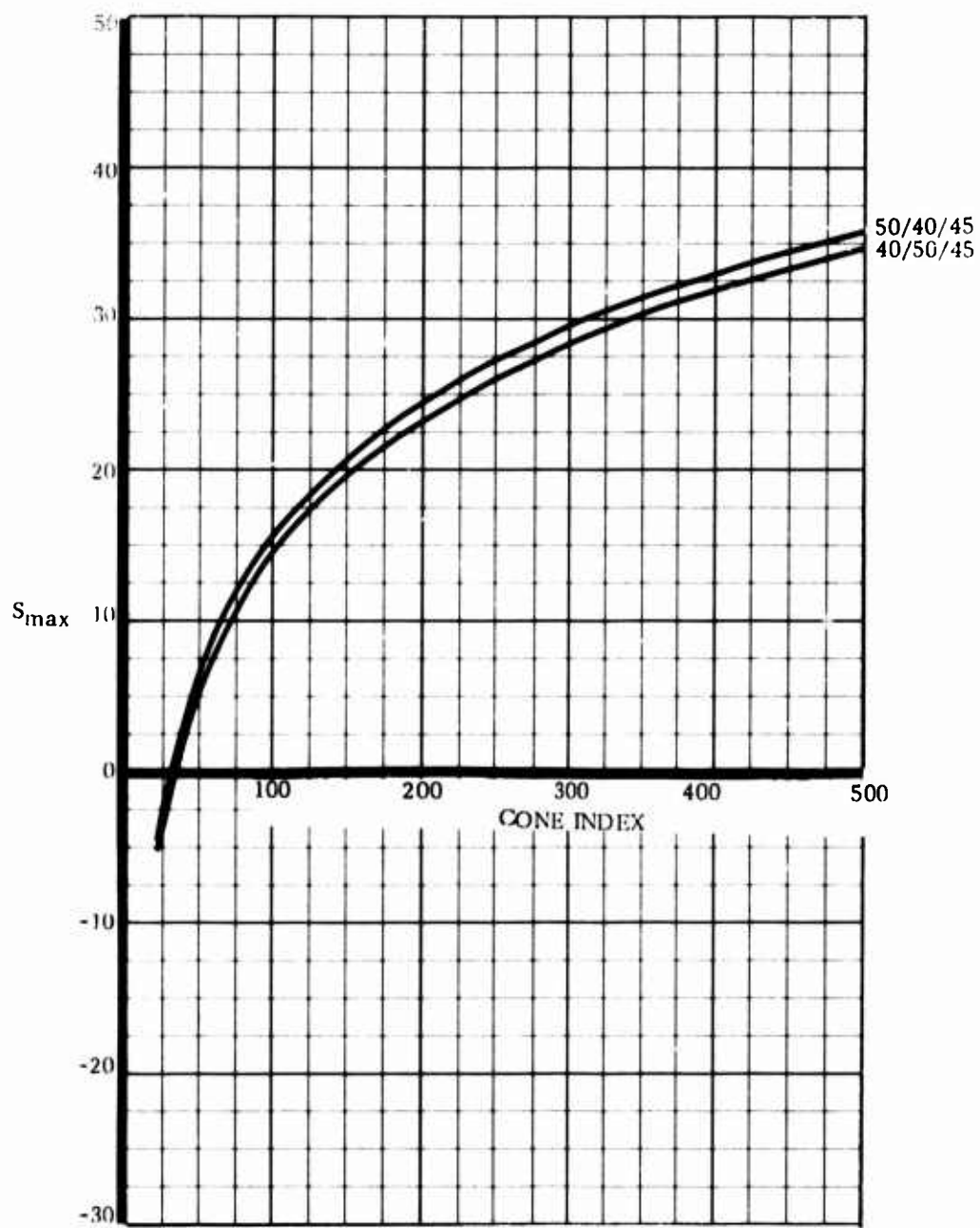
10K RTFLT



Graph 50

Radial Tires
Equal axle load

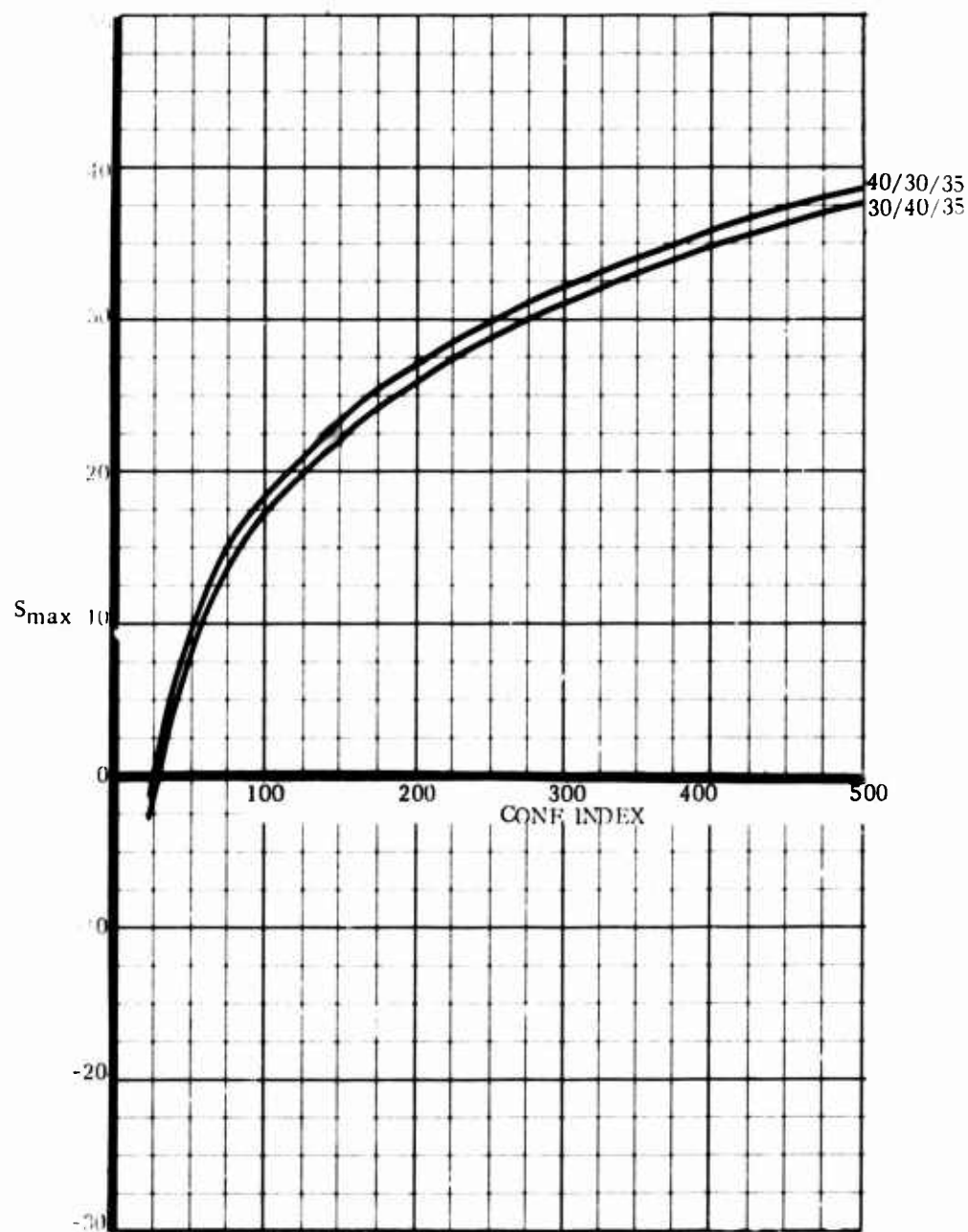
10K RTFLT



Graph 51

Radial Tires
Equal axle load

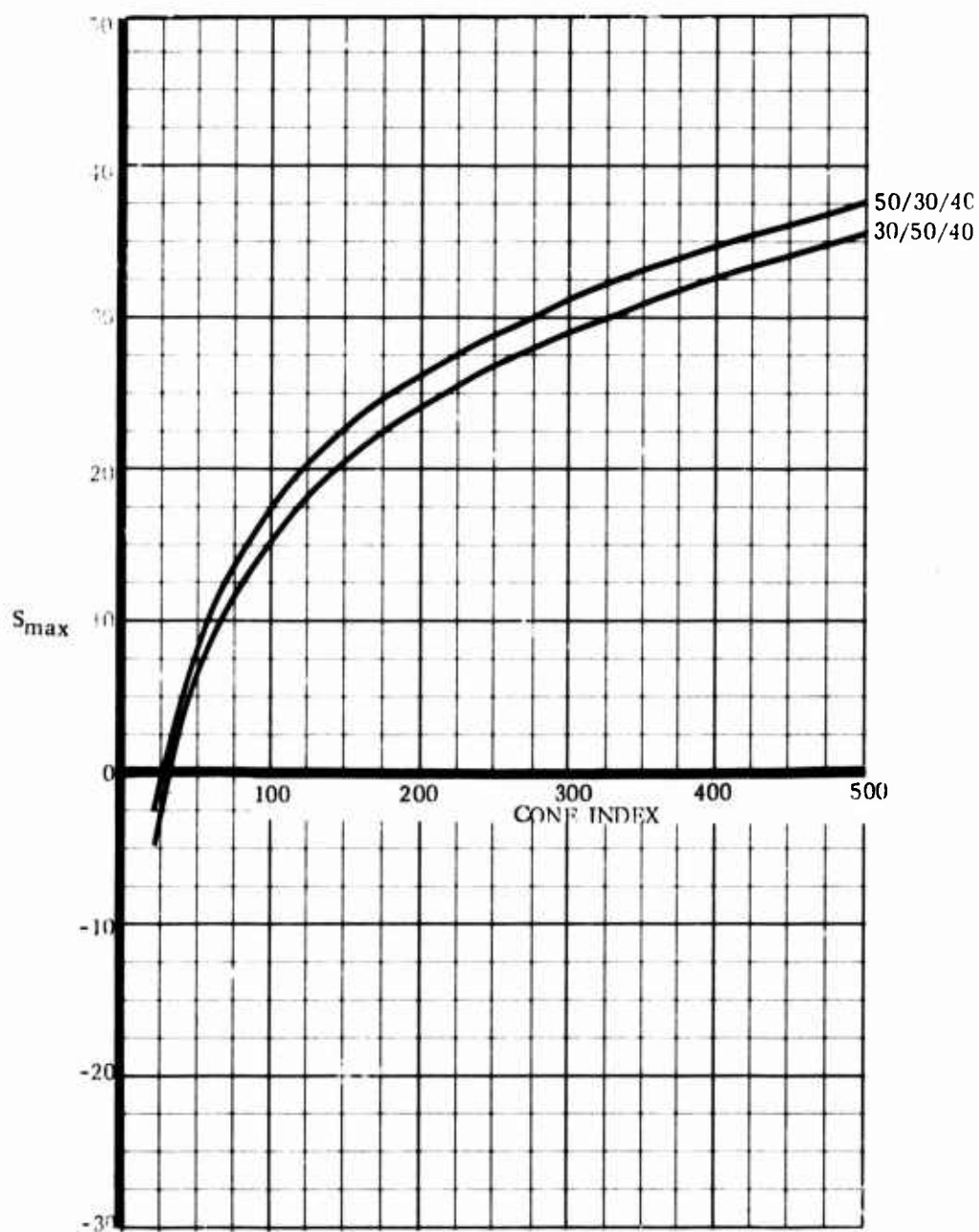
10K RTFLT



Graph 52

Radial Tires
Equal axle load

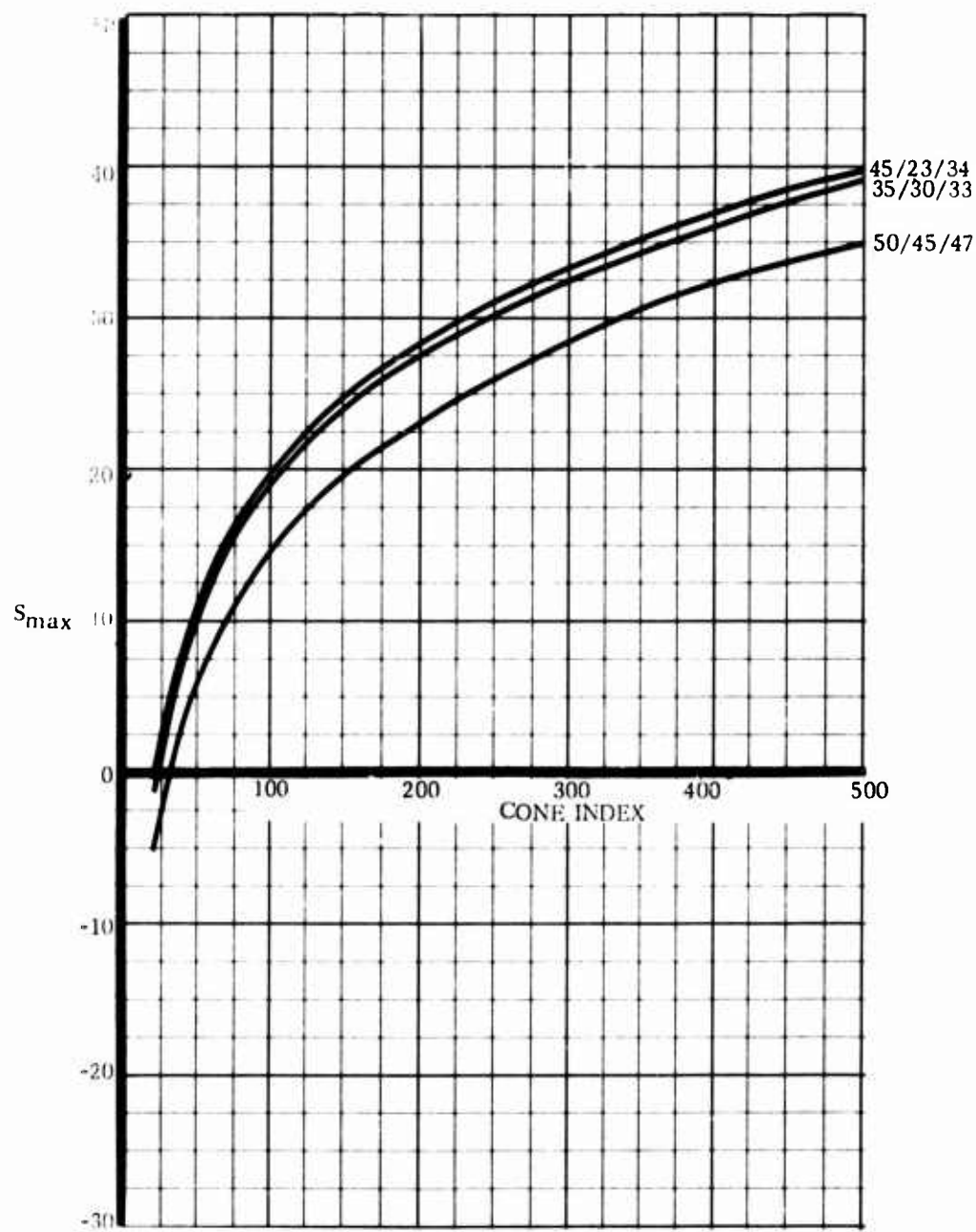
10K RTFLT



Graph 53

Radial Tires
Equal axle load

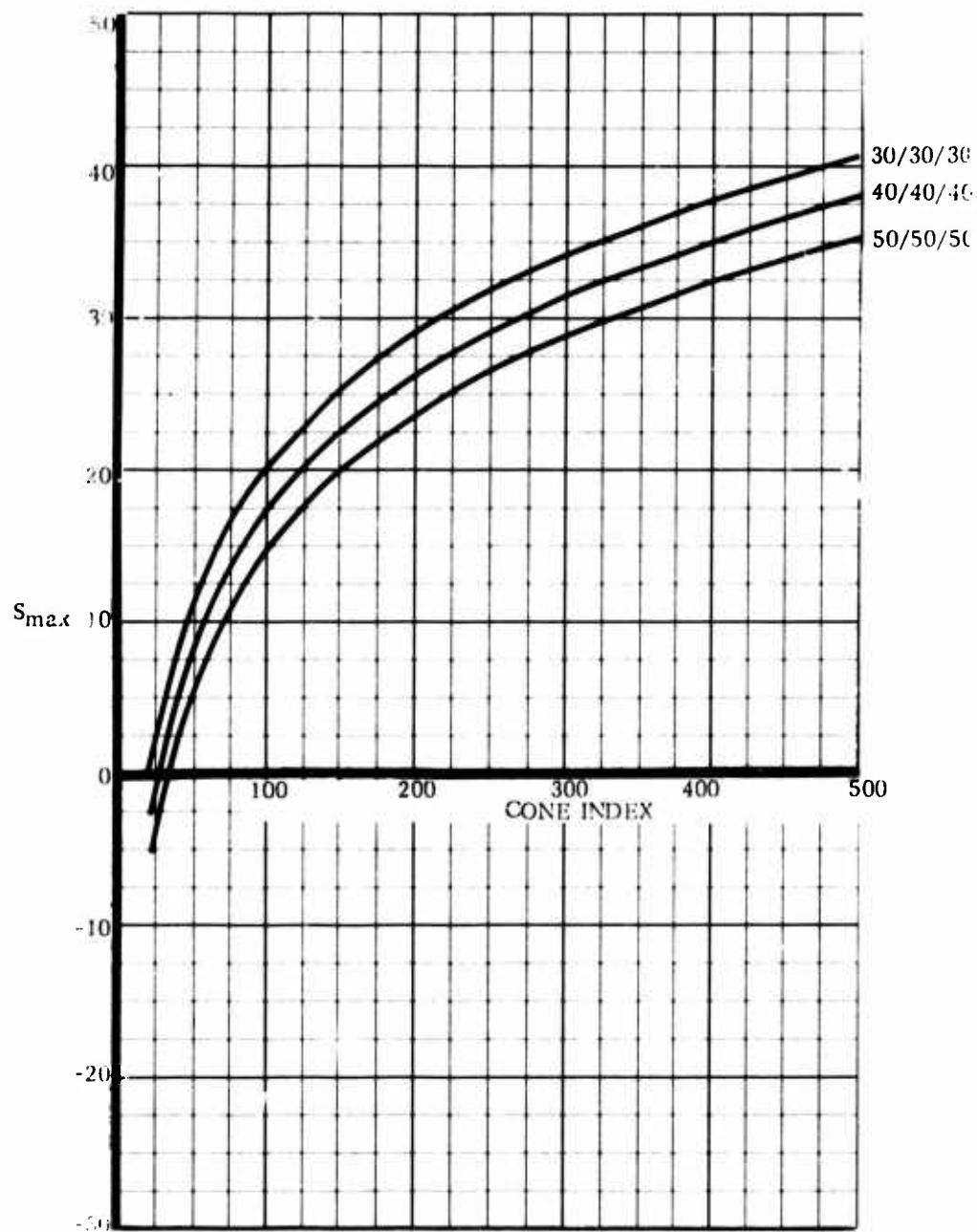
10K RTFLT



Graph 54

Radial Tires
Equal axle load

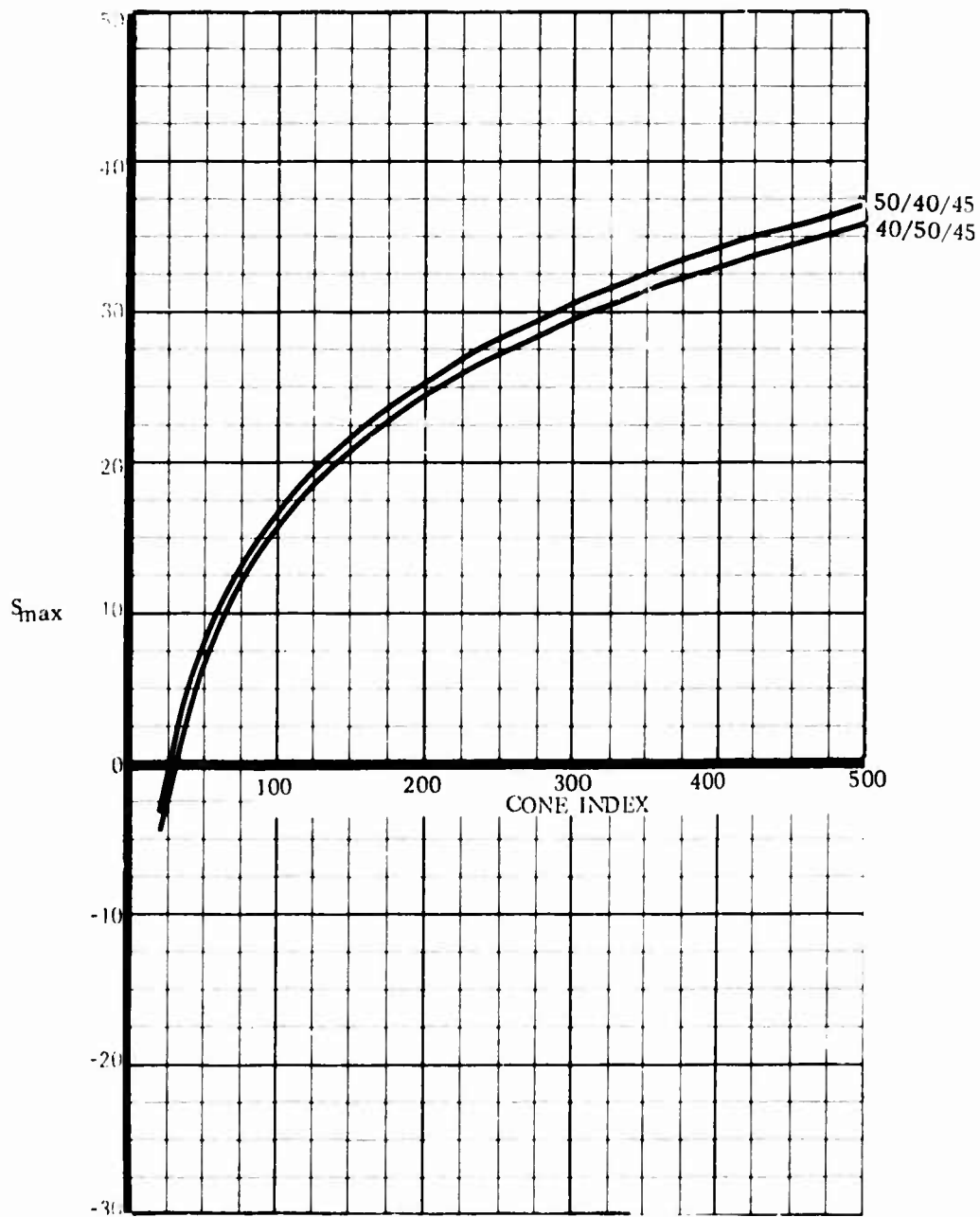
10K RTFLT



Graph 55

Radial Tires
Unequal axle load

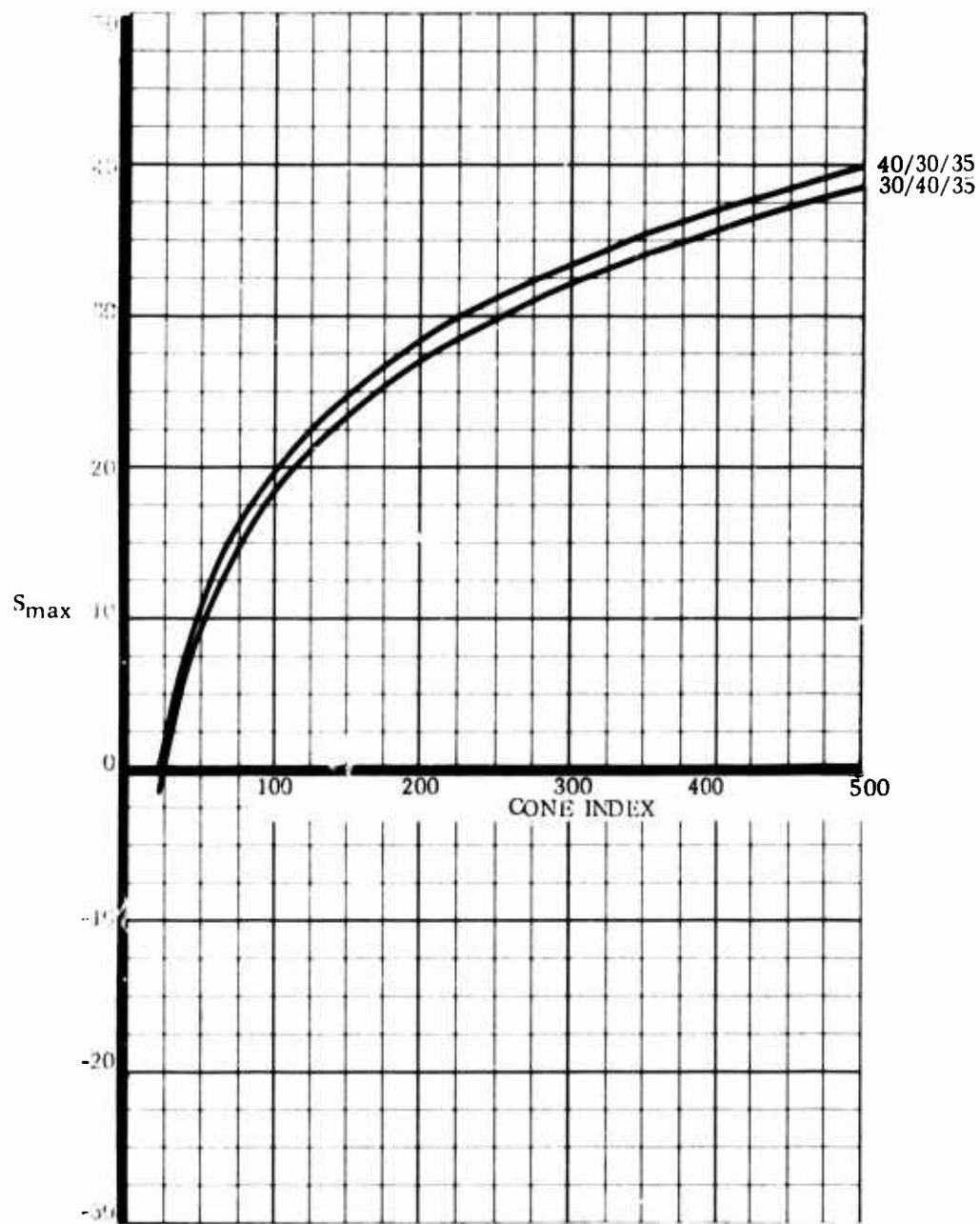
10K RTFLT



Graph 56

Radial Tires
Unequal axle load

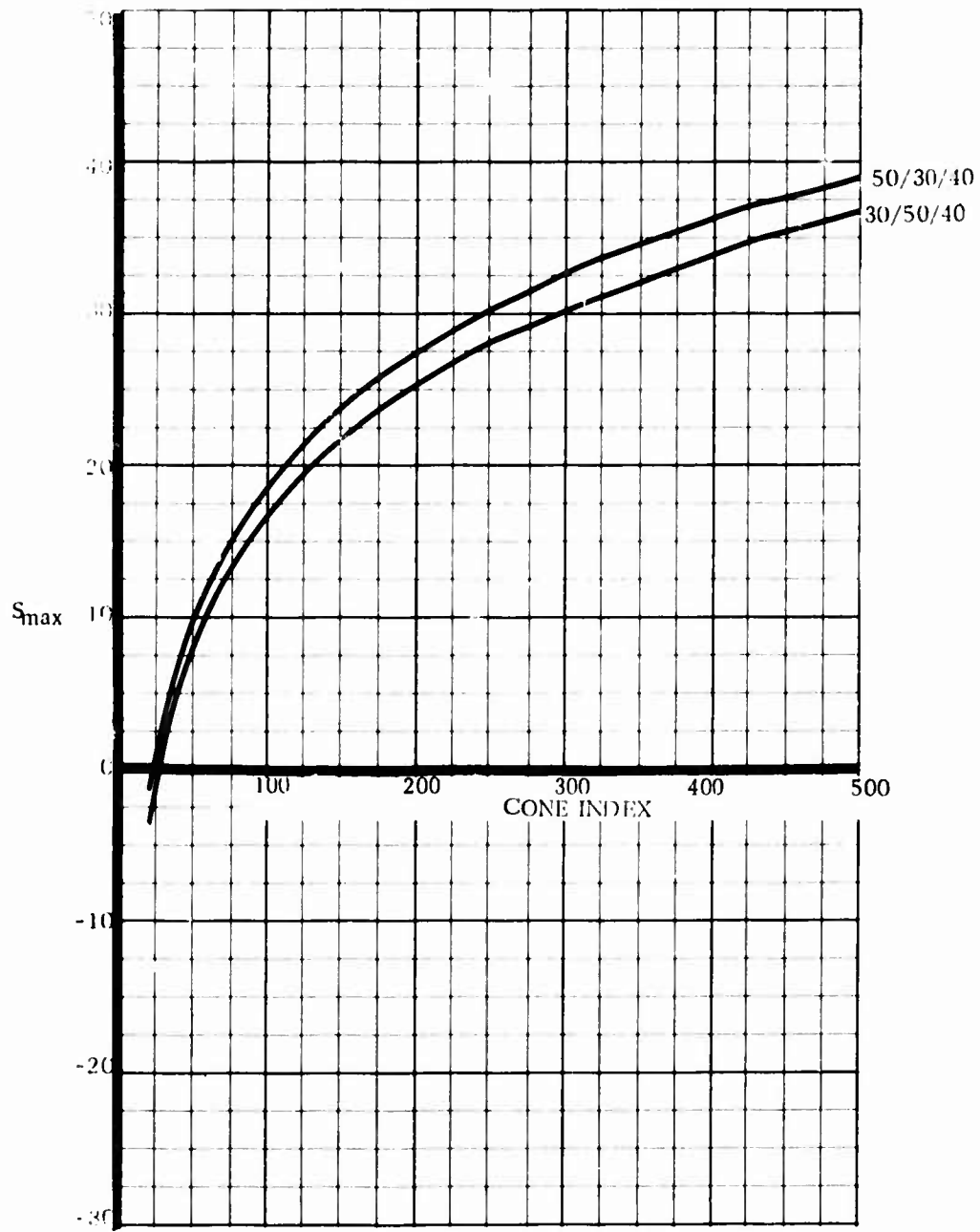
10K RTFLT



Graph 57

Radial Tires
Unequal axle load

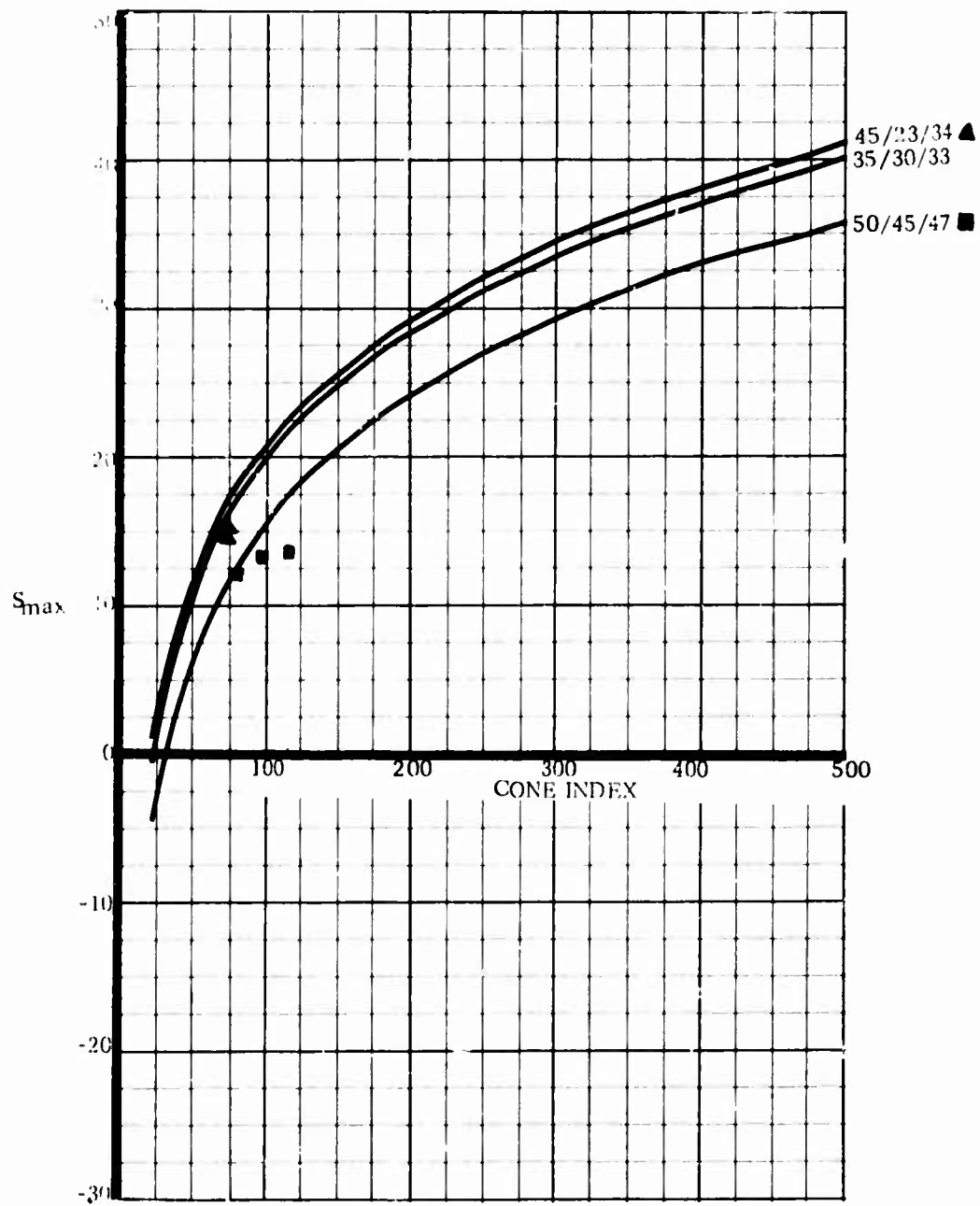
10K RTFLT



Graph 58

Radial Tires
Unequal axle load

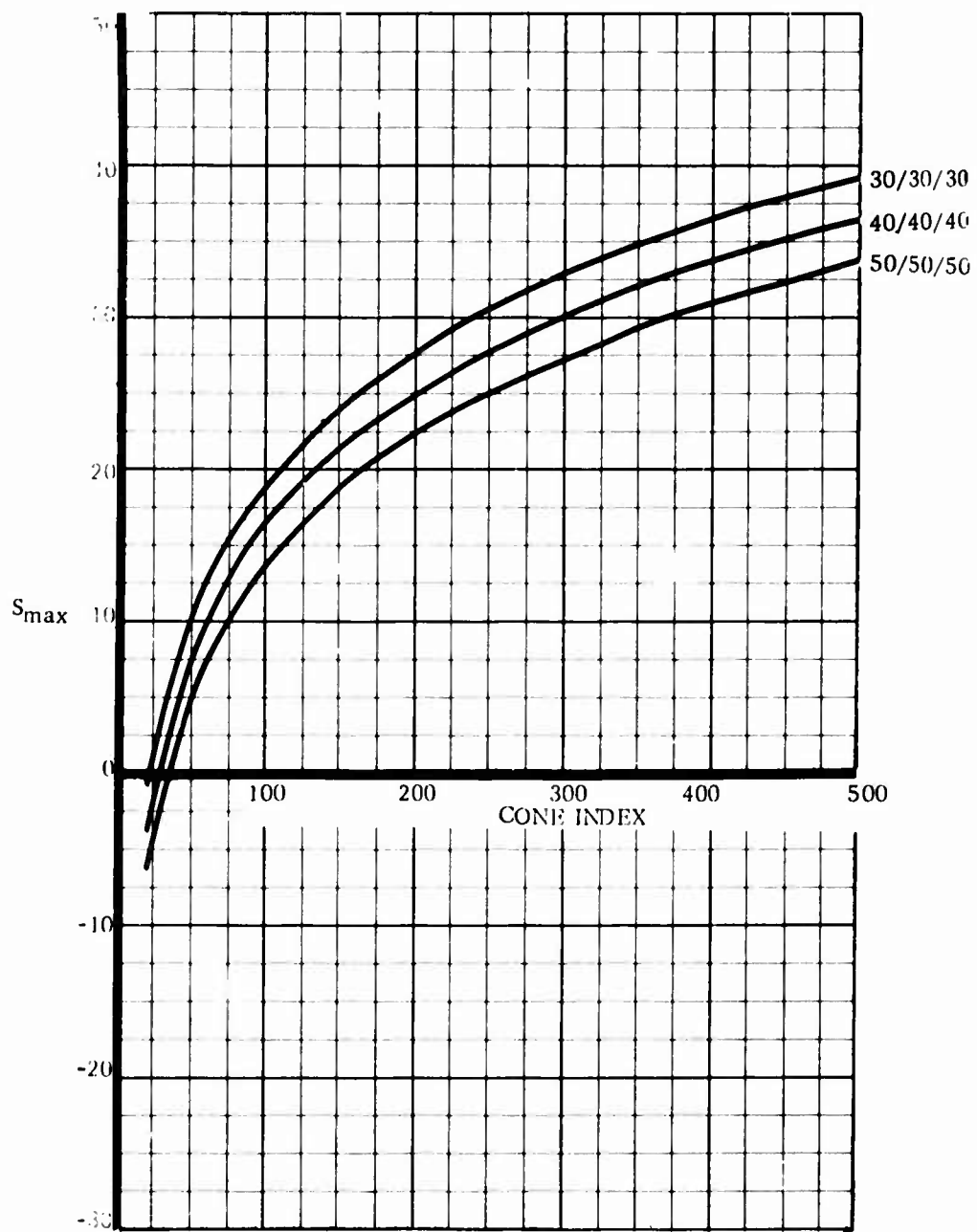
10K RTFLT



Graph 59

Radial Tires
Unequal axle load

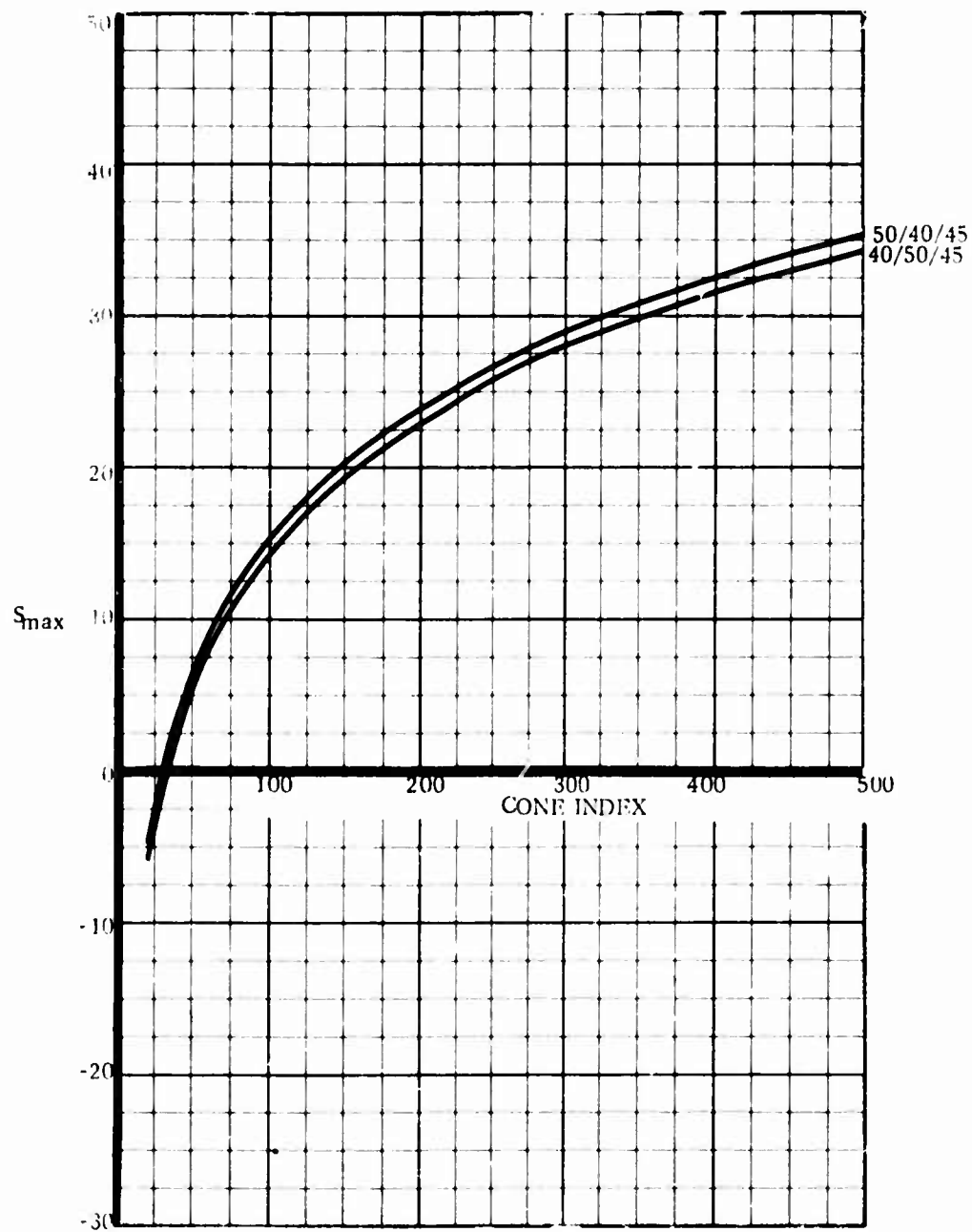
10K RTFLT



Graph 60

Radial Tires
No axle load

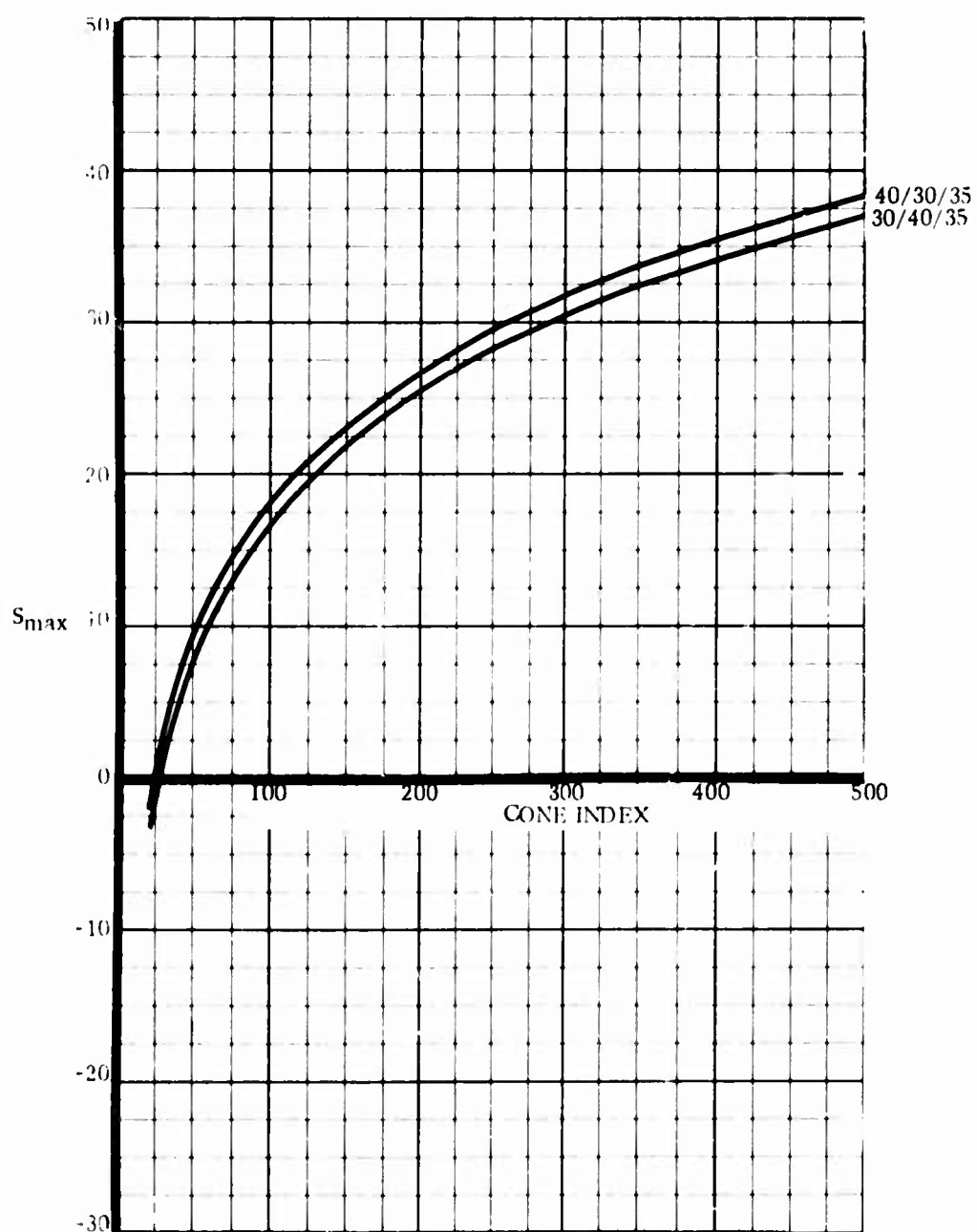
10K RTFLT



Graph 61

Radial Fires
No axle load

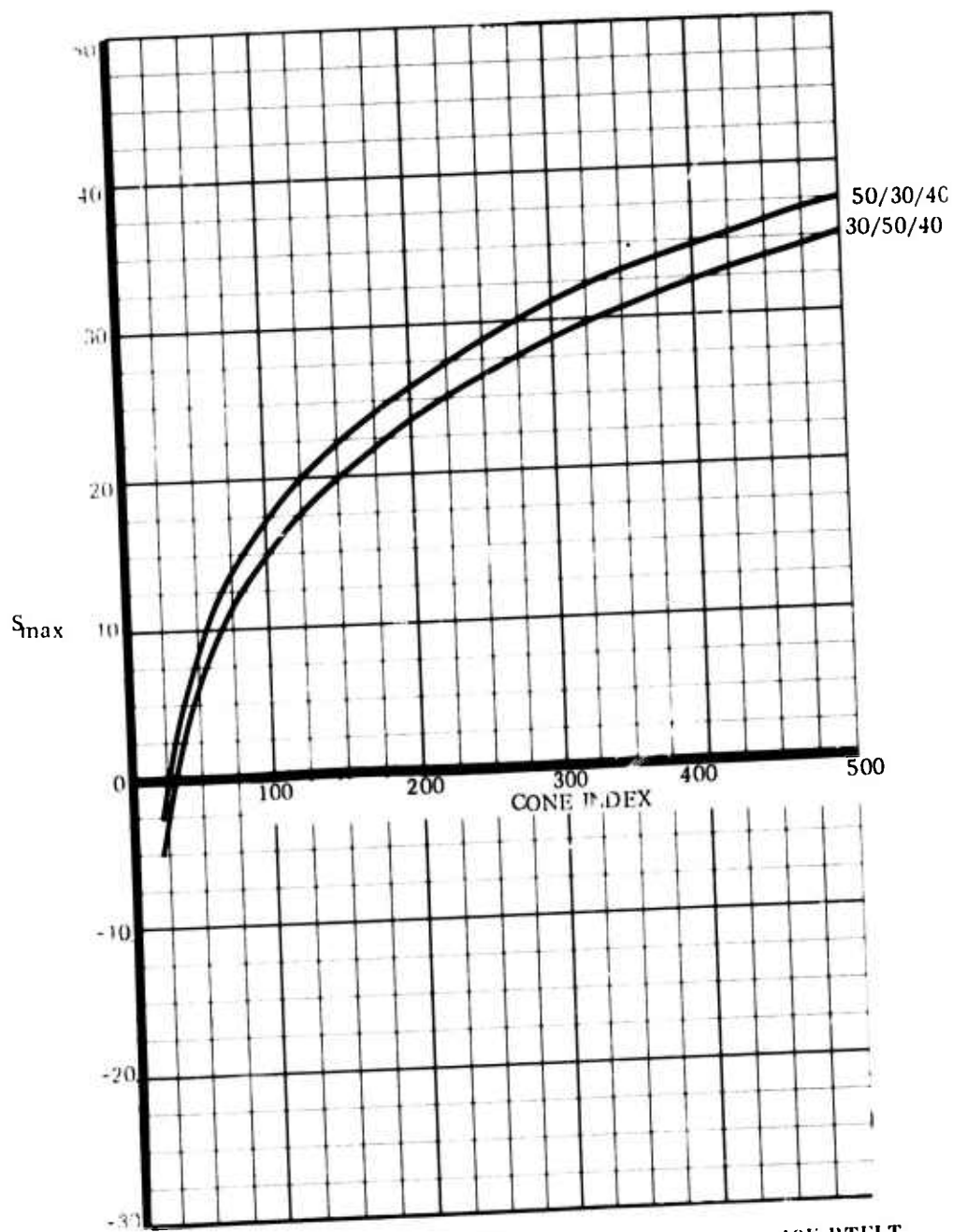
10K RTFLT



Graph 62

Radial Tires
No axle load

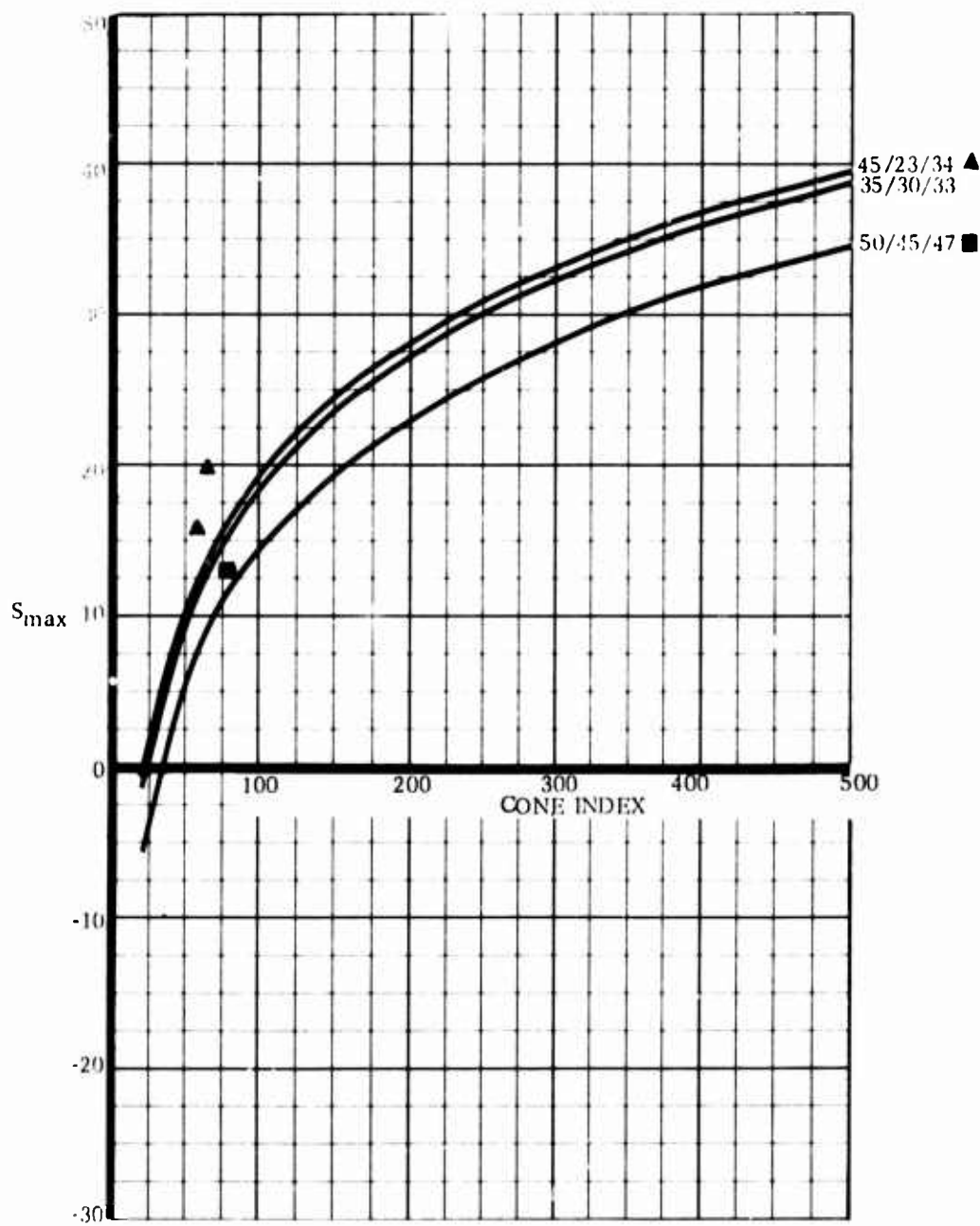
10K RTFLT



Graph 63

Radial Tires
No axle load

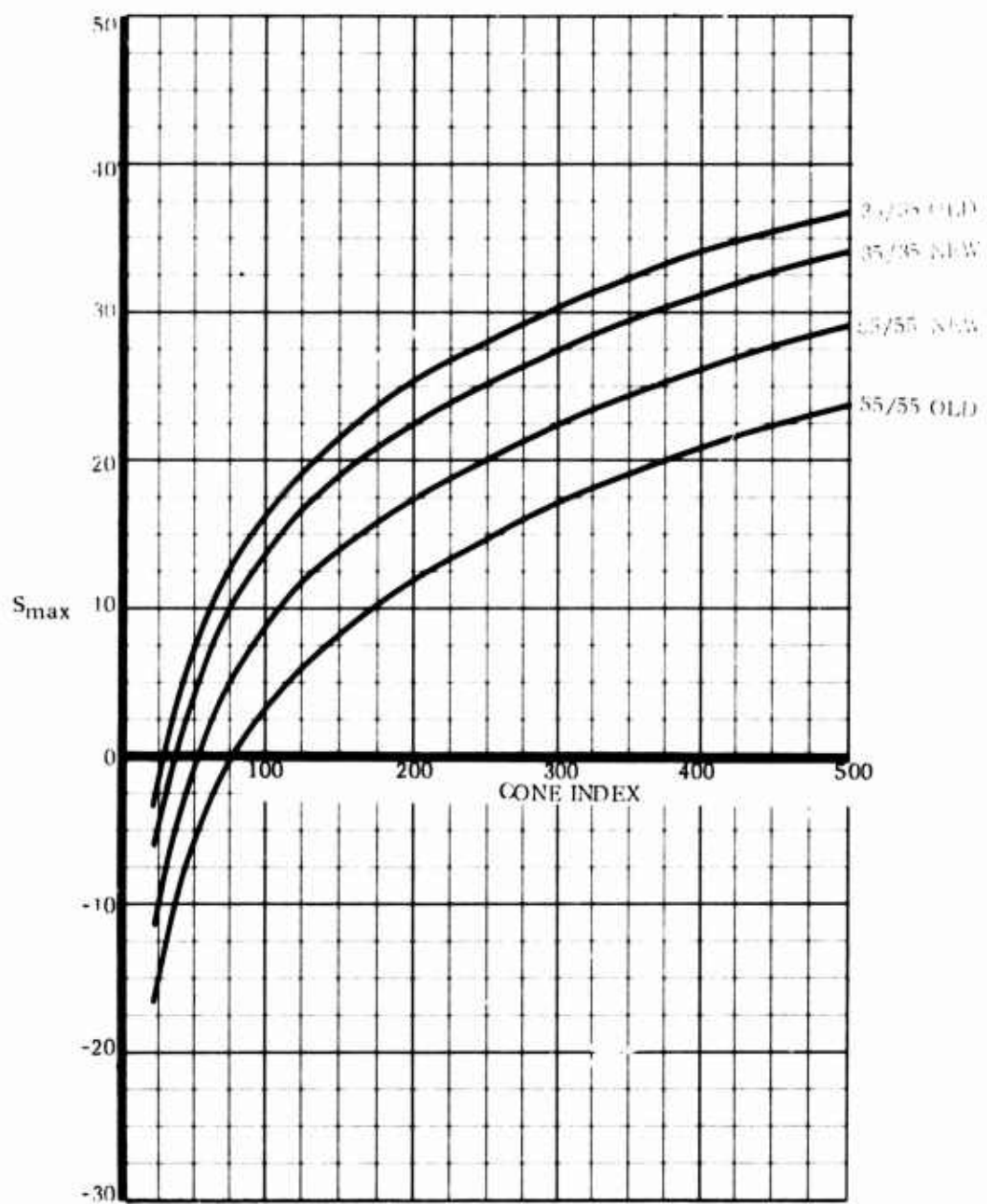
10K RTFLT



Graph 64

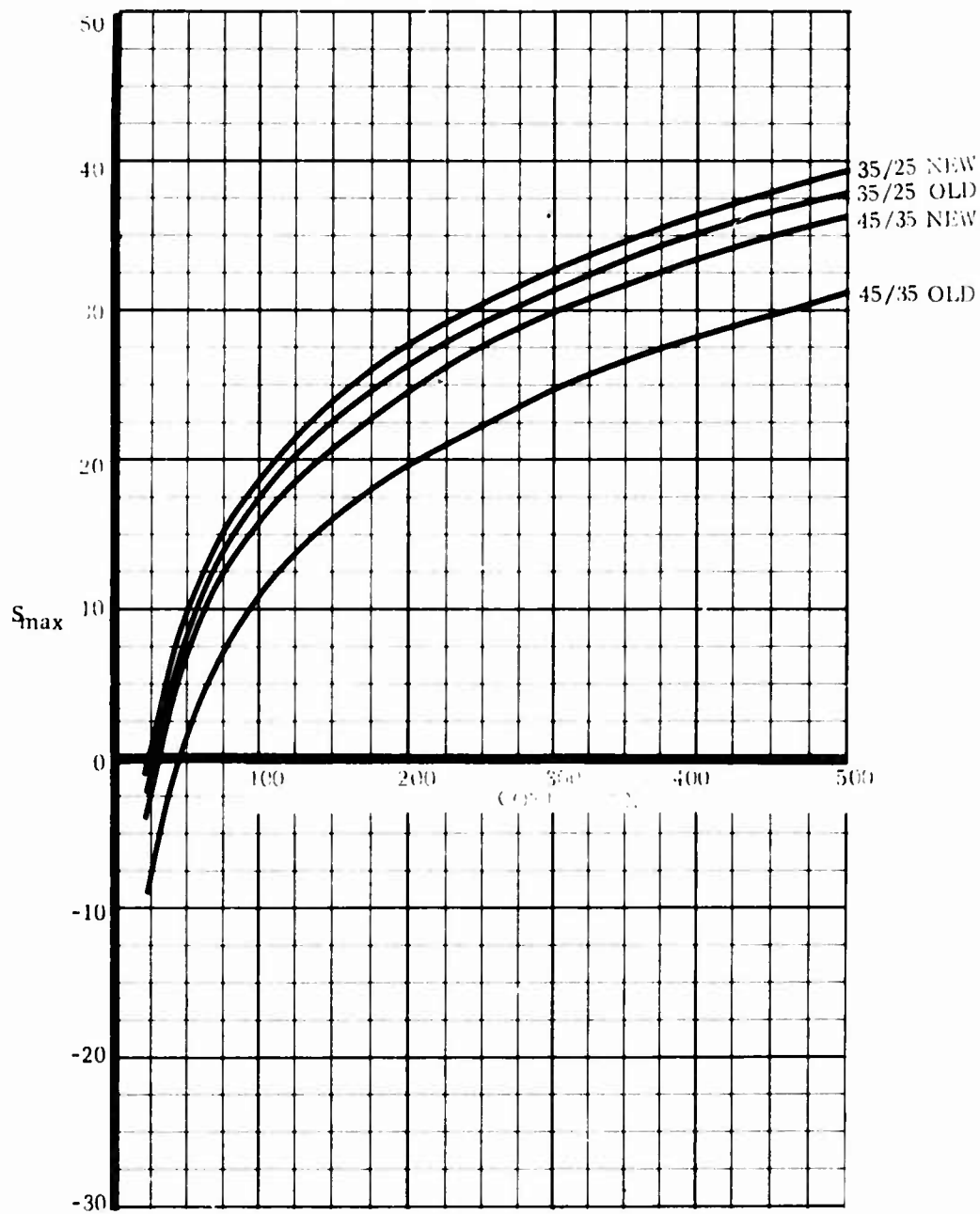
Radial Tires
No axle load

10K RTFLT



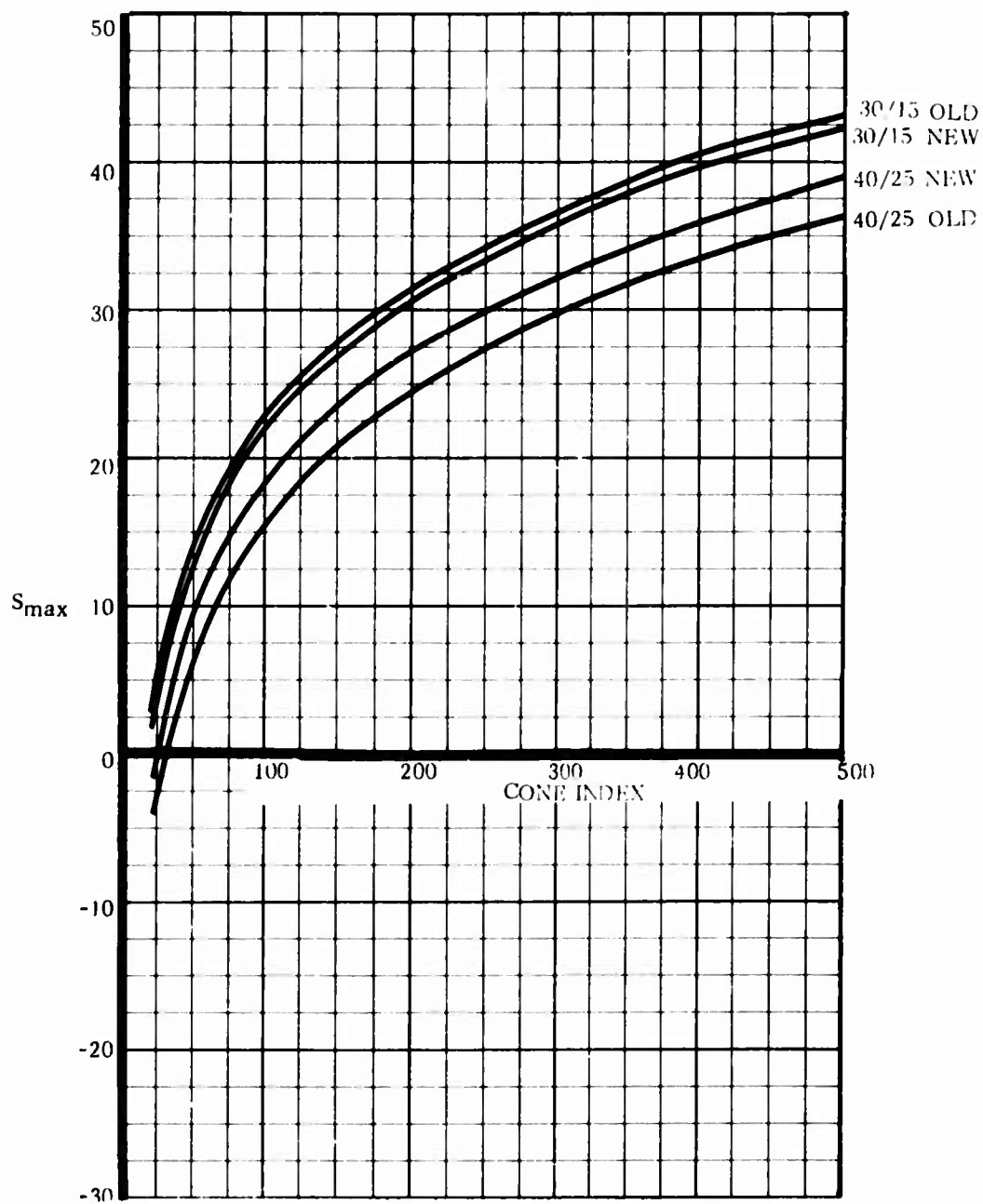
Graph 65

20-ton RTC



Graph 66

6K RTFLT



Graph 67

6K RTFLT

ABBREVIATIONS, ACRONYMS, and SYMBOLS

AL	Axle Load (pounds)
C	Collection of Terms in CIMM Formula
CAF	Contact Area Factor
CI	Cone Index (psi)
CIMM	Cone Index Mobility Model
D	Tire rut depth (inches)
DBP	Drawbar Pull (measured in pounds but made dimensionless)
EQ AX	Equal Axle Load
FLT	Forklift Truck
GVW	Gross Vehicle Weight (pounds)
k,K	Constants
MHE	Materials Handling Equipment
NPW	Number of powered wheels
PSI	pounds per square inch
RTC	Rough Terrain Crane
RTFLT	Rough Terrain Forklift Truck
S	Slope on which vehicle is operating (percent)
S_{max}	Maximum negotiable slope
SFC	Surface
TP	Tire Inflation Pressure
VCI	Vehicle Cone Index
W	Weight
Wd	Tire rut width (inches)
WES	Waterways Experiment Station
6K	6,000-lb Capacity, or payload
10K	10,000-lb capacity, or payload
50K	50,000-lb capacity, or payload
20-T	20-Ton Rough Terrain Crane
Δ	Change in Variable
θ	Angle of Inclination
μ	Friction coefficient
\propto	Proportional to
SUBSCRIPTS:	
ave	average value
F	Front Axle
FL	Floating Constant
ID	related to F-R inflation differences
Proj	Projected value
R	Rear Axle